THÈSE

PRÉSENTÉE À

L'UNIVERSITÉ BORDEAUX 1

ÉCOLE DOCTORALE DES SCIENCES CHIMIQUES

PAR

PARANTAP SARKAR

POUR OBTENIR LE GRADE DE DOCTEUR

SPÉCIALITÉ: ORGANIC-CHIMIE DE LA MATIÈRE CONDENSÉE

THE CERAMIDONINE AND PERKIN APPROACHES TO AROMATIC NANORIBBONS

DIRECTEUR DE RECHERCHE : HARALD BOCK

SOUTENUE LE 20 JUILLET 2012

DEVANT LA COMMISSION DÉXAMEN FORMÉE DE

M. Roger Hiorns	Chargé de Recherche, IPREM/CNRS	Rapporteur
M. Stéphane Baudron	Chargé de Recherche, LCCO/CNRS	Rapporteur
M. Benoît Colasson	Maître de Conférences, Univ. Paris 5	Examinateur
Mme Corine Mathonière	Professeur, Univ. Bordeaux 1	Examinateur
M. Philippe Richetti	Directeur de Recherche, CRPP/CNRS	Président,Examinateur
M. Harald Bock	Directeur de Recherche, CRPP/CNRS	Directeur de Thèse

This Thesis is
dedicated to my
Mom and Dad for
their Love and
Support

Résumé

Vers des nanorubans aromatiques : approches par formation de céramidonines et par réaction de Perkin

Les nanorubans de graphène (NRGs) sont des matériaux prometteurs pour l'organique électronique, à mi-chemin entre polymères conjugués et nanotubes de carbone. Deux approches différentes pour la synthèse de nanorubans aromatiques sont développées et évaluées. La première est fondée sur la formation de céramidonines par cyclisation d'arylamino-anthraquinones en milieu acide. Plusieurs tétraaza-arènes incorporant deux de ces unités sont obtenus, mais l'approche s'est uniquement avérée appropriée dans le cas de courts substrats. La seconde approche repose sur la condensation d'acides aryle-acétiques avec des formyl-arènes ou acides aryle-glyoxyliques, suivie soit de cyclo-deshydrogénations en présence de quinone, soit de deshydrodebromation catalysée par le palladium, pour donner des arenes carboxy-substitués allongés. La méthode impliquant la quinone s'avère limitée à des substrats suffisamment réactifs tels que des thiophènes et laisse envisager des poly(arènodithiophènes) en partie rigidifiés et carboxy-substitués. La catalyse au palladium s'avère plus générale, ouvrant des perspectives d'obtention d'une grande variété de rubans aux propriétés électroniques ajustables.

Abstract

The Ceramidonine and Perkin Approaches to Aromatic Nanoribbons

Graphene nanoribbons (GNRs) are promising materials for organic electronics, as they bridge the gap between single-stranded conjugated polymers and carbon nanotubes. Two different synthetic approaches to GNRs are developed and evaluated. The first approach is based on the acid-promoted cyclisation of arylamino-anthraquinones to ceramidonines. Tetraazaarenes with two ceramidonine units are obtained, but the approach is found to be appropriate only to such small systems. The second approach is based on the condensation of arylacetic acids with arenecarboxaldehydes or arylglyoxylic acids, followed either by quinone-assisted oxidative cyclodehydrogenation or palladium-catalysed dehydrodebromination to yield carboxy-substituted elongated arenes. The quinone-based variant is found to be limited to reactive substrates such as thiophene derivatives and offers the perspective of partially rigidified carboxy-substituted poly(arenodithiophenes). The palladium-based variant is found to be more general, opening the prospect of obtaining a variety of ribbon-type structures with tunable electronic properties.

Foreword

This research work was performed at Centre de Recherche Paul Pascal (CRPP, UPR 8641) of University Bordeaux 1. I am thankful to Philippe Richetti hosting me during these three years within the team $(AO)^2$. I am also thankful to the University of Bordeaux 1, Erasmus Mundus (external co-operation window with Asia) and CNRS for funding and organizing my research project and offering me a great atmosphere during last three years. I would like to express my gratitude to the rapporteurs Mr. Roger Hiorns and Mr. Stéphane Baudron for approving to judge this thesis. Likewise, I am also grateful to Mr. Benoît Colasson and Mme. Corine Mathonière for joining as juries of the defense.

I want to especially thank Mr. Harald Bock for supervising my thesis. I think that, I am fortunate to have such an enthusiastic and supportive person as a supervisor. He is not only an ideal researcher but also a great person. I learned a lot in last three years from his knowledge and enthusiasm. I would like to thank Mr. Fabien Durola for his inspiring and random ideas with his own specific humor (which helped a lot to 'evaporate' my pressure) and Mr. Rodolphe Clérac for his continious and immense support throught my doctoral studies.

CRPP was always been a wonderful place for me, not only for work but also as a place of relief. So I am thankful to all the CRPP members for helping me to finish such a massive work. So, a big "thank you" to all of them, especially to W. Neri, M. Rajaoarivelo, Ie-Rang Jeon, Pierre dechambenoit, Julien kelber, Anirban Pradhan, A. Bentaleb for their time, they spent for my work and my 'office-mates' Julien vieaud, Octavian Blaj, Alexis de la Cotte, Emilie Pouget and Déborah Mirbel for providing me an enjoyable office atmosphere.

Finally, I must mention about my familiy, my parents, my brother Sayantan and my sweetheart Swarnali for their splendid support, without which I could never achive such a difficult milestone in my life. Thank you, you are what is most precious to me.

Table of Contents

Chapter 1

Introduction to functionalised polycyclic aromatic nanoribbons

Graphene nanoribbons are a potential alternative to carbon nanotubes on the one hand and to conventional conjugated polymers on the other hand, uniting some of the advantages and eliminating some of the shortcomings of both.

1.1. Carbon nanotubes

The two allotropes of carbon extensively present in nature are diamond and graphite. Diamond is made up exclusively of tetracoordinated sp^3 carbon atoms that form an extended three-dimensional network of fused chair-configured cyclohexane rings. It is the hardest of all minerals. Due to its fully saturated, single-bonded make-up, diamond only absorbs in the ultraviolet and is transparent in the visible spectral range. The sparkle of diamond, which made it so precious throughout history, results from its exceptionally high refractive index and thus its ability to fractionate visible light into its spectral components. Graphite consists exclusively of tricoordinated sp^2 carbons in loosely stacked sheets of fused benzene rings. Unlike diamond, graphite is black and a very good conductor due to its bidimensionally conjugated aromatic structure. As bonding interactions between the aromatic graphene layers are weak, graphite is an anisotropic conductor and far softer than diamond. Its light absorption and its softness give rise to its most prominent traditional use in pencils.

Newer, non-polymeric carbon allotropes are the fullerenes, which are fully unsaturated cage-like spheres or ellipsoids. The best-known and most easily accessible fullerene is C_{60} (Buckminsterfullerene), first prepared by Kroto et al. in 1985.[1] The key feature that leads to the curvature necessary to form spherical surfaces with a sp^2 hybridized carbon network in such spherical carbon macromolecules is the presence of a dozen five-membered rings. There are always exactly twelve such pentagons, the only suitable number to impart the necessary curvature to close a sphere; the number of hexagons varies and defines the size of the fullerene: C_{60} for example consists of 12 pentagons and 20 hexagons, whilst C_{540} consists of 12 pentagons and 265 hexagons. Even though the five-membered rings constitute a marked difference between fullerenes and graphite, fullerenes may be considered as spherical forms of graphene.

In 1991, Iijima[2] first prepared carbon nanotubes (CNTs), which can be described as rolled up graphene layers. In an idealised representation (that does not always fit with reality), the tube is closed at either end by a half-fullerene end cap (that comes with six five-membered rings). CNTs can be single-walled (SWNTs) or multi-walled (MWNTs), the latter consisting of multiple concentric graphitic cylinders assembled like Russian dolls. A number of different preparation methods have been developed in the last two decades, including the evaporation of graphite in an electric arc, laser ablation, chemical vapour deposition, and vapour phase decomposition of carbon containing molecules.[3] All these harsh synthetic processes require cumbersome purification because in all cases the resulting carbon nanotubes contain impurities such as amorphous carbon and graphite nanoparticles as well as particles of the transition metal catalysts used to nucleate tube growth. Structural defects due to the formation of nonhexagonal rings such as pentagons or heptagons within the honeycomb carbon network may occur in the resulting carbon nanotubes, promoting additional curvatures (pentagons promoting bowl-type curvature and heptagons promoting saddle-type curvature).

As a graphene sheet can curl into a cylinder along many different directions with respect to the orientation of the carbon-carbon bonds, nanotubes with different bond orientations can be observed. The two extreme cases are termed are *zig-zag* and *armchair* nanotubes, in allusion to the form of the rim formed when cutting the nanotube perpendicular to its axis. In zig-zag nanotubes, one third of the C-C bonds is parallel to the tube axis, whilst in armchair nanotubes one third of the bonds lie in the plane normal to the tube axis. All other tubes with intermediate (oblique) bond orientations between these two extremes are termed *chiral*, because the combination of this oblique bond orientation with the tubular curvature makes the tube a chiral object (i.e. without mirror symmetry) that is either the left- or the right-rotating enantiomer.

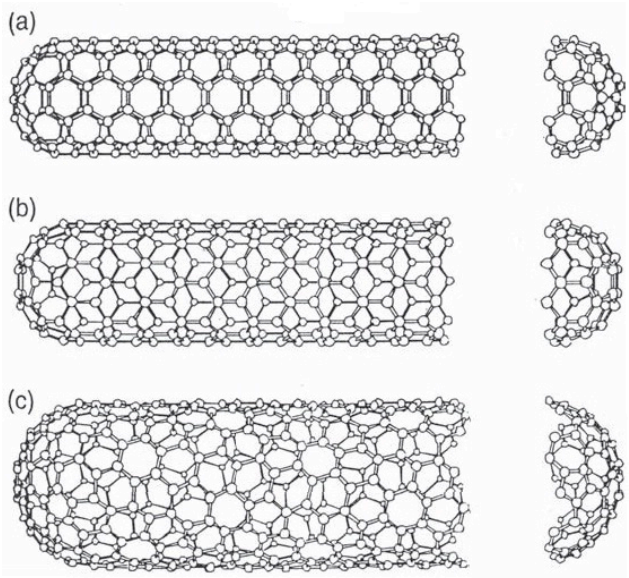

Fig. 1. Models of (a) armchair, (b) zigzag, and (c) chiral nanotubes (reproduced from ref. 4)

The structure of a nanotube is usually defined by the index (n,m), where n and m are the numbers of side-joined hexagons in two directions, different by 60°, that have to be crossed to come back to the point of origin after a journey around the tube. n and m yield the chiral angle $\theta = \arctan[-(3)^{1/2}m]/2n+m$ and, together with the (average) C-C bond length a, the tube diameter $d = a[(m^2+mn+n^2)^{1/2}]/\pi$. If $n \neq 0$ and $m = 0$, the tube is zig-zag. If $n = m \neq 0$, the tube is armchair. In all other cases the tube is chiral.

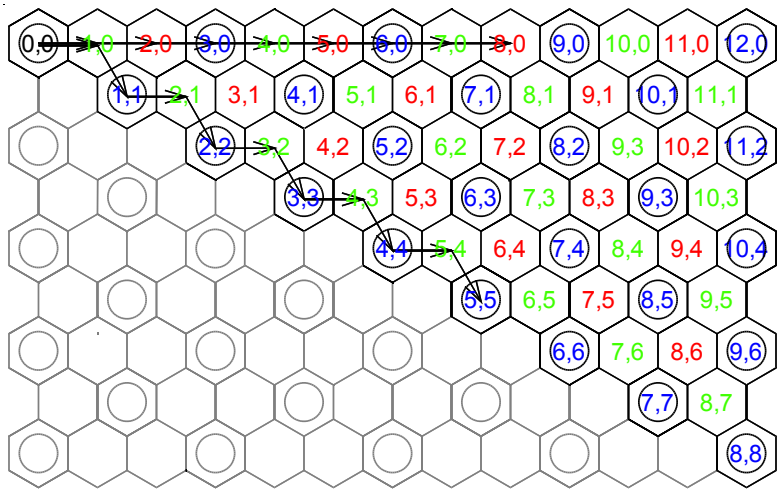

Fig. 2. Diagram for the construction of the roll-up indices n,m for any given CNT. If the graphene sheet is rolled up to make a given hexagon marked n,m coincide with the 0,0-hexagon, the n,m-CNT is formed. As examples, the horizontal set of arrows describes a tour around a 8,0-zig-zag-CNT (8 hexagons in one direction, 0 in the other), and the descending set of arrows describes a tour around a 5,5-armchair-CNT (5 hexagons in one direction, 5 hexagons in the other). The indices of fully benzenoid = metallic nanotubes with n–m = 3p are

marked in blue, the indices of semiconducting CNTs with n–m = 3p+1 are marked in green, and those of semiconducting CNTs with n–m = 3p+2 are marked in red.

Nanotubes for which n – m = 3p, where p is an integer, are metallic (blue in the above roll-up diagram). This includes all armchair nanotubes. The others, i.e. nanotubes for which n – m = 3p + 1 (green in above diagram) or n – m = 3p + 2 (red in above diagram) have a non-vanishing band gap and are thus semiconductors. Nanotubes with n – m = 3p can all be described by a fully sextetted Clar structure. Clar structures are representations of PAHs where circles are written to represent a benzenic sextet wherever they can replace three double bonds that would otherwise be written on a same hexagon, whilst double bonds are maintained in writing wherever else. Circles thus can never be written into adjacent hexagons; those Clar structures that contain the maximal number of circles, called "maximally sextetted" in the following, are considered to represent best which hexagons of the molecule are most aromatically stabilised and which bonds are most olefinically reactive.[4] It follows that all nanotubes that can be fully constructed by joining benzenes via single bonds are metallic, whilst all others (those where not only benzenes but also additional ethylenes have to be joined by single bonds to construct the CNT) are semiconductors. This is quite counter-intuitive when compared to the band gaps of polycyclic aromatic hydrocarbons (PAHs), where fully sextetted isomers have much larger HOMO-LUMO energy gaps than minimally sextetted isomers: Triphenylene ($C_{18}H_{12}$ with three sextets) has a gap so large that it appears uncoloured, whereas tetracene ($C_{18}H_{12}$ with one sextet and six non-sextetted double bonds) is orange.

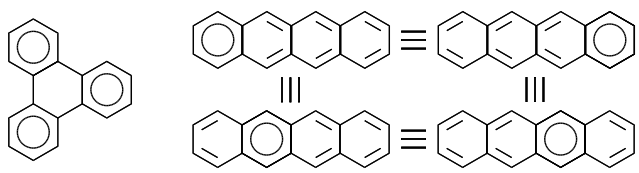

Fig. 3. Clar structures of triphenylene (fully sextetted, single Clar structure, uncoloured) and its isomer tetracene (minimally sextetted, four equivalent Clar structures, orange)

But on second view, this paradox between the vanishing gap of fully sextetted nanotubes and the maximal gap of fully sextetted PAHs may be explained by the overwhelming edge effect on bond fixation in PAHs, which is absent in CNTs: In fully sextetted PAHs such as triphenylene only one Clar structure is possible, leading to localisation and isolation of the aromatic sextets and strong single bond character of the bonds in-between benzene units, whereas in less sextetted isomers like tetracene several Clar structures are possible, no bond has strong single bond character and the aromatic electron system is strongly delocalised all over the molecule and not split up in isolated benzene units. In

bidimensionally infinite graphene on the other hand, which has a fully sextetted Clar structure, all hexagons can be split into three subsets of benzene networks of equal contribution to the bond character, and thus the aromatic electron system is fully delocalised (infinite) and all bonds are equal. The latter is true also for nanotubes (rolled-up graphene) if we ignore the weak effect of curvature on bond lengths, *but only if the nanotube is of the fully sextetted type (n – m = 3p)!* If double bonds have to be drawn in addition to the sextet circles, these double bonds have to be drawn preferentially (i.e. in the majority of equivalent Clar structures) parallel or near-parallel to the tube axis to fill the gap lines between sextet rows running along the tube. Bond lengths should therefore not be identical any more in not fully sextetted CNTs, leading to a less ideal delocalisation of the aromatic electron system over the tube. Thus whilst in PAHs, dominated by edge effects, fully sextetted structures lead to maximal diversity of bond lengths and maximal separation of sextets, in CNTs, with no edges but with variably sextet-commensurable circumference, fully sextetted structures lead to the contrary: minimal diversity of bond character and maximal homogeneity of the aromatic electron system all over the tube.

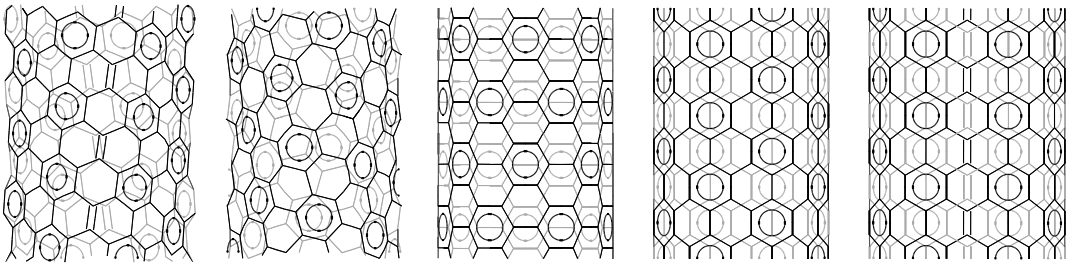

Fig. 4. Clar structures of CNTs. From left to right: a) chiral (12,2), partially sextetted, semiconducting, b) chiral (10,4), fully sextetted, metallic, c) armchair (7,7), fully sextetted, metallic d) zig-zag (12,0), fully sextetted, metallic, e) zig-zag (13,0), partially sextetted, semiconducting.

The electronic properties of CNTs may also be modified by doping. Boron substitution results in p-type doping whilst nitrogen substitution corresponds to n-type doping.[5] Intercalation of alkali metals inside SWNTs gives rise to metallic character, whilst intercalation of alkali metals in the intershell spaces of MWNTs disrupts the cohesion of the tubes, resulting in partial or complete destruction of the shells of the nanotube in line with its Russian doll morphology. Thus MWNTs can be opened longitudinally by alkali metal intercalation to obtain flat graphene ribbons.[3]

The reactivity of fullerenes are driven by the enormous strain that arises from their strongly bent spherical geometry. An sp^2-hybridised carbon atom favours a planar geometry with a pyramidalisation angle $\theta_P = 0^0$, whilst an sp^3-hybridised carbon atom favours a tetrahedral geometry with $\theta_P = 19.5^0$. In C_{60} all carbon atoms have $\theta_P = 11.6^0$ which is more adapted to tetrahedral than to planar hybridisation.

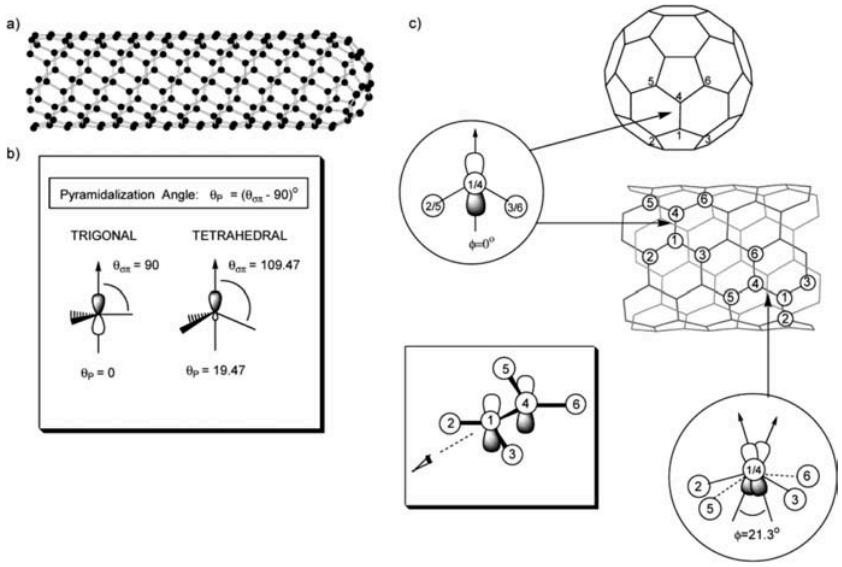

Fig. 5. Diagrams of (a) a metallic (5,5)-SWNT, (b) pyramidalization angle (θ_P), and (c) the orbital misalignment angles (ϕ) along C–C bonds in the (5,5)-SWNT and its capping fullerene, C_{60}

This is the main reason why C_{60} easily undergoes addition chemistry to relieve strain at the point of attachment and simultaneously lower the strain at the 59 remaining atoms. In contrast, carbon nanotube cylinders are chemically quite inert though possibly more reactive than a flat graphene sheet.[6] The chemical inertness of the sidewall of a cylindrical nanotube structure in comparison to its end cap is linked to the misalignment of π-orbitals and relatively lower pyramidalization angles in the sidewall compared to the end cap. Furthermore, since the pyramidalization angles and the π-orbital misalignment angles of SWNTs are inversely proportional to the diameter of the tube, reactivity varies with diameter. The chemical inertness of nanotubes renders difficult their solubilisation or other property modification by chemical functionalization. CNTs are insoluble in most common solvents. Various derivatisations of CNTs, in order to solubilise them in various solvents, have nevertheless been achieved in the recent past, such as covalent modification (halogenation, end group functionalization, cycloaddition, radical addition, nucleophilic addition, defect functionalization etc.), wrapping with polymers or surfactants, and donor-acceptor interactions with electron-rich polycyclic aromatics.[3]

1.2. Conjugated polymers

In 1977, the report of metallic conductivity in doped polyacetylene[7] initiated an enormous surge of interest in conjugated polymers as promising materials for "next-generation" electronic and optical devices. In the more than three decades elapsed since, a great variety, structural and electronic, of

conjugated polymers has been developed. Undoped conjugated polymers with low band gaps are one of the major research interests in the field of organic semiconducting materials and solar cells. In order to reduce the band gap, the energy difference between HOMO and LUMO should be decreased either by raising the HOMO or lowering the LUMO level of the polymer or both.

Unimpeded conjugation of the π-electrons of alternating double bonds over a large number of monomer units is a main factor determining the extent of band gap reduction between a monomer and the corresponding polymer,[8,9] and good coplanarity of adjacent monomer units and a low density of chemical or configurational defects are key to such an efficient long range conjugation. Polythiophenes are a particularly important class of conjugated polymers in this respect because of their good coplanarity induced by geometrically favourable S-H interactions between adjacent thiophene units, leading to a sulphur-bridged highly coplanar all-trans polyacetylene chain with, compared to free polyacetylene, improved chemical and thermal stability.[8, 9]

Another factor that greatly influences the width of the band gap is the energy difference between the *aromatic* form of the polymer, i.e. the form where aromatic monomer units are linked only by single bonds, and the *quinoid* form, where, via a one-carbon bond shift with respect to the aromatic form, the monomer units are linked by double bonds to give a polymer that is intrinsically more conjugated and more coplanar, and is thus prone to show a lower band gap. Resonating structures of aromatic forms and quinoid forms in the simple conjugated polymers polyphenylene, poly(phenylenevinylene), and polythiophene are shown in the following fig.6, which indicates that in all three cases, the aromatic form is energetically much more stable than the quinoid form because aromaticity with confined π-electrons results in stable benzenoid configurations whilst the quinoid form is olefinic in character and thus energetically less stable. In contrast to the three mentioned polymers, poly-isothianaphthene prefers the quinoid form because this allows the conservation of the higher benzenoid resonance energy of the six-membered rings, whilst the aromatic form only allows the conservation of the lower benzenoid resonance rings of the thiophene rings (1.56 eV vs. 1.26 eV).

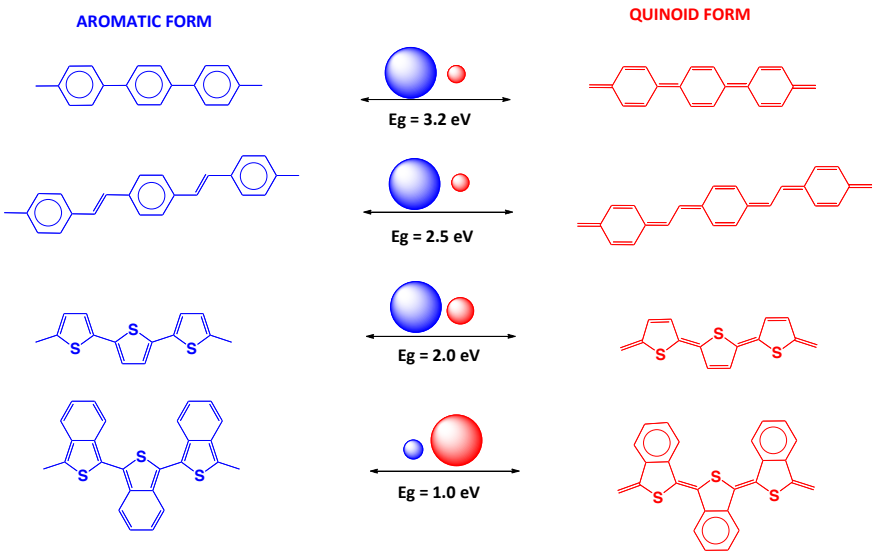

Fig 6. Aromatic and quinoid resonance forms of poly(*p*-phenylene), poly(*p*-phenylenevinylene), polythiophene, and polyisothianaphthene. The relative contribution of the mesomeric structures is represented by the size of the coloured circles over the arrows (reproduced from ref. 7).

A further means of lowering the band gap is the rigidification of pairs or larger subsets of monomer units by planarising bridges. Rigidifying two adjacent thiophene units by methylene bridges remarkably lowers the band gap (Fig. 7, polymer P1), and extending the rigidification to triplets of monomers reduces the band gap further (Fig. 7, polymer P2).

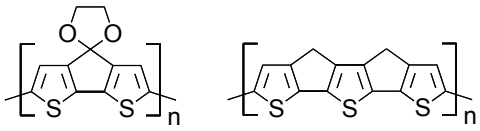

P1
E_g = 1.2 eV

P2
E_g = 1.1 eV

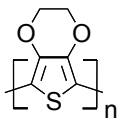

P3
E_g = 1.5 eV

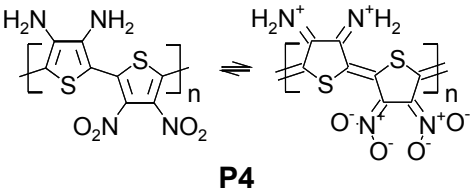

P4
E_g = 1.1 eV

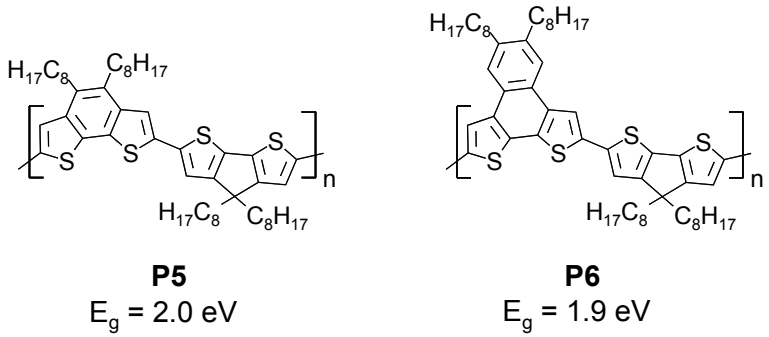

Fig 7. Top: Polymers from rigidified bi- and terthiophenes, with band gap energies. Centre: Polythiophenes with electron-donating (**P3**) and -withdrawing (**P4**) substituents, with band gap energies. Bottom: Polymers from rigidified bithiophenes with solubilizing *n*-octyl chains, with band gap energies.

The incorporation of electron-donating or electron-withdrawing substituents in monomeric aromatic units also reduces the energy difference between HOMO and LUMO, with electron-donating groups (Fig. 7, polymer P3) raising the HOMO energy and electron withdrawing groups lowering the LUMO energy. A combination of alternating monomeric units containing electron-donating and electron-withdrawing substituents respectively may favour a zwitterionic quinoid form (Fig. 7, polymer P4), which causes a dramatically reduced band gap energy compared to that of the parent polythiophene.

Solubility is another major issue in terms of accessibility, characterisation and processability of conjugated polymers. Due to strong interchain π-π stacking, most aromatic conjugated polymers are insoluble without solubilising substituents attached. Aliphatic side chains of most often at least six carbons are frequently introduced into the monomeric units to induce an adequate solubility of the resulting conjugated polymer. But excess incorporation of insulating aliphatic side chains reduces the charge mobility as it impedes interchain π orbital interactions and also may reduce the intrachain coplanarity and thus conjugation. The right dosage of chain length and an optimised choice of chain attachment points are thus important to maintain good conductivity and small band gap.

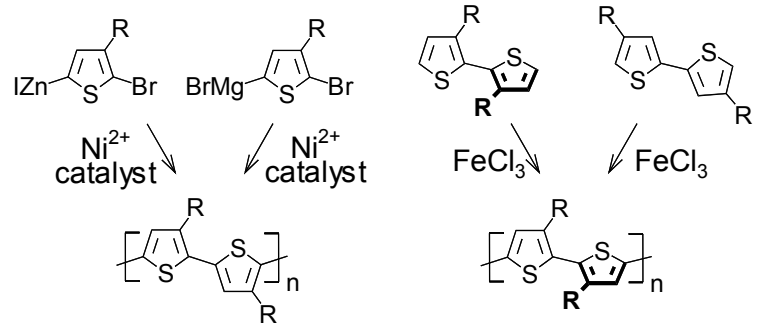

Fig 8. Syntheses of the two extreme types of regioregular 3-alkylthiophenes, the maximally coplanar all-HT-polymer and the minimally coplanar all-HH-TT-polymer.

The polymerisation of unsymmetrical 3-alkylthiophenes gives raise to regioisomers depending upon the mode of coupling between two monomeric units. The coupling between two 3-substituted thiophenes occurs either at the 2- or at the 5-position of each thiophene brick. If the 2-position of one such 3-alkylthiophene couples with the 5-position of the other (2,5'-coupling), a "head-to-tail" (HT) coupling takes place. Alternatively, a 2,2'- or "head-to-head" (HH) coupling and a 5,5'- or "tail-to-tail" (TT) coupling may occur. These different modes of coupling may lead to a mixture of chemically distinct regioisomers,[10] where unfavourable HH couplings cause a sterically driven twist of thiophene rings, resulting in a deviation from the parallel alignment of p-orbitals, *i.e.* loss of conjugation. On the other hand, regioregular all-HT poly(3-substituted) thiophene allows a predominantly planar conformation, leading to a highly conjugated polymer. The opposite, least conjugated worst-case configuration would be a regioregular all-HH-TT coupled polythiophene with minimal conjugation, maximal band gap and low charge mobility. Regioregular all-HH-TT poly-3-alkylthiophenes can be obtained by polymerisation of HH- or TT-dimers.[10] Highly regioregular all-HT poly-3-alkylthiophenes have been obtained from monometalated monomers such as 2-bromo-3-alkyl-5-bromomagnesio-thiophene or 2-bromo-3-alkyl-5-iodozincio-thiophene[10] (Fig. 8) and has found widespread use in organic electronic prototype devices.

1.3. Structural types of graphene nanoribbons

If we define graphene nanoribbons (GNRs) as graphene segments of (near-)infinite length and limited width, they may not only be conceptually (and practically) obtained by slicing open SWNTs, but they also offer themselves to structural classifications similar to those of SWNTs. Whilst they differ from CNTs by the presence of edges, a feat they have in common with PAHs, they share with CNTs the presence of an axis of elongation with respect to which the bond orientations may be classified. One might consider classifying them into zig-zag edge, armchair edge and oblique edge (GNRs), but this may lead to confusion as zig-zag edge GNRs would correspond to armchair CNTs and vice versa, and besides this, the edges may be of various shapes independently of bond orientation, with bays, coves and protrusions. We therefore propose the terms "acene-like bond orientation" (AO, fig. 9), "phenacene-like bond orientation" (PO, fig. 10) and "slanted bond orientation" (SO, fig. 11, centre), corresponding respectively to armchair, zig-zag and chiral geometries of CNTs regarding the relative orientations of the bonds to the macromolecular axis. Whilst the Clar structure and electronic character of CNTs is only defined by bond orientation and width, edge effects may dominate the aromatic and electronic character of GNRs and lead to greatly different Clar structures between ribbons of same bond orientation and similar width. The most striking example is the comparison of polyacene, which

has a completely olefinic (non-sextetted) Clar structure and is thus exceedingly unstable and small-bandgapped, with its AO isomers where some or all hexagons are meta-diannellated instead of para (fig. 9): Without changing the bond orientation, the number of sextetted hexagons varies between nil and maximal, i.e. equal to phenacene. The instability of polyacene itself is easily illustrated by the huge gain in sextets upon oxidation to the corresponding polyquinone (in general, ribbons that gain sextets when oxidised to quinones should be considered unstable). No such gain of sextets by oxidation is possible with maximally sextetted kata-annellated ribbons such as polyacene (the term *kata* designates annelation without sharing any carbon between three rings, which would be termed *peri*).

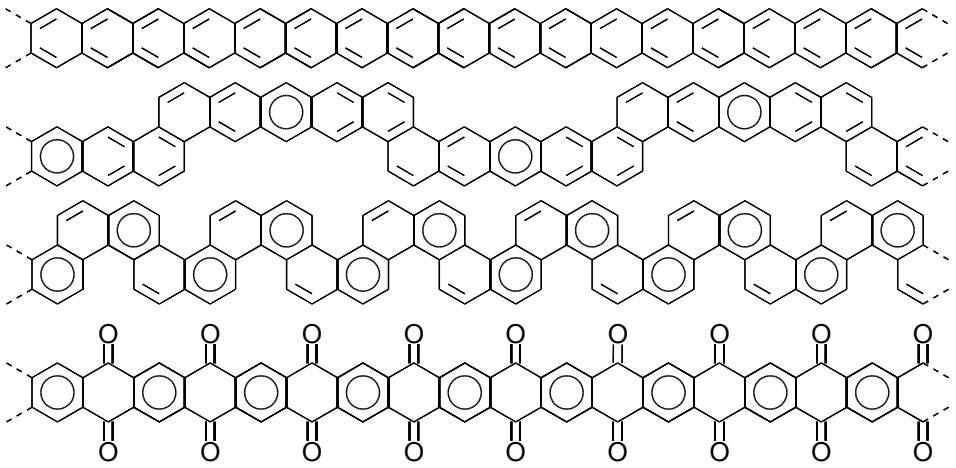

Fig 9. Kata-annellated GNRs with acene-like bond orientation (AO) and different degrees of sextet stabilisation, and the highly sextet-stabilised polyquinone obtained by oxidation of polyacene.

Similarly, whilst polyphenacene is highly sextet-stabilised, kata PO isomers with far less sextet stabilisation are readily constructed by insertion of para-diannellated hexagons (fig. 10).

If we go from exclusively kata-annellated systems to larger peri-annellated ribbons, we are able to construct fully benzenoid ribbons independently of bond orientation, i.e. with AO, PO and SO alike (fig. 11).

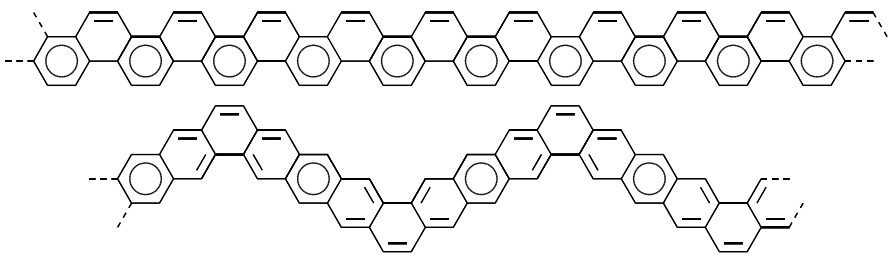

Fig 10. Kata-annellated GNRs with phenacene-like bond orientation (PO) and different degrees of sextet stabilisation

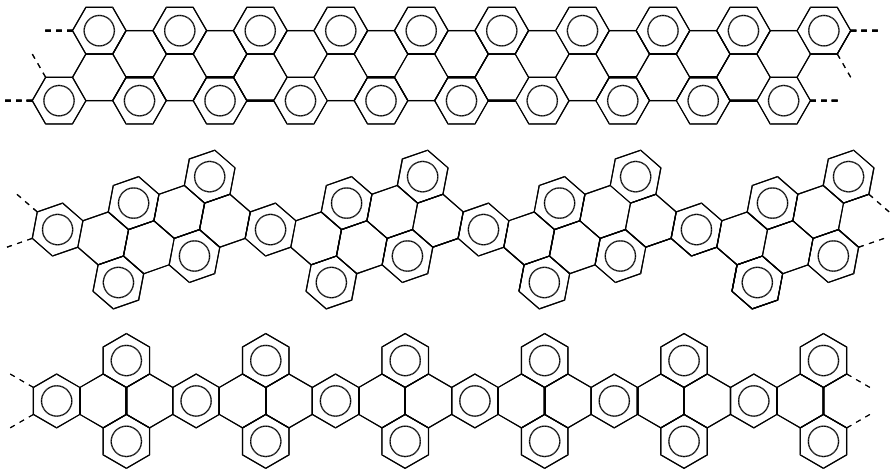

Fig 11. Fully benzenoid GNRs with phenacene-like, slanted and phenacene-like bond orientations (PO, SO and AO).

This illustrates that in GNRs, the degree of benzenoid character is much less dependent on bond orientation than on edge geometry.

If one notes in figures 10 and 9 that the two maximally benzenoid kata ribbons (phenacene in fig.10 and most benzenoid AO isomer in fig.9) are vinylene-bridged poly-para- and -meta-phenylenes, one may wonder about the ortho isomer, which leads us to poly-helicene (i.e. vinylene-bridged poly-ortho-phenylene, fig. 12), the simplest member of a completely different class of ribbons, which are helical and where the macromolecular axis is roughly perpendicular to all bonds. A similar but larger ("kekulenic") helical ribbon can be obtained by an alternative vinylene bridging of meta-polyphenylene, and an alternative vinylene bridging of para-phenylene leads to an "anthracenoid" iso-polyphenacene; the latter two are less resonance-stabilised than the three previously discussed isomers because the sextetted rings and the bridge rings are not equivalent: shifting of the sextets to the bridge rings would lead to biradicals in the formerly sextetted rings. These helicenic ribbons cannot be "cut out" from graphene sheets; they are thus not GNRs in the strict sense.

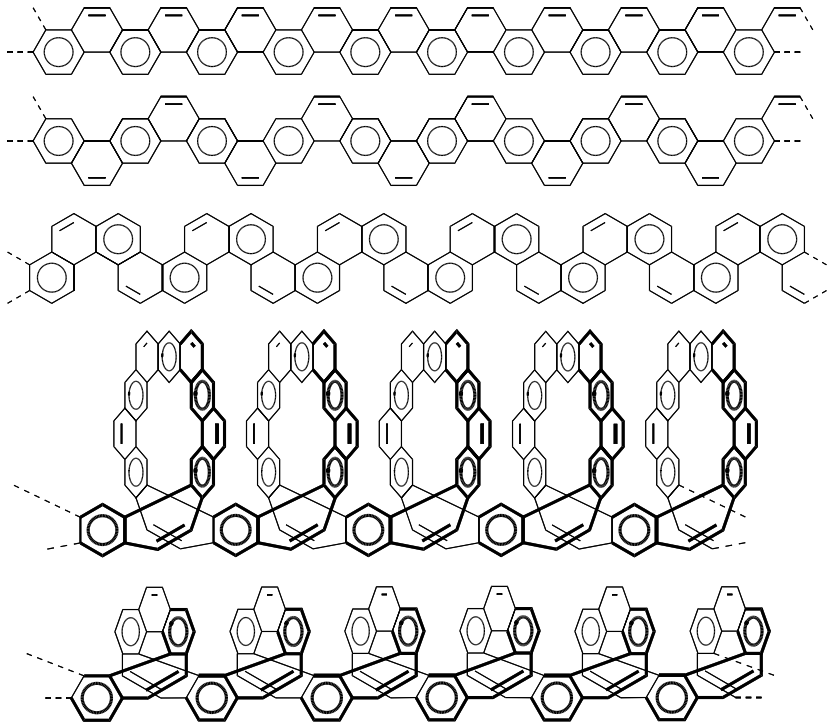

Fig 12. The five ribbons that are simple regularly vinylene-bridged poly-phenylenes, including polyphenacene (top) and polyhelicene (bottom). Note that in the top, middle and bottom polymers all six-membered rings are equivalent, whereas the second and fourth polymers lack such optimal resonance stabilisation.

Whereas properly zig-zag edged AO ribbons are fully olefinic, and can be seen sets of parallel polyacetylene chains that are extremely prone to oxidation to more sextetted quinones, strictly armchair-edged PO ribbons merit special interest because of their simple and symmetric structures as well as their sextet configurations that are analogous to zig-zag nanotubes in the fact that they fall into three classes of n=3p, n=3p+1 and n=3p+2 width, with n being the number of carbon rows parallel to the ribbon axis and p being an integer: The 3p series is fully sextetted, with only one maximally sextetted Clar structure (ie. benzenes linked by single bonds), and thus maximal bond fixation and maximal band gap (Fig. 13, centre). The 3p+2 series shows the most olefinic Clar structures and minimal bond fixation; all hexagons can be assigned a benzenic sextet in one of the several resonant maximally sextetted Clar structures, exemplified in figure 13 (top) for the thinnest representative, polyrylene (p=1, n=5). The 3p+1 series is of intermediate character between the other two, with more than one maximally sextetted Clar structure, but in which not all hexagons are sextetted (Fig. 13, bottom).

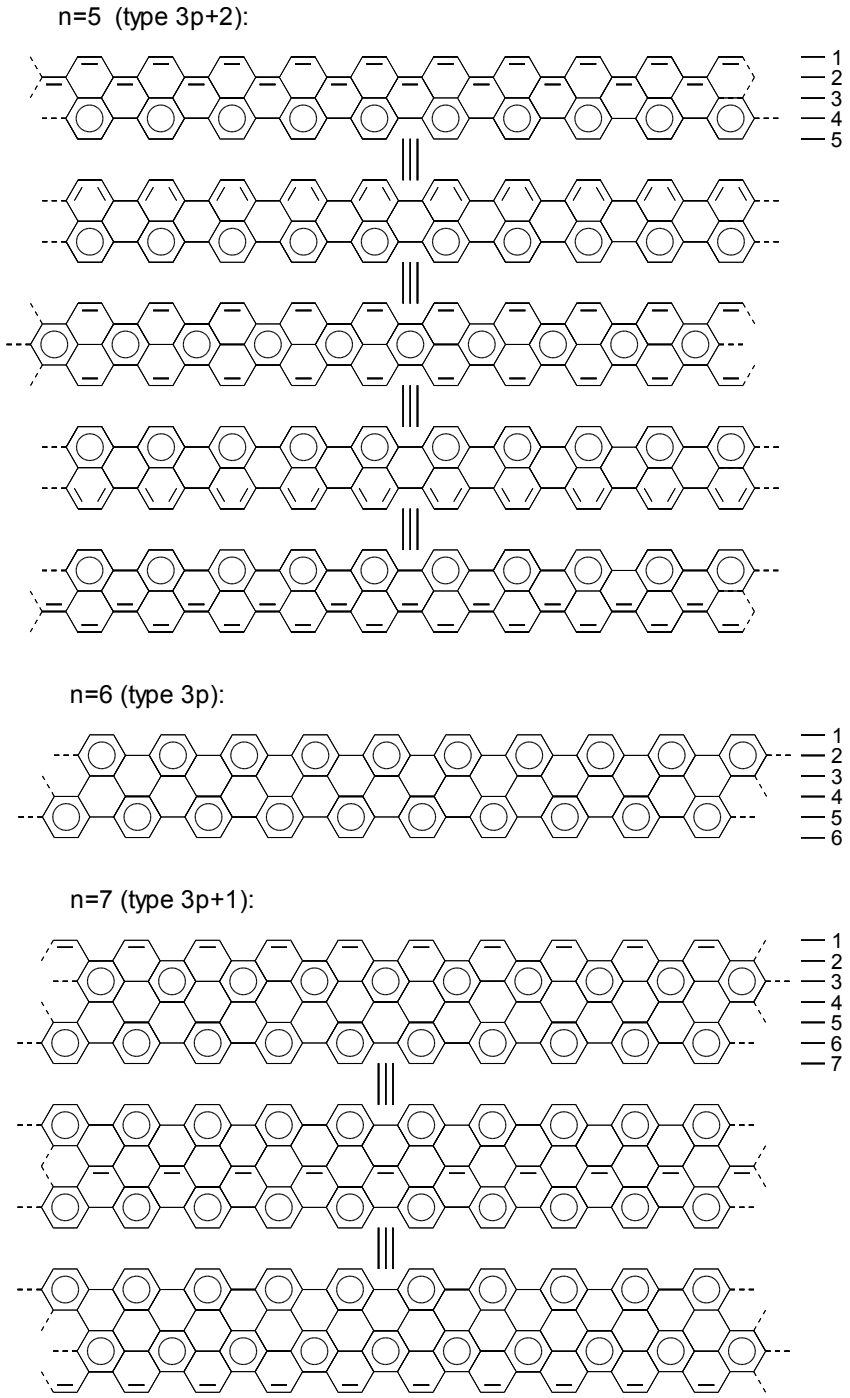

Fig 13. Sets of maximally sextetted Clar structures of the three thinnest peri-annellated armchair-edge PO ribbons. Note that all hexagons are sextetted in at least one resonance structure of n=5, whereas the two inner rows of hexagons in n=6 and the central row in n=7 are never sextetted.

This simple Clar structure analysis points to smallest band gaps in the 3p+2 series and largest band gaps in the 3p series, which is in partial agreement with first principle calculations[11] that predict considerably smaller band gaps for the 3p+2 series, starting with 0.4eV for n=5 (polyrylene), the thinnest, largest-gap representative. The two other series start with much larger values: The 3p+1

series starts with 2.5 eV for n=4 (polyphenacene) followed by 1.6 eV for n=7 ("perbenzo-polyrylene"), and the 3p series starts with 1.7 eV for n=3 (poly-*p*-phenylene, not quite a ribbon, but presumably calculated in fully coplanar configuration) followed by 1.0 eV for n=6 ("perbenzo-polyphenacene"). The limits of our simple Clar analysis are illustrated by it not accounting for the fact that according to first principle calculations the 3p series has smaller band gaps at similar ribbon width than the 3p+1 series. It is notable that simple tight-binding calculations predict very similar band gaps at similar width for the two latter series, and metallic character (no band gap) for all 3p+2 ribbons including polyrylene[11] (fig. 14).

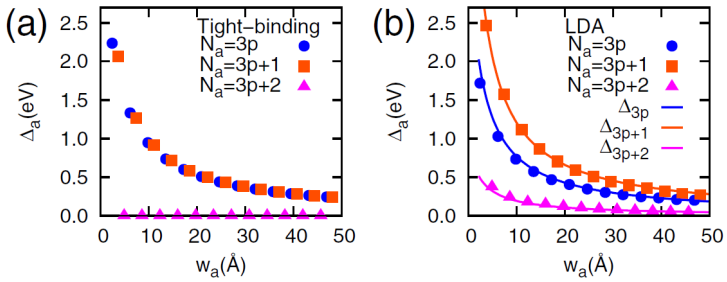

Fig 14. Variation of band gaps in armchair-edge PO ribbons as function of width w_a obtained (a) from tight binding calculations and (b) first-principle calculations (reproduced from ref. 11).

1.4. Graphene nanoribbons from carbon nanotubes

Nanoribbons of relatively controlled width have been obtained recently from CNTs.[12, 13] Ribbon-shaped fragments have also been obtained from graphene by chemical attack, but the the control of shape (width, edge geometry) is poor in that case.[14, 15, 16, 17] A method that uses a geometrically better related precursor than graphene is the unzipping of CNTs, either by strong oxidants[18] or by slicing open nanotubes partially embedded in, and protected by, a polymer matrix with an argon plasma.[17]

In the strong oxidant approach ,[18, 19] a suspension of MWCNTs in sulfuric acid is treated with potassium permanganate under heating. The GNRs obtained are well soluble in polar solvents due to a multitude of carboxylic acid and ketone edge groups introduced by the procedure. It may be presumed that in a first step a double bond on the nanotube is opened into a diketone, which creates sterical strain on neighbouring bonds and thus transforms these into preferred sites for further attack, which again fragilises the environment, leading eventually to a clean slicing of the tube in longitudinal direction. The nanoribbons obtained display uniform widths herited from the parent nanotubes, predominantly straight edges and, of course, oxidised defects, which makes them electronically much less homogeneous than graphene sheets.

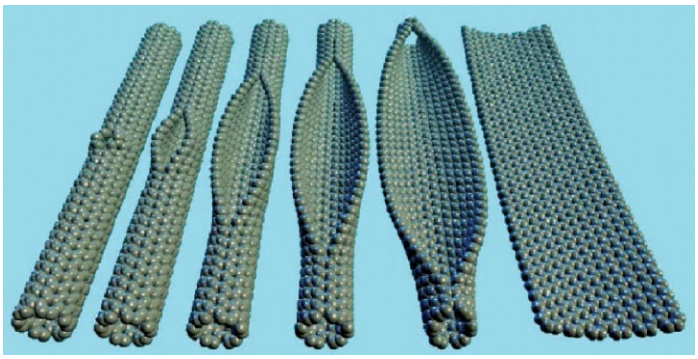

Fig. 15. Unzipping of a carbon nanotube by oxidative self-perpetuating attack. Reproduced from (reproduced from ref. 12).

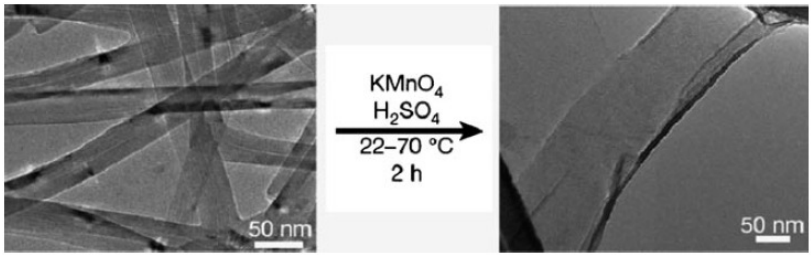

Fig. 16. Transmission electron microscopy (TEM) images of MWCNTs before and after unzipping oxidation into an oxidised GNR (reproduced from ref. 12).

In the embedded plasma etching approach,[17] MWCNTs are embedded in a poly(methyl methacrylate) (PMMA) layer, and then the polymer layer is thinned by plasma etching until the uppermost rim of the nanotube is etched away, opening the outermost wall of the MWCNT. Etching may be continued for various periods, allowing to obtain single-, bi- and multilayer GNRs. The remaining PMMA film with embedded GNRs may then be contact deposited on a solid substrate and the polymer removed with solvent vapour (Figure 17).

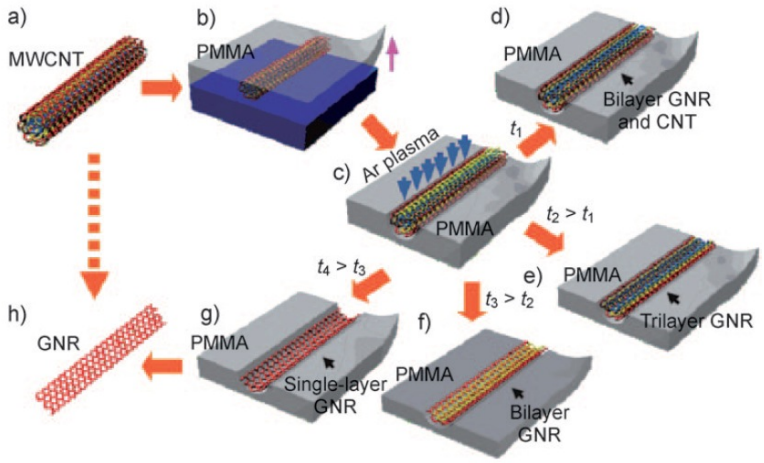

Fig. 17. GNRs by Ar plasma etching of a polymer matrix with embedded MWCNTs (reproduced from ref. 12).

The edges of these ribbons produced by matrix etching are very smooth, and, as before, their widths (of the order of 10nm) are quite uniform as consequence of the uniformity of the CNTs used. Field effect transistors made with these ribbons showed charge carrier mobilities only one order of magnitude smaller than those observed with large graphene sheets.

1.5. Synthetic approaches to graphene nanoribbons

Whilst the CNT unzipping approach to GNRs is relatively new, ribbon-type fully condensed aromatic oligomers and polymers have been a target of synthetic efforts for several decades.[20, 21]

Not fully unsaturated, but fully planarised poly-para-phenylenes where the phenylene units are bridged by side-chain-bearing methylene units, termed ladder polymers, where obtained by modification of acyl-substituted nonbridged polyphenylenes of considerable length (about 150 phenylene units).

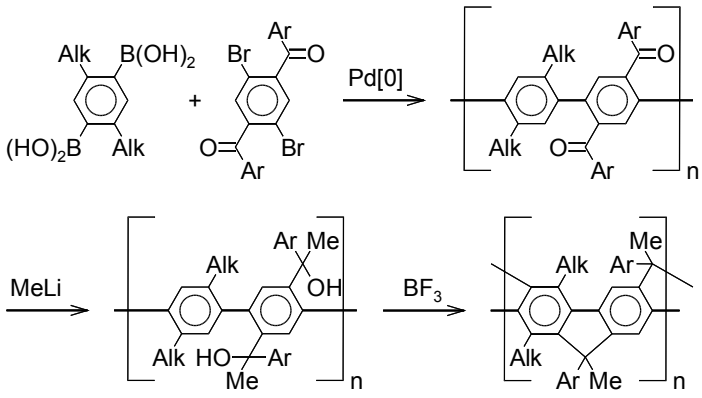

Fig 18. Methylene-bridged polyphenylenes from nonbridged precursors.[20]

Acenes quickly become highly unstable towards oxygen with increasing length, and already the greenish-black heptacene (ie. [7]acene) is too unstable to be obtained in pure form.[22] In contrast, phenacenes up to fulminene (ie. [6]phenacene) are stable enough to be present in coal tar, and alkyl-chain substituted derivatives of longer phenacenes up to [11]phenacene have been obtained by photocyclisation of stilbene-type precursors.[23, 24] Solubilities drop quickly with increasing length, and unsubstituted [7]phenacene is extremely insoluble. By the same photocyclisation approach, helicenes (which do not need solubilising substituents to be characterised due to their much better solubilities) have been obtained up to [14]helicene.[25, 26]

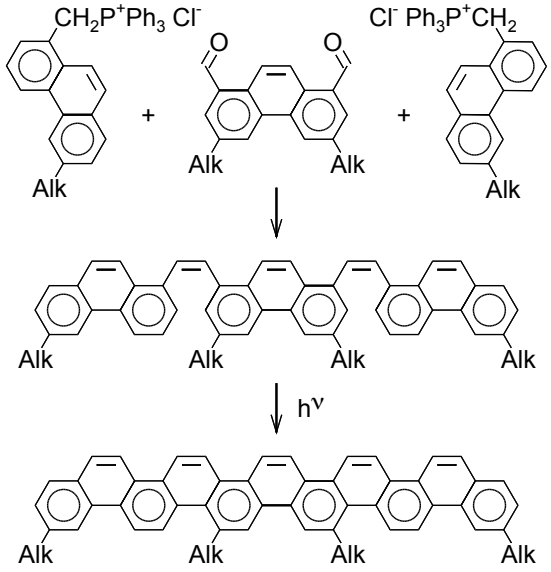

Fig. 19. Photosynthesis of a [11]phenacene with solubilising alkyl chains.[23]

Soluble alkoxyphenyl-substituted "isophenacene" polymers (ie. derivatives of the second polymer in figure 12) where obtained in the nineties by vinylene bridging of suitably substituted poly-para-phenylenes, either via McMurry-type coupling of two acyl substituents[27, 28] or via acid-promoted isomerisation of alkynyl substituents.[29] The former ribbons were obtained with lengths of about 25 phenylene units, the latter ribbons were about 50 phenylene units long.

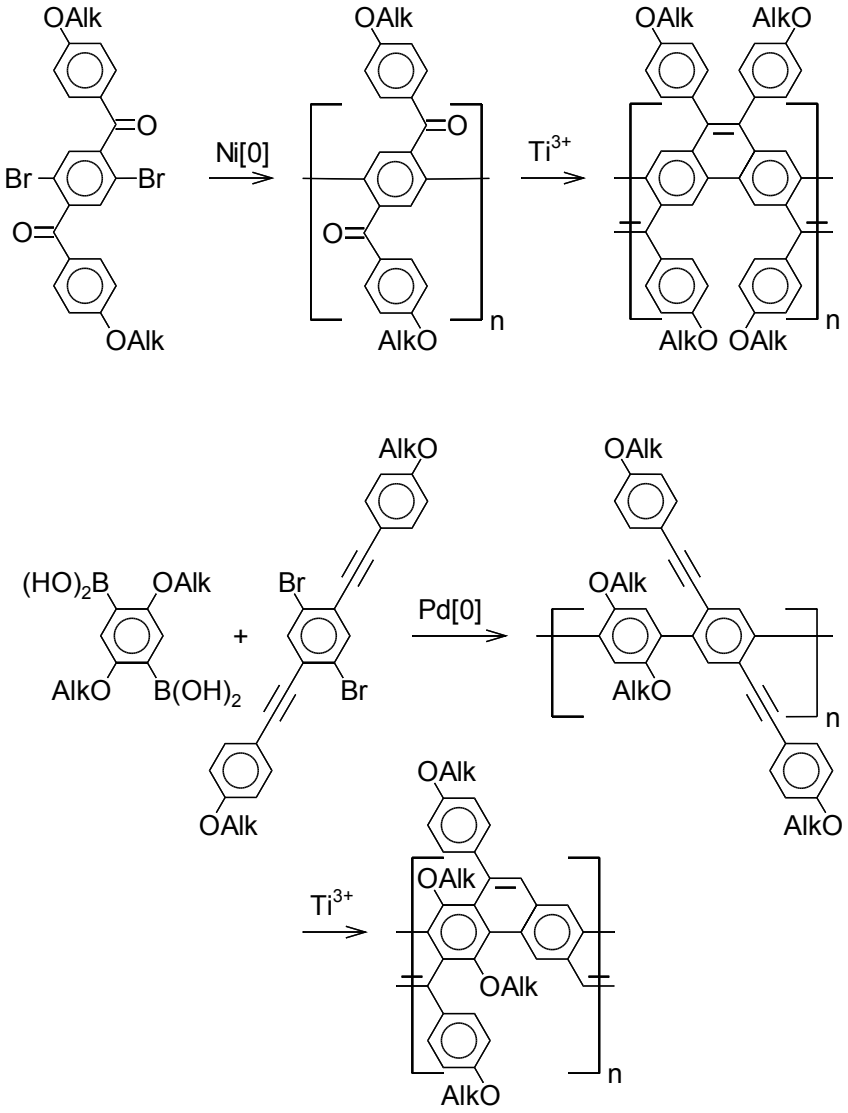

Fig. 20. Poly-isophenacenes by bridging of poly-para-phenylenes.[20]

Fully condensed aromatic ribbon polymers that are not truly graphene ribbons because they include five-membered rings have been obtained by Diels-Alder cycloaddition between a bis-furan as bis-diene and a bis-pyracycleno-anthracene as dienophile, with a length of about 20 pyracyclenoanthracene subunits and a band gap of 2.1 eV.[30]

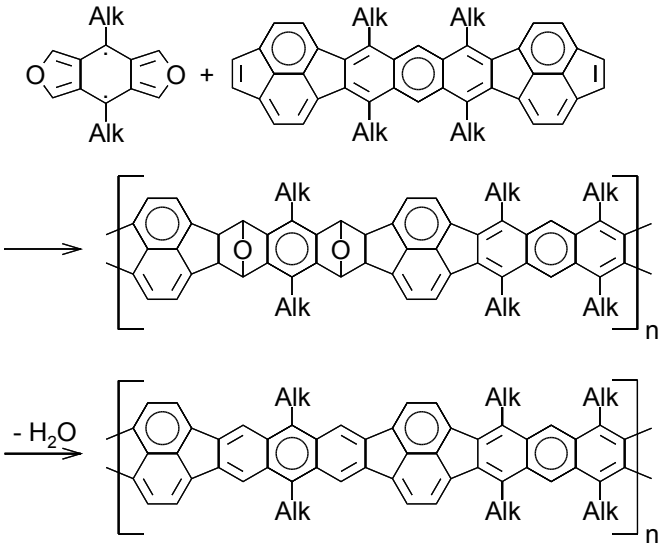

Fig. 21. Pyracycleno-anthracene based ribbons by Diels-Alder reaction.[30]

Rylenes with lateral solubilising alkylaryloxy substituents and terminal imide groups have been synthesised up to hexarylene,[31] and this series shows a rapidly decreasing band gap that drops from about 2.0 eV for perylenediimides to about 1.1 eV for hexarylenediimides whose absorption maximum consequently is in the near infrared. These diimides are reported to be of good chemical and photo-stability.

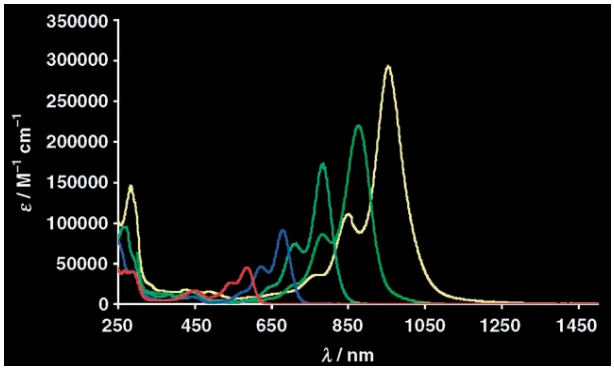

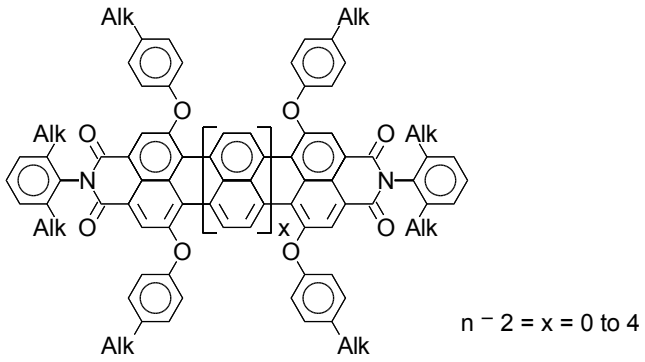

Fig. 22. Absorption spectra of tetraphenoxy-substituted [n]rylenediimides (n = 2 to 6) in chloroform solution (reproduced from ref. 31).

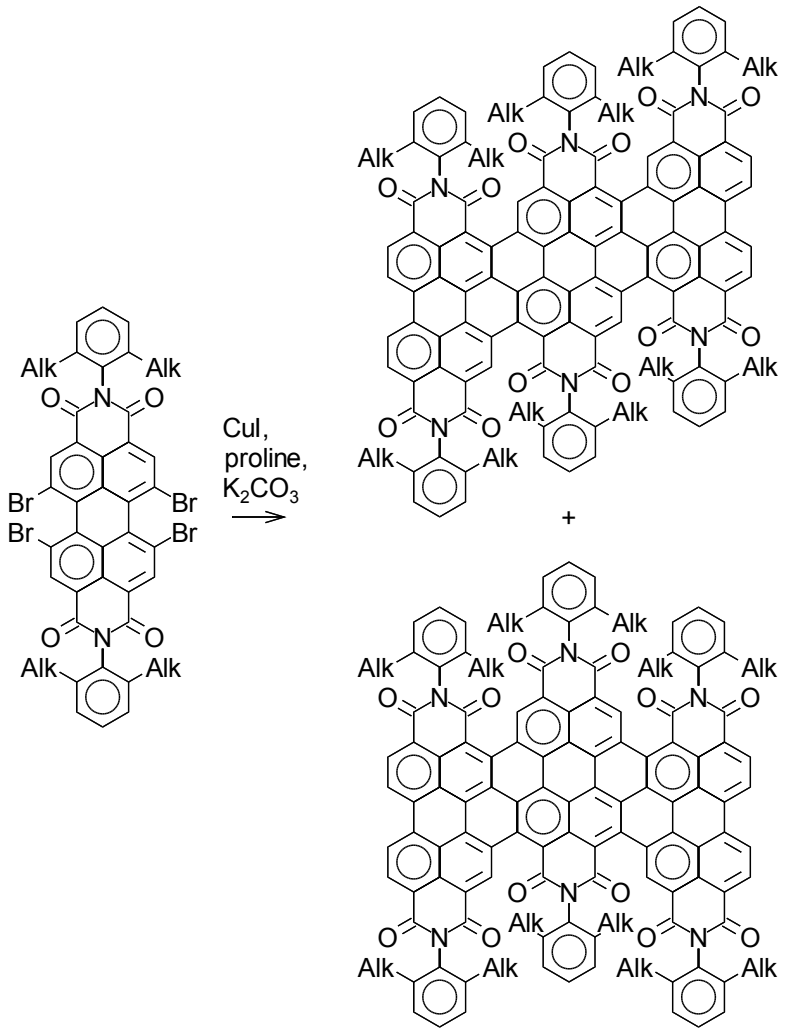

Fig. 23. Lateral perylenediimide trimers by CuI-mediated coupling.[33]

Another perylenediimide-based approach towards ribbons is the copper iodide promoted coupling of bay-region halogenated perylenediimides, by which so far dimers and trimers have been isolated.[32, 33] The green trimers form as two HPLC-separable isomers, whose arene cores are twisted out of planarity due to the bulky substituents.

Fully benzenoid armchair-edge PO ribbons of tetracene width with solubilising alkyl substituents have been obtained by highly parallel Scholl cyclisations with ferric chloride of polyphenylene precursors with a length of around 20 phenylene units.[34] Similar ribbons but with some benzene units missing to give a benzannellated poly-isophenacene structure have been obtained by the same approach with a length of around 40 phenylene units.[35]

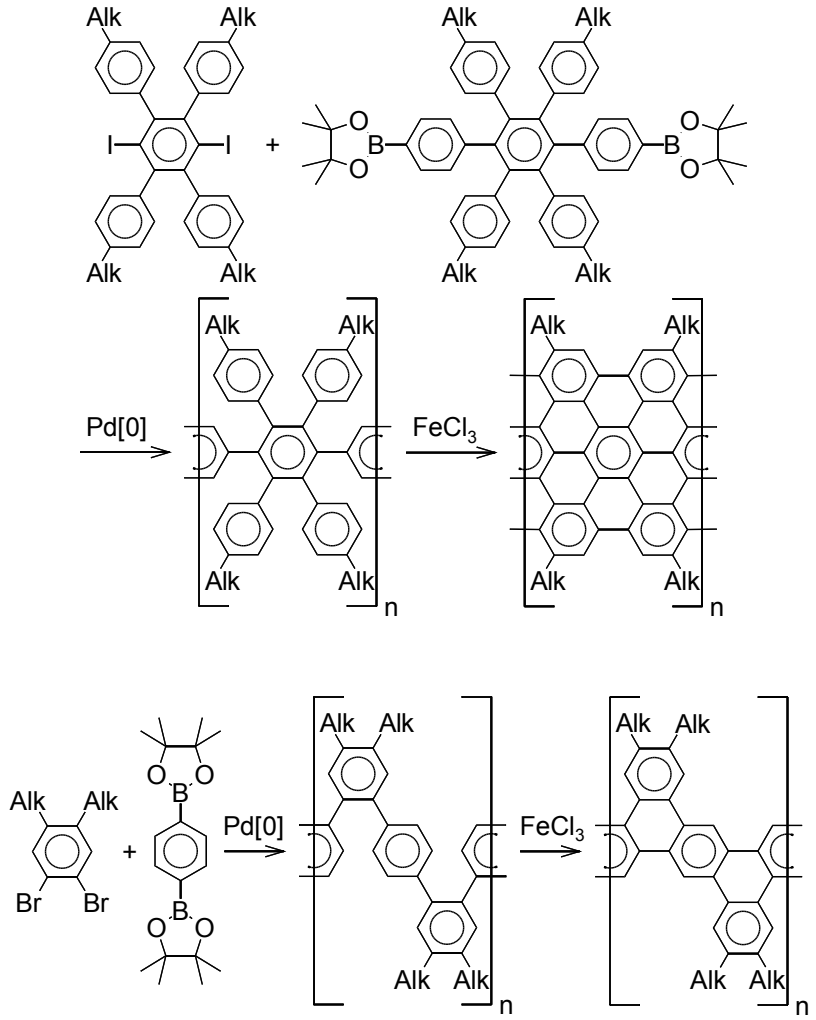

Fig. 24. Fully benzenoid ribbons by cyclodehydrogenation with $FeCl_3$.[33, 35]

Extended straight and chevron-type PO GNRs without solubilising substituents have been obtained by the dehydrogenation of polyanthrylene and polyphenylene precursors on gold surfaces at 400 to 440°C and observed by STM.[36]

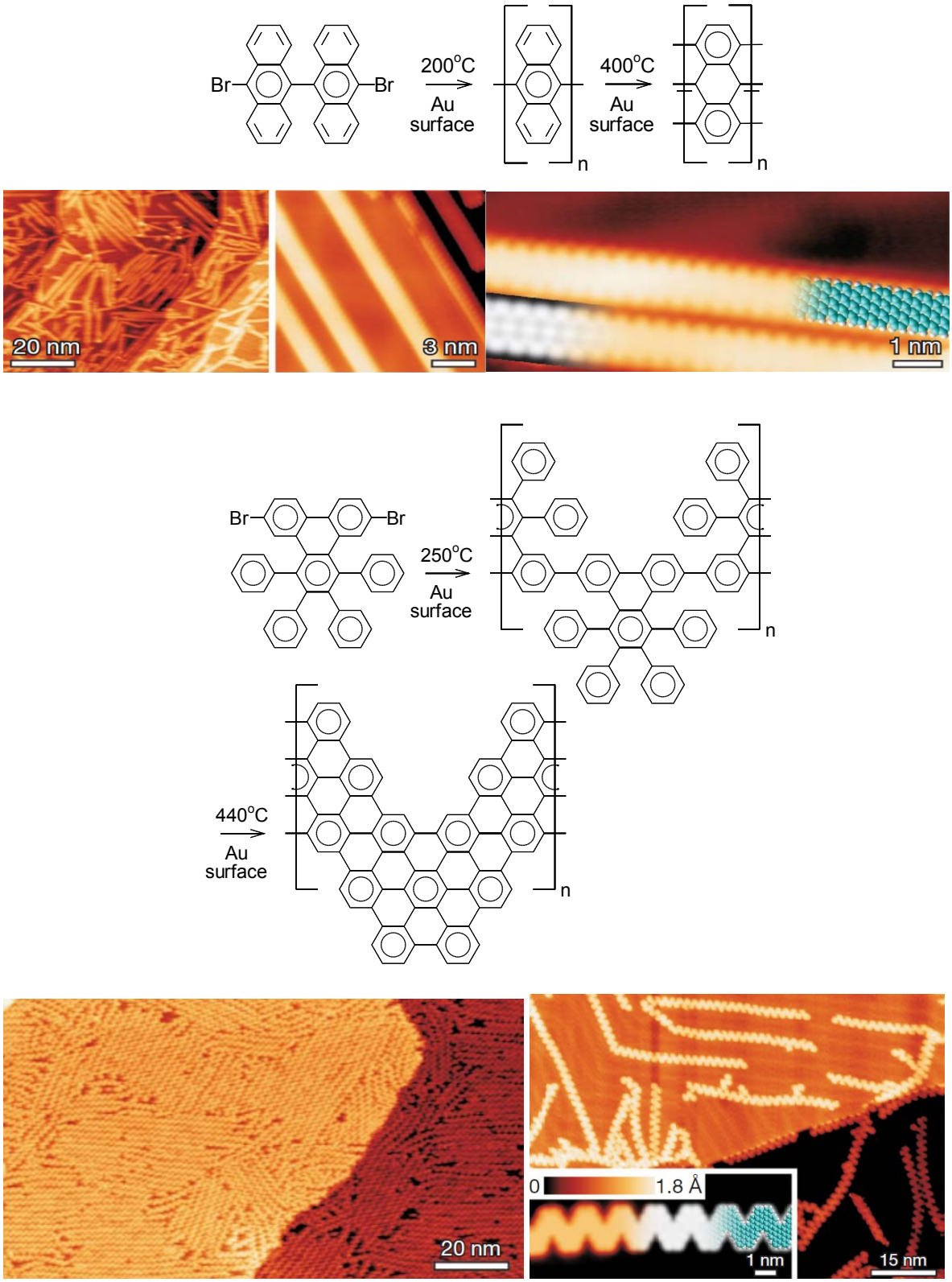

Fig. 25. Surface-assisted formation of unsubstituted nanoribbons (STM images with partial overlays of molecular models) (reprod. from ref. 36).

1.6. Heteronanoribbons

Doping of GNRs and CNTs with heteroatoms such as boron or nitrogen should lead to p- or n-doped (i.e. excess hole or electron possessing) conjugated π electron structures.

Not only theoretical studies,[37, 38, 39] but also a successful synthetic approach to N-doped graphene by chemical vapour deposition,[40] have recently established the existence of structurally different types of nitrogen atoms in N-doped graphene, which may be termed graphitic, pyridinic and pyrrolic (fig 26).

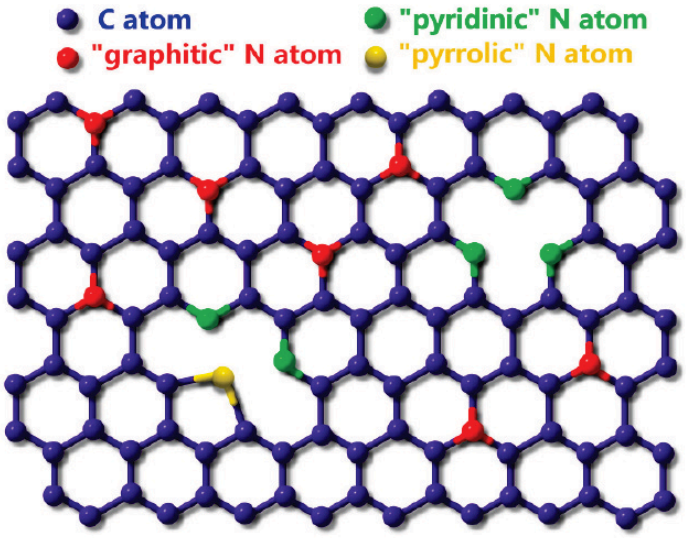

Fig. 26. Schematic representation of the N-doped graphene. Blue, red, green, and yellow spheres represent the C, "graphitic" N, "pyridinic" N, and "pyrrolic" N atoms in the N-doped graphene, respectively (reproduced from ref. 40).

Synthetic "bottom-up" approaches towards heterographene sheets and ribbons are scarce. Early efforts in the 1960s led to poly-heteroacenes with nitrogen, oxygen and sulphur heteroatoms, that in contrast to homoaromatic polyacene are stabilised by benzenic sextets arising from the altered distribution of double bonds that is a consequence of the incorporation of single-bonded heteroatom sites. Most of these poly-heteroacenes lacked solubilising substituents allowing full characterisation, but a few poly-azaacenes with solubilising side groups were obtained as well (fig. 27).[20]

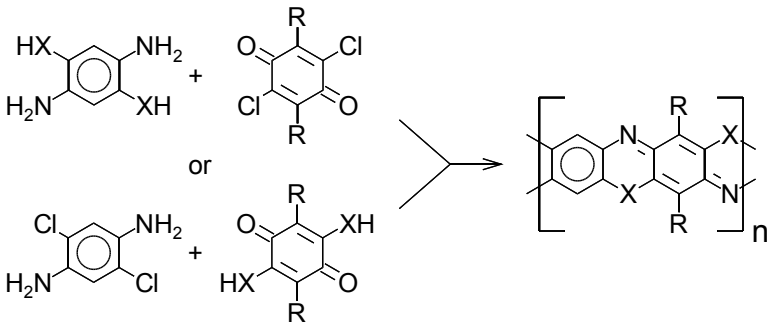

Fig. 27. Synthetic approach to poly-heteroacenes with single-bonded NR, O and S sites,[20] X = NH, O or S; R = H or solubilising substituent.

Limited evidence for the formation of holey graphene sheet structures of composition $(C_3N_4)_n$ has been obtained upon high temperature treatment of *s*-triazine derivatives (fig. 28).[41, 42]

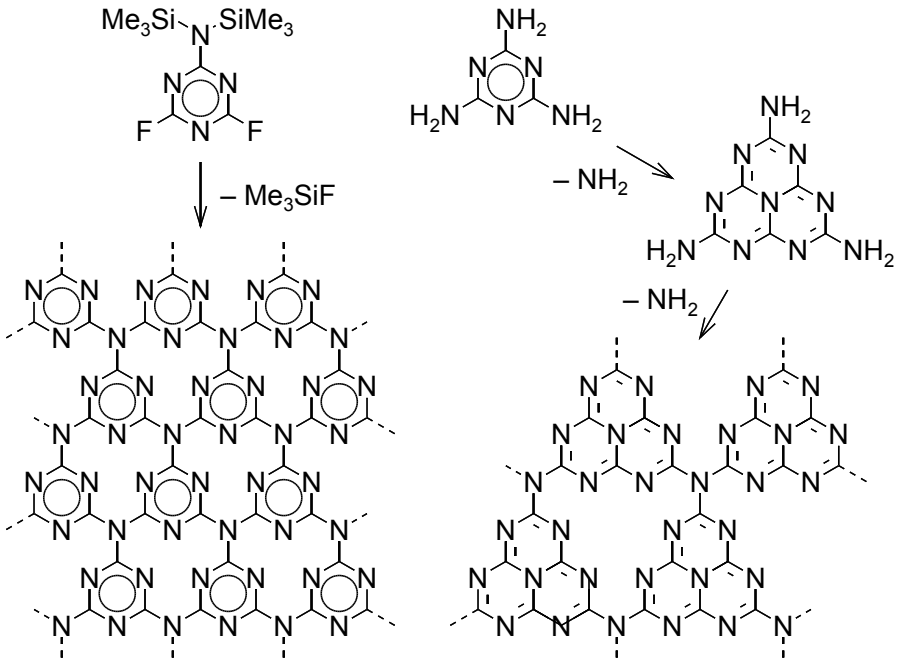

Fig. 28. Assumed formation of carbon nitride sheets of composition $(C_3N_4)_n$ from triazine precursors.[41, 42]

1.7. Heteronanoribbons with metal atom chelating periphery and carboxysubstituted nanoribbons with removable donor/acceptor-tuning substituents as perspectives

Whilst the elaboration of new approaches to novel aromatic ribbon-type structures appears from the foregoing in itself to be a research target of high actuality, two structural aspects of such nanoribbons had particular appeal to us at the outset of this work:

First, even though rare examples of heteronanoribbons have been obtained already, no such structures with metal ligating rim sites have been reported. Ribbons able to complexate transition metal atoms should open an entire new field of conjugated materials with novel electronic and magnetic properties. Simple polycyclic arenes with two chelation sites on opposite sides of the molecule exist and conceptionally constitute thus monomeric analogues of polyligating nanoribbons. One simple example amongst others is the eilatin/isoeilatin/dibenzoeilatin family of tetraazaperylene derivatives, that has been shown to yield both mono- and dinuclear complexes with transition metals (fig. 29).[40, 41, 42]

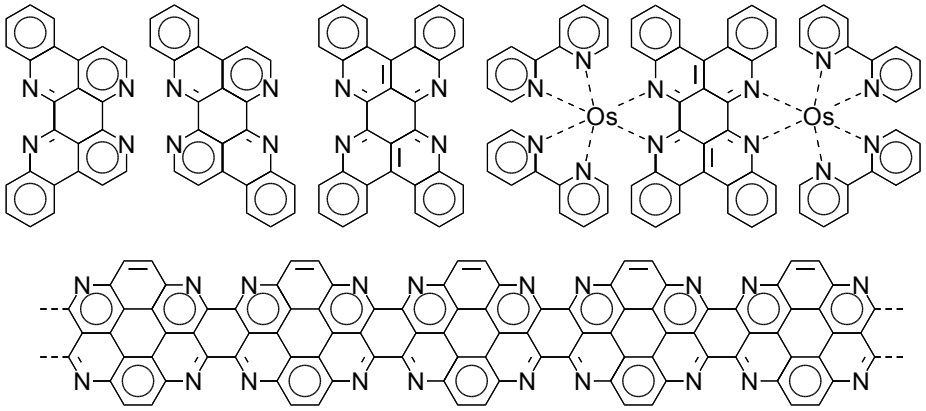

Fig. 29. eilatin, isoeilatin, dibenzoeilatin and a dinuclear complex of the latter,[41] together with a hypothetical example of a structurally related polymeric ribbon.

Second, it transpires from the various existing examples of fully condensed conjugated polymers that

1. Any bulk synthetic approach has to incorporate flexible side groups within the monomer units to avoid serious problems with reactivity and characterisability caused by low solubility.
2. As side-group-free nanoribbons nevertheless constitute a particularly neat and fundamentally most interesting target, it would be of great convenience to have solubilising side groups that could be eliminated after the completion of the ribbon build-up.
3. In view of electronic applications, side groups that allow easy modification of their electron

donating/withdrawing effect without destroying their solubilising character would be of great utility.

A class of side groups that in principle satisfy these three criteria are carboxylic substituents such as alkyl esters and alkyl imides:

1. The alkyl chain length and bulkiness can easily be adjusted via hydrolysis to the carboxylic acid and reesterification/reimidification.
2. Decarboxylation to eliminate $–CO_2H$ substituents after hydrolysis is a well established and controlled procedure for the access to unsubstituted parent systems.[4(a)]
3. Replacement of vicinal diester moieties by imide groups via ester hydrolysis has been shown by our group to be a powerful means of changing the donor/acceptor character of condensed aromatic systems. [43, 44]
4. Ester hydrolysis to carboxylic acids gives access to systems with pH-modulable solubility and electron density.

The following chapters describe our attempts to establish the bases for new synthetic approaches to ribbons with multiple chelation sites and to multiply carboxy-substituted ribbons.

1.8. References

[1] H. W. Kroto, J. R. Heath, S. C. O'Brien, R. F. Curl and R. E. Smalley, Nature, 318, 162, 1985.

[2] S. Iijima, Nature, 354, 56, 1991.

[3] Chapter 1. Carbon Nanotubes," in *RSC Nanoscience & Nanotechnology*, 2nd ed., vol. 0, Cambridge: Royal Society of Chemistry, pp. 1–242.

[4] *(a) Clar, E. Polycyclic Hydrocarbons; Academic Press: New York, 1964; Vol. I/II. (b) Clar, E. The Aromatic Sextet; Wiley-VCH: London, 1972. (c) Scholl, R.; Seer, C.; Weitzenböck, R. Chem. Ber. 43, 2202, 1910. (d) Scholl, R.; Seer, C. Liebigs Ann. Chem, 394, 111, 1912. (e) Scholl, R.; Seer, C. Chem. Ber, 55, 330, 1922. (f) Clar, E.; Stewart, D. G. J. Am. Chem. Soc., 75, 2667 1953. (g) Clar, E.; Schmidt, W. Tetrahedron, 35, 2673. 1979.*

[5] M. Terrones, A. Jorio, M. Endo, A. M. Rao, Y. A. Kim, T. Hayashi, H. Terrones, J.-C. Charlier, G. Dresselhaus and M. S. Dresselhaus, Mater. Today, 30, 2004.

[6] S. Niyogi, M. A. Hamon, H. Hu, B. Zhao, P. Bhowmik, R. Sen, M. E. Itkis and R. C. Haddon, Acc. Chem. Res., 35, 1105, 2002.

[7] C. K. Chiang, C. R. Fincher, Y. W. Park, A. J. Heeger, H. Shirakawa, E. J. Louis, S. C. Gau, A. G. MacDiarmid. Phys. Rev. Lett. 39, 1098–1101, 1977.

[8] Y.-J. Cheng, S.-H. Yang, and C.-S. Hsu; *Chemical Reviews*, vol. 109, no. 11, pp. 5868–5923, Nov. 2009.

[9] M. Kertesz, C. H. Choi, and S. Yang; *Chemical Reviews*, vol. 105, no. 10, pp. 3448–3481, Oct. 2005.

[10] R. D. McCullough, *Advanced Materials*, vol. 10, no. 2, pp. 93–116, Jan. 1998.

[11] Y.-W. Son, M. L. Cohen, and S. G. Louie; *Physical Review Letters*, vol. 97, no. 21, Nov. 2006.

[12] A. Hirsch, *Angewandte Chemie International Edition*, vol. 48, no. 36, pp. 6594–6596, Aug. 2009.

[13] M. Terrones, *ACS Nano*, vol. 4, no. 4, pp. 1775–1781, Apr. 2010.

[14] S. S. Datta, D. R. Strachan, S. M. Khamis, and A. T. C. Johnson, *Nano Lett.*, vol. 8, no. 7, pp. 1912–1915, 2008.

[15] L. Ci, Z. Xu, L. Wang, W. Gao, F. Ding, K. F. Kelly, B. I. Yakobson, and P. M. Ajayan; *Nano Research*, vol. 1, no. 2, pp. 116–122, Jul. 2008.

[16] X. L. Li, X. Wang, L. Zhang, S. Lee, H. Dai, Science, 319, 1229, 2008.

[17] L. Jiao, L. Zhang, X. Wang, G. Diankov, H. Dai, Nature, 458, 877, 2009.

[18] D. V. Kosynkin, A. L. Higginbotham, A. Sinitskii, J. R. Lomeda, A. Dimiev, B. K. Price, J. M. Tour, Nature, 458, 872, 2009.

[19] Higginbotham, A. L.; Kosynkin, D. V.; Sinitskii, A.; Sun, Z.; Tour, J. M. , ACS Nano, 4, 2059– 2069, 2010.

[20] U. Scherf, *Journal of Materials Chemistry*, vol. 9, no. 9, pp. 1853–1864, 1999.

[21] A. C. Grimsdale and K. Müllen, *Macromolecular Rapid Communications*, vol. 28, no. 17, pp. 1676–1702, Sep. 2007.

[22] E. Clar, Polycyclic Hydrocarbons, Academic Press & Springer Verlag 1964.

[23] F. B. Mallory, K. E. Butler, A. C. Evans, E. J. Brondyke, C. W. Mallory, C. Yang, and A. Ellenstein, *Journal of the American Chemical Society*, vol. 119, no. 9, pp. 2119–2124, Mar. 1997.

[24] F. B. Mallory, K. E. Butler, A. C. Evans, and C. W. Mallory, *Tetrahedron Letters*, vol. 37, no. 40, pp. 7173–7176, Sep. 1996.

[25] Y. Shen and C.-F. Chen, *Chemical Reviews*, vol. 112, no. 3, pp. 1463–1535, Mar. 2012.

[26] R. H. Martin and M. Baes, *Tetrahedron*, vol. 31, no. 17, pp. 2135–2137, 1975.

[27] K. Chmil and U. Scherf, *Makromol. Chem., Rapid Commun.*, vol. 14, no. 4, pp. 217–222, 1993.

[28] K. Chmil and U. Scherf, *Acty Polymerica*, vol. 48, no. 5–6, pp. 208–211, 1997.

[29] M. B. Goldfinger and T. M. Swager; *Journal of the American Chemical Society*, vol. 116, no. 17, pp. 7895–7896, Aug. 1994.

[30] M. Löffler, A.-D. Schlüter, K. Gessler, W. Saenger, J.-M. Toussaint, and J.-L. Brédas, *Angewandte Chemie International Edition in English*, vol. 33, no. 21, pp. 2209–2212, Nov. 1994.

[31] N. G. Pschirer, C. Kohl, F. Nolde, J. Qu, and K. Müllen, *Angewandte Chemie International Edition*, vol. 45, no. 9, pp. 1401–1404, Feb. 2006.

[32] H. Qian, Z. Wang, W. Yue, and D. Zhu, *Journal of the American Chemical Society*, vol. 129, no. 35, pp. 10664–10665, Sep. 2007.

[33] H. Qian, F. Negri, C. Wang, and Z. Wang; *Journal of the American Chemical Society*, vol. 130, no. 52, pp. 17970–17976, Dec. 2008.

[34] X. Yang, X. Dou, A. Rouhanipour, L. Zhi, H. J. Räder, and K. Müllen; *Journal of the American Chemical Society*, vol. 130, no. 13, pp. 4216–4217, Apr. 2008.

[35] L. Dössel, L. Gherghel, X. Feng, and K. Müllen, *Angewandte Chemie International Edition*, vol. 50, no. 11, pp. 2540–2543, Mar. 2011.

[36] J. Cai, P. Ruffieux, R. Jaafar, M. Bieri, T. Braun, S. Blankenburg, M. Muoth, A. P. Seitsonen, M. Saleh, X. Feng, K. Müllen, and R. Fasel, *Nature*, vol. 466, no. 7305, pp. 470–473, Jul. 2010.

[37] Martins, T. B.; da Silva, A. J. R.; Miwa, R. H.; Fazzio, Nano Lett. 2008, 8, 2293–2298.

[38] Deifallah, M.; McMillan, P. F.; Cora, F. ; J. Phys. Chem. C, 112, 5447–5453, 2008.

[39] Y. Li, Z. Zhou, P. Shen, and Z. Chen, *ACS Nano*, vol. 3, no. 7, pp. 1952–1958, 2009.

[40] Wei, D.; Liu, Y.; Wang, Y.; Zhang, H.; Huang, L.; Yu, G.; Nano Lett., 9, 1752–1758, 2009.

[41] J. Kouvetakis, M. Todd, B. Wilkens, A. Bandari, and N. Cave, *Chemistry of Materials*, vol. 6, no. 6, pp. 811–814, Jun. 1994.

[42] B. Jürgens, E. Irran, J. Senker, P. Kroll, H. Müller, and W. Schnick; *Journal of the American Chemical Society*, vol. 125, no. 34, pp. 10288–10300, Aug. 2003.

[43] S. Alibert-Fouet, I. Seguy, J.-F. Bobo, P. Destruel, and H. Bock, ; *Chemistry - A European Journal*, vol. 13, no. 6, pp. 1746–1753, Feb. 2007.

[44] J. Kelber, H. Bock, O. Thiebaut, E. Grelet, and H. Langhals, *European Journal of Organic Chemistry*, vol. 2011, no. 4, pp. 707–712, Feb. 2011.

Chapter 2

The ceramidonine approach towards azaaromatic ribbons

The synthesis of extended heteroarenes via the acid-promoted dehydrocyclisation of arylamino-anthraquinones is examined as an approach to highly conjugated electron-acceptor materials and eventually to heterographene nanoribbons. Whilst the latter perspective is found to remain challenging, the former is exemplified by the synthesis of extended tetraazaheterocycles bearing solubilising alkyl substituents.

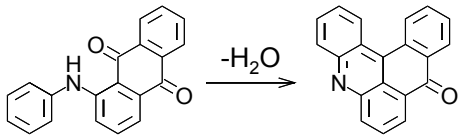

2 **1**

2.1. Bifunctional bricks for the build-up of conjugated systems with multiple ceramidonine fragments

Ceramidonine **1**, the heart-shaped cyclodehydration product of 1-phenylamino-anthraquinone **2**, is efficiently obtained by treatment of the latter in sulphuric acid at elevated temperature.[1, 2] We assumed thus that oligo- and polymers with multiple 1-arylaminoanthraquinone fragments are convenient precursors to extended polycyclic heteroarenes. Such extended azaheterocyclic nanoribbons should exhibit pronouncedly electron-deficient and thus electron-acceptor type electronic character that may be of interest for organic electronics. They also are more stable against oxidation than their homoaromatic counterparts, and may represent novel chelating ligands for transition metal complexation, if further aromatic nitrogens are introduced by the choice of appropriate azaarylamine precursors.

1-arylaminoanthraquinones are most conveniently obtained by a condensation of an aminoarene with a 1-substituted anthraquinone such as 1-bromo-or 1-triflyloxyanthraquinone. A ceramidonine-based approach to oligomers requires bifunctional diaminoarenes and dianthraquinone bricks with substituents on opposing sides. The most obvious choice of a diaminoarene brick that could lead to phenanthroline-type chelating sites is o-phenylenediamine, but its only moderate stability due to the high electron density in the doubly donor-substituted phenylene moiety make it a questionable choice

for harsh cyclisation reactions. As conveniently stable diaminoarenes with ring nitrogen atoms in vicinal positions to the amino groups for possible chelation, the 1,6- and 1,9-diaminophenazines **3** and **4** appear promising. They are accessible from phenazine via nitration under harsh conditions (fuming nitric and sulphuric acids at 100°C)[3] and separation of the two obtained dinitrophenazines by selective crystallisation.[4] As concerns bifunctional anthraquinones, the 1,4- and 1,5-dihydroxy derivatives are cheap and easily transformed into the corresponding triflates **5** and **6**.[5]

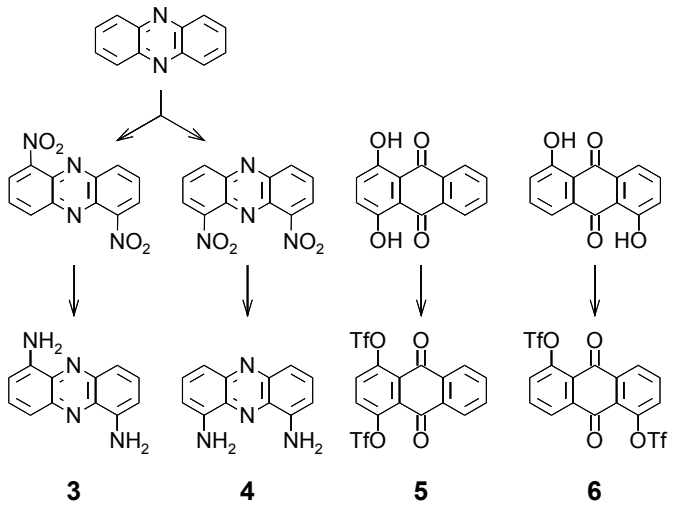

Replacement of the triflate leaving groups on **5** or **6** by the amino functions of **3** or **4** followed by loss of water leads to four hypothetical polymers; these ribbon-like polymers are linear in the cases **poly35**, **poly36** and **poly46**, and helicoidal in the case of **poly45** (a hexameric macrocycle can also be imagined). It may anecdotically be noted that, if the three linear ribbons are classified in analogy to carbon nanotubes[6, 7], all three different basic types of hexagon orientations (with respect to any perpendicular cut through the ribbon) are present: zigzag (**poly35**), oblique (**poly36**) and armchair (**poly46**).

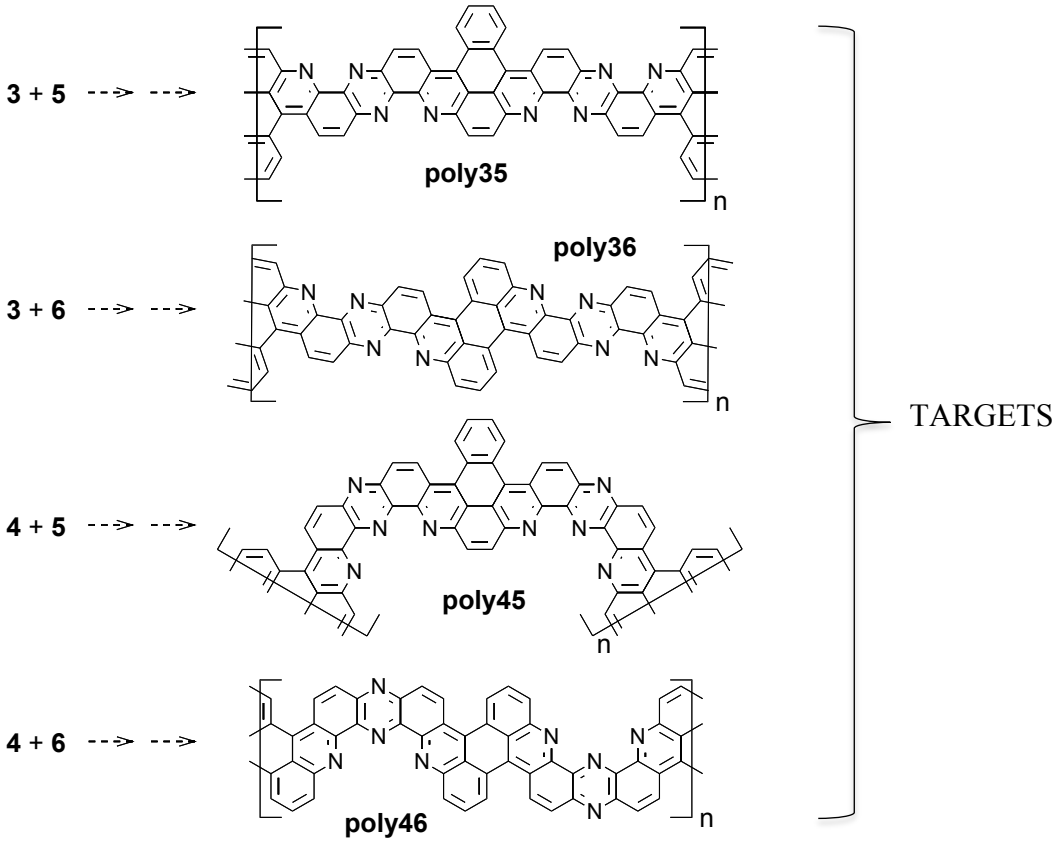

2.2. Monofunctional bricks with solubilising alkyl substituents

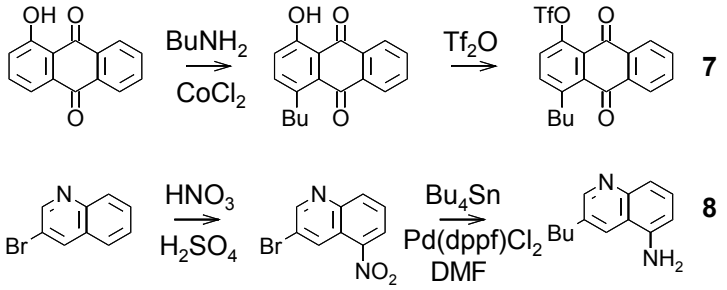

To obtain soluble ceramidonine dimers with these bifunctional bricks **3**-**6**, we aimed at condensing them with monofunctional counterparts bearing solubilising *n*-butyl chains, i.e. 4-butyl-1-triflyloxy-anthraquinone **7** and 3-butyl-5-aminoquinoline **8**. 4-butyl-1-hydroxy-anthraquinone is available by the atypical reaction of butylamine with 1-hydroxyanthraquinone in the presence of $CoCl_2$ reported by M. Matsuoka et al.,[8] and we aimed at obtaining **8** from 3-bromoquinoline via nitration, alkylation and reduction.[9, 10] To our surprise, when trying to obtain 3-butyl-5-nitroquinoline from 3-bromo-5-nitroquinoline with excess tetrabutyltin and catalytic $Pd(dppf)Cl_2$ [dppf = 1,1'-bis(diphenylphosphino)ferrocene] in DMF under argon, we isolated 3-butyl-5-aminoquinoline directly

in 39% yield. This points to DMF acting as reducing agent and hydrogen source, in concordance with the recently reported reduction of nitro substituents to amino groups during the palladium-catalysed coupling of nitro-substituted 2-haloanilines with alkynes to amino-substituted indoles in DMF.[11, 12]

Previous reports about the isomeric outcome of the mononitration of 3-bromoquinoline are ambiguous [9, 13], leaving some doubt about whether the main product is the 5- or the 8-nitro-derivative, both being poorly distinguishable by NMR. It was in this respect fortunate that we obtained single crystals of the derived amine **8** suitable for crystallographic structure determination, confirming that nitration predominately happens in position 5. In quinoline, dication formation in strong acid by benzene ring protonation following N protonation occurs fastest at C-8 and then relaxes to C-5, meaning that if nucleophilic substitution is kinetically controlled, it leads to 8-substituted quinolines, whilst 5-substituted ones are obtained under thermodynamic control.[14]

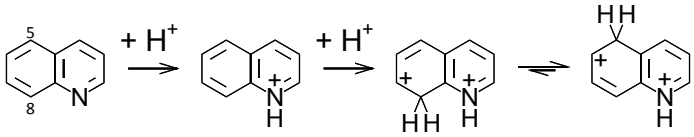

3-butyl-5-aminoquinoline crystallises in the trigonal *R-3* space group. Three molecules of the compound are arranged in a triangle held together by hydrogen bonds between one of the amino hydrogen atoms and the quinoline ring nitrogen of adjacent molecules (dotted lines in figure 1). The triangular units are arranged into a hexagonal geometry in the *ab* plane.

The four bifunctional and two monofunctional bricks **3**-**8** should yield the two quinones **737** and **747** and the two oxygen-free azaarenes **858** and **868** via their precursors **pre737**, **pre747**, **pre858** and **pre868**.

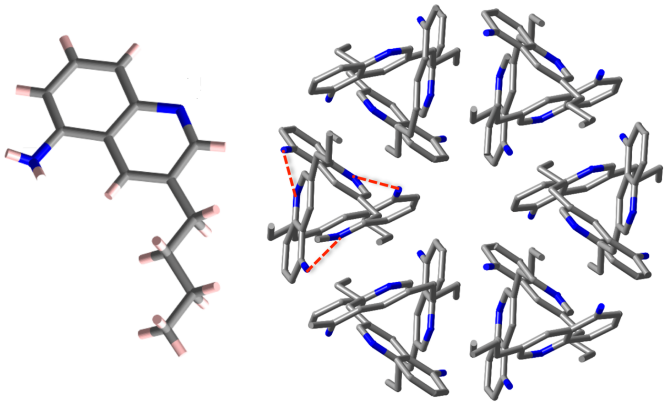

Fig. 1 Crystal structure of 3-butyl-5-aminoquinoline.

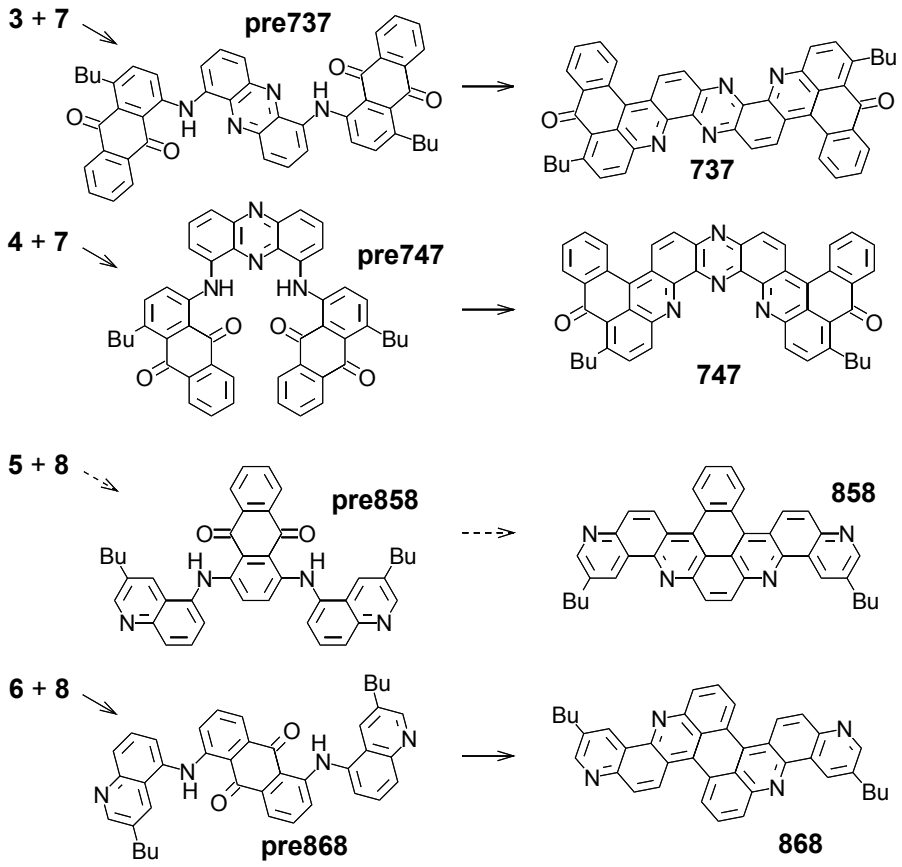

2.3. Condensations with mono- and bifunctional bricks

Before using dearly obtained **8** in condensation attempts with bifunctional anthraquinones **5** or **6**, we investigated the condensation of commercial aminoarenes with mono- and bifunctional anthraquinones **7**, **6** and **5**. The uncatalysed reaction of aryl triflates with aryl amines in the presence of base requires long reaction times and high temperatures or microwave irradiation. The copper mediated addition of amines to aryl triflates also requires harsh reaction conditions[15, 16] A more attractive option is the palladium catalysed triflate-amine coupling pioneered by Hartwig and co-workers: following their procedure, we achieved the coupling of singly triflate-subsituted anthraquinone **7** with 8-aminoquinoline as monofunctional aminoarene to give **9** first in moderate yields (25%) with a combination of catalytic $Pd(dba)_2$ [dba = dibenzylideneacetone] and dppf as chelating ligand in the presence of sodium *t*-butoxide as strong base.[17] The yields were significantly improved (57%) by addition of lithium chloride in order to deactivate the liberated triflate in the reaction medium which may poison the palladium catalyst, and slow addition of the triflate-subsituted anthraquinones to the reaction in order to prevent base catalysed dissociation to hydroxyanthraquinones. Cyclisation of quinolinylamino-butyl-anthraquinone **9** in 70% H_2SO_4 (10 ml) at 130^0 C for 8 min gave pyridino-ceramidonine **10** in about 50% yield. Having thus in hand a feasible method of condensation to obtain arylamino-substituted anthraquinones, we investigated the feasibility of double cyclisations in the

presence of solubilising alkyl chains, using the condensation products **11** (63% yield) and **13** (60% yield) of p-butylaniline with the bifunctional anthraquinones **6** and **5**. To our regret, whilst these bifunctional anthraquinones underwent condensation with a monofunctional aniline, all our many tries to couple o-phenylenediamine with monofunctional triflyloxyanthraquinone led only to untractable mixtures of dyes.

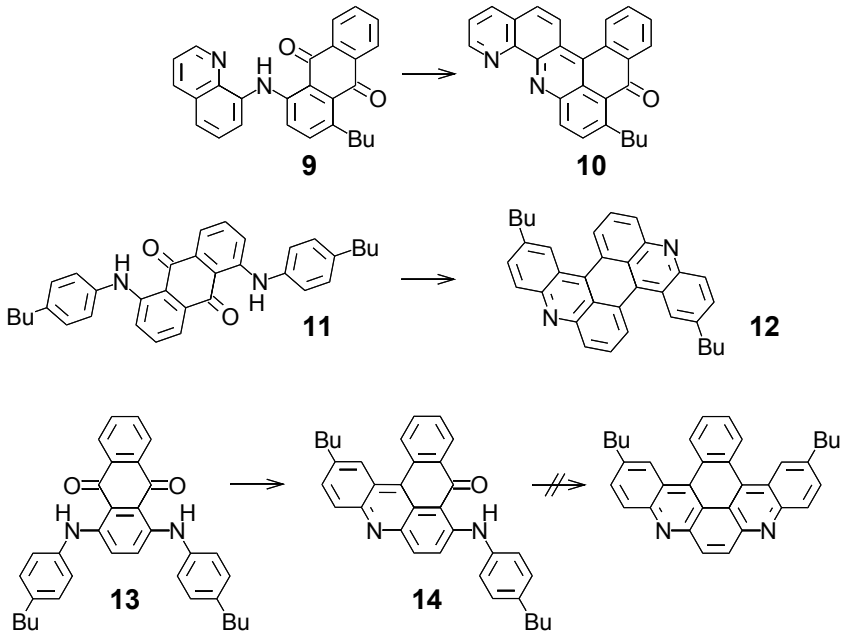

Whereas 1,5-bis(p-butylphenylamino)-anthraquinone **11** yielded the corresponding bisceramidonine **12** upon double dehydration in hot sulphuric acid, the 1,4-isomer **13** did only give, depending on the reaction time and temperature, either the monodehydrated intermediate **14** or tar; tar was also obtained when 70% sulphuric acid was replaced by concentrated sulphuric acid or polyphosphoric acid as dehydrating medium. This difference in outcome is puzzling. The expected double dehydration product from **13** may be formally considered as consisting of a benzene and a 5,8-diaza-pentaphene fragment linked by two single bonds, and 5,8-diaza-pentaphene has been reported to be exceedingly resistant to further oxidation even with CrO_3 in sulphuric acid.[18] Fragility of the double cyclisation product from **13** under the harsh reaction conditions therefore does not seem to be an evident explanation for our failure to isolate it.

We thus abandoned **5** as building block and did not attempt the synthesis of **pre858** and **858**. The three other cyclisation precursors **pre737**, **pre747** and **pre868** were obtained by our above-mentioned improved procedure with LiCl in 40%, 52% and 40% yield respectively. The three tetraazaarene targets **737**, **747** and **868** were obtained from their precursors by dehydration in 70% sulphuric acid at 170ºC in 53%, 41% and 64% as best yields, respectively. The yields proved to be strongly dependent

on the reaction time, short times giving incomplete cyclisations and long times giving substantial degradation. Optimised reaction times were 8 minutes for **737** and **747**, and 30 minutes for **868**.

2.4. Attempts to obtain bifunctional anthraquinone bricks with solubilising substituents

As the synthesis of oligomeric ceramidonines that are longer than dimers, such as tetramers or hexamers, clearly necessitates more than just two terminal solubilising alkl chains (it is known e.g. from the [n]phenacene series [19, 20] that the insolubility, i.e. the need for solubilising substituents, increases dramatically with increasing length of the arene systems), we also tried to incorporate side chains into bifunctional bricks. As the further functionalisation of arylenediamines appeared to us more cumbersome than the further functionalisation of dihydroxyanthraquinones, we aimed at the latter by transformations of anthrachrysone (1,3,5,7-tetrahydroxy-anthraquinone) **15**. In anthrachrysone, the two inner and the two outer hydroxyl groups are of different acidity and reactivity: Those in positions 1 and 5 are strongly hydrogen-bound to the adjacent carbonyls. So in a Williamson etherification, the hydroxyls in positions 3 and 7 can be selectively converted to alkoxy substituents if only two equivalents of etherification reagent are used. Anthrachrysone is prepared from 3,5-dihydroxybenzoic acid by dehydration in concentrated sulphuric acid at 130°C in 31% yield [21], doubly etherified with 2-ethylhexyl bromide to diether **16** in 43% yield and doubly triflated with triflic anhydride in pyridine in 90% yield to give the appropriately difunctionalised, doubly alkyl chain decorated, anthraquinone brick **17**, which we reacted under our optimised palladium coupling conditions with aniline to obtain the cyclisation precursor **18** in 80% yield. To our great dismay, all attempts to cyclise **18** to the expected doubly alkoxysubstituted diaza-dibenzoperylene **19** failed, as even at only 130°C in 70% sulphuric acid, **18** turns into intractable black tar within a few minutes.

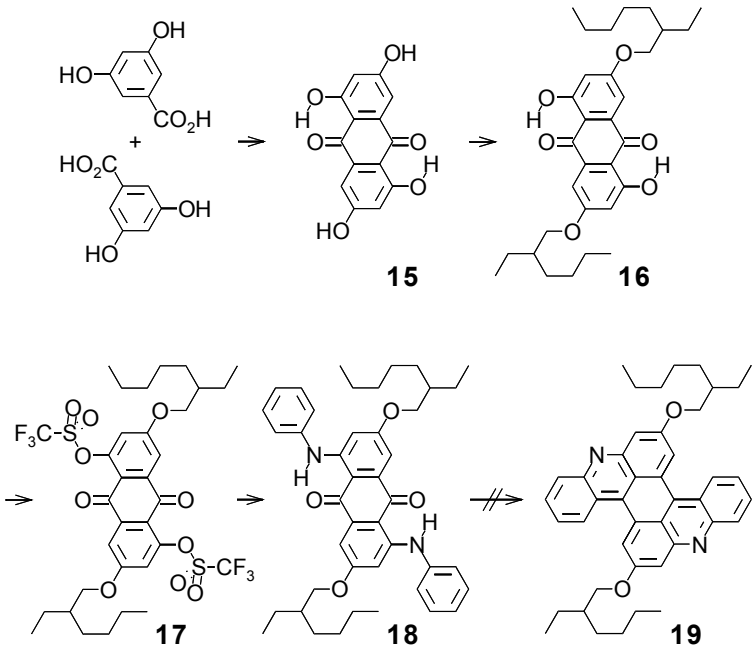

2.5. Perspectives

In view of these dismal results with solubilising ether substitutents on a bifunctional anthraquinone brick, considering that there is no evident efficient approach to similar alkyl instead of alkoxy functionalised central bricks, and, most of all, in view of the moderate yields accompanied by relatively fast decomposition under the necessary stringent reaction conditions leading to **737**, **747** and **868**, this synthetic approach appears practical only for the synthesis of relatively small extended azaarenes that may offer potential for a variety of applications such as electron acceptor behaviour in organic electronics or double metal chelation for metal-to-metal spin-spin interactions. To render this approach sufficiently efficient to lead to extended electron-deficient, potentially metal-chelating, heterographene nanoribbons such as **poly36** and **poly46**, considerable further innovative effort may be needed.

2.6. Electronical and structural characterisations

The absorption spectra (fig. 2) of the two tetraaza-diketones **737** and **747**, which both can be seen as doubly benzoylene-substituted tetraaza-naphthopentaphenes, show very similar, relatively unpronounced spectra typical of kata-annellated arenes with relatively continuous absorption up to about 500nm. In contrast, the tetraaza-dinaphthoperylene **868** exhibits the typical absorption features of a rylene, i.e. a gap zone of low absorption between a zone of intense short-wavelength absorption (below 350nm) and intense three-peaked long-wavelength absorption (between 450 and 560nm). [22]

To assess the electron-deficient character of the three materials, we tried to perform cyclic

voltammetry on all three, but the still limited solubility in dichloromethane of the two diketones impeded the obtention of meaningful curves.

Azahydrocarbon **868** on the other hand showed two clearly discernable reversible reduction peaks at –0.85V and –1.25V vs. ferrocene (inset in fig. 2). These values are closer than 0.1V to the values for C_{60}, a prominent prototype acceptor material in organic electronics, whose reduction peaks are found at –0.92V and –1.32V vs. ferrocene under identical conditions.[23] This indicates that multiple azasubstitution in moderately long-wavelength absorbing (i.e. moderately low band-gap) arenes such as benzannellated perylenes leads to pronouncedly electron-deficient azaarenes of suitable reduction potentials for organic electronic applications.

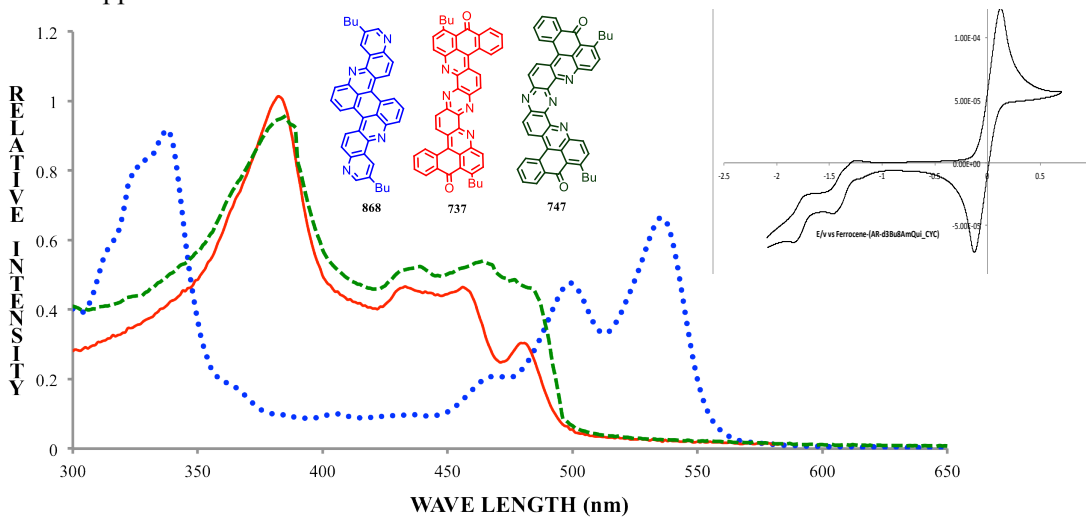

Fig. 2 Absorption spectra of **737** (red, continious), **747** (green, dashed) and **868** (blue, dotted) in chloroform. Inset: Cyclic voltammogram against ferrocene of **868** in 1mM solution in dichloromethane in the presence of 0.1M tetrabutylammonium hexafluorophosphate (scan rate: 100mV/s).

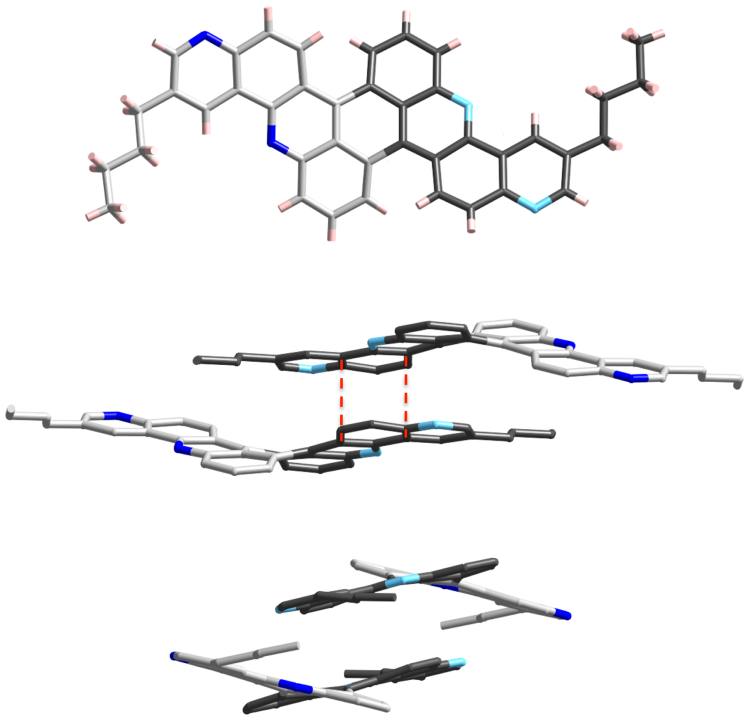

Fig. 3 Crystal structure of nonacyclic dialkyl-tetraazaarene **868**.

We were able to obtain single crystals of **868**, which allowed us to assess the degree of non-planarity forced upon the arene system by the two [4]helicenic bay regions (fig. 3). **868** crystallises in the centrosymmetric triclinic space group *P-1*, with two molecules per unit cell that are closely stacked by π-π interactions with shortest carbon-carbon distances of 3.44 Å (dashed lines in fig. 3). The planes of the two diazatetraphene fragments (light and dark grey in figure 3), which both are in themselves roughly planar, are tilted with respect to each other by an angle of 24 degrees (when observed along the two central bonds between the two fragments).

2.7. Conclusion

In summary, we have explored an approach towards extended polycyclic azaarenes based on the acid-promoted cyclising dehydration of arylamino-anthraquinone fragments to ceramidonine fragments. The potential of this approach towards extended polycyclic azaarenes is found to be geometry-dependent with respect to anthraquinone disubstitution: 1,5-disubstituted anthraquinones yield the desired products, whilst 1,4-substituted ones do not. On the other hand, the approach is geometry-independent with respect to phenazine disubstitution, with both 1,6- and 1,9-disubstituted phenazines being similarly reactive. Whilst the yields observed do not allow an efficient access to polymeric nanoribbon structures, they are adequate for double cyclisations (of the order of 50%) leading to

twisted tetraazaarenes such as **868** whose reduction potentials come close to those of C_{60}, the archetypal, but weakly absorbing and weakly soluble, acceptor material in organic electronics.

2.8. Experimental

1,6 dinitrophenazine and 1,9-dinitrophenazine

To a solution of phenazine (9 g,) in conc. H_2SO_4 (90 ml), fuming H_2SO_4 (50 %, 45 ml) and fuming HNO_3 (d= 1.52, 90 ml) were added under cooling. The temperature were gradually raised to 100 ^{0}C over period of 1 h and held there for 30 min. The reaction mixture was cooled and poured into ice. The precipitate was filtered and dried and refluxed with glacial AcOH (900 ml) to complete solution, concentrated to a volume of about 600 ml and cooled to room temperature. The crystals that separated out after 6 h at room temperature were collected and recrystallised from acetone to yield 1,6-dinitrophenazine. Yield: 4 g (30 %) as yellow solid.

The mother liquor was concentrated to a volume of about 300 ml and kept in the freezer over night. The precipitate was filtered and recrystallized twice from acetic acid to yield 1,9-dinitrophenazine. Yield: 4.7 g (35 %) yellow needles.

1,6 diaminophenazine (3) and 1,9-diaminophenazine (4)

1,6-dinitrophenazine (500 mg, 1.85 mmol), 10 % palladium on carbon (500 mg, 0.47 mmol Pd) and hydrazine monohydrate (10 ml, 10.27 g, 0.205 mol) were refluxed in ethanol (30 ml) for 5 h. The reaction mixture was concentrated under reduced pressure followed by chromatography through silica in chloroform. The product was crystallised from butanol. Yield: 190 mg (48 %) of **3** as deep red powder; ^{1}H NMR (400 MHz, DMSO-d_6): ∂ = 7.53 (dd, 2H, J=7Hz), 7.28 (d, 2H, J=7 Hz), 6.82 (d, 2H, J=7 Hz), 6.24 (broad s, 4H) ppm.

1,9-dinitrophenazine was reduced by the same protocol and purified by column chromatography through silica with 2:1 toluene:EtOAc. Yield: 290 mg (74 %) of **4** as deep red powder; ^{1}H NMR (400 MHz, DMSO-d_6): ∂ = 7.52 (t, 2H, J=9 Hz), 7.16 (d, 2H, J= 9 Hz), 6.71 (d, 2H, J=9 Hz), 6.67 (broad s, 4H) ppm.

1,4-bis-(trifluoromethanesulfonyloxy)-anthraquinone (5)

Pyridine (10 ml) was added at 0 ^{o}C to a suspension of 1,4 dihydroxyanthraquinone (3 g, 12.5 mmol) in 50 ml 1:1 dichloromethane (DCM) : chloroform and stirred at 0^o C for 15 min. Then trifluoromethanesulfonic anhydride (4.6 ml, 27.5 mmol) was added dropwise at 0^o C and stirring was continued at room temperature for 24 h. The reaction mixture was diluted with 100 ml of chloroform

and washed with brine. The organic phase was concentrated and purified by column chromatography through silica with chloroform. Yield: 5.9 g (94 %) of orange flakes. ^{1}H-NMR (400 MHz, $CDCl_3$,): ∂ = 8.34 (AB, 2H, J= 3.5 Hz & 5.5 Hz); 7.90 (AB, 2H, J= 3.5 Hz & 5.5 Hz), 7.73 (s, 2H) ppm.

1,5-bis-(trifluoromethanesulfonyloxy)-anthraquinone (6)

Pyridine (10 ml) was added at 0 ^{o}C to a suspension of 1,5 dihydroxyanthraquinone (3 g, 12.5 mmol) in 50 ml 1:1 DCM:chloroform and stirred at 0^o C for 15 min. Then trifluoromethanesulfonic anhydride (4.6 ml, 27.5 mmol) was added dropwise at 0^o C and stirring was continued at room temperature for 24 h. The precipitate was filtered and washed with chloroform. Yield: 5.6 g (89 %) of grey powder .^{1} H NMR (400 MHz, DMSO-d): ∂ = 8.32 (d, 1H, J=8 Hz); 8.06 (t, 1H, J=8Hz); 7.92(d, 1H, J=8 Hz) ppm.

4-butyl-1-hydroxyanthraquinone

A mixture of 1-hydroxyanthraquinone (1.12 g, 5 mmol), $CoCl_2$ (650 mg, 5 mmol), butylamine (22.5 ml) and butanol (7.5 ml) was refluxed for 5 h, then cooled and poured into 200 ml of 10% HCl solution. The precipitate was filtered, washed with water, dried and chromatographed through silica with toluene to give the products in the order of first 4-butyl-1-hydroxyanthraquinone **6**, then 4-butylamino-1-hydroxyanthraquinone and finally a trace amount 2,4-bis-(butylamino)-1-hydroxyanthraquinone. Yield: 700 mg (50%) of yellow solid. ^{1}H NMR (400 MHz, $CDCl_3$): ∂ = 13.00 (s, 1H), 8.30 (m, 2H), 7.77 (m, 3H), 7.52 (d, 1H, J= 13 Hz), 2.75 (t, 2H, J=7Hz), 1.65 (m, 2H), 1.39 (m, 2H), 0.95 (t, 3H, J=7Hz) ppm.

4-butyl-1-(trifluoromethanesulfonyloxy)-9,10-anthraquinone (7)

4-butyl-1-hydroxyanthraquinone (6 g, 21.4 mmol) was triflated following the procedure for **5**, with trifluoromethanesulfonic anhydride (7.5 g, 26.6 mmol) and pyridine (20 ml) in 1:1 DCM:chloroform (100 ml). The product was purified by chromatography through silica with chloroform. Yield: 7.9 g (90%) of yellow powder. ^{1}H NMR (400 MHz, $CDCl_3$): ∂ = 8.31 (m, 2H), 8.25 (m, 1H), 7.80 (pseudo t, 2H), 7.75 (d, 1H, J=8Hz), 2.85 (t, 2H, J=8Hz), 1.66 (m, 2H), 1.41 (m, 2H), 0.95 (t, 3H, J=7Hz) ppm.

3-bromo-5-nitroquinoline

Nitration of 3-bromoquinoline (Alfa Aesar) and separation of 3-bromo-5-nitroquinoline from small quantities of 3-bromo-8-nitroquinoline by crystallization were performed following the procedure of Crowley et al.[9], which is identical to the procedure of Doherty et al.[13], with the sole exception that Doherty et al. misassign the main product, isolated by recrystallisation from ethyl acetate, as being the 8-nitro isomer.

To a solution of 3-bromoquinoline (10 g, 48 mmol) in conc. H_2SO_4 (20 ml), cooled in a ice/water/NaCl bath, was added 16 ml of conc. H_2SO_4/conc. HNO_3 mixture (6:2) dropwise at -10^0 C. The mixture was stirred at 0^0 C for 2 h and then diluted with water (50 ml) and NaOH was added until the solution reached pH 10-11. The resulting solution was extracted with diethyl ether (2× 50 ml). The organic phase was dried over anhydrous $MgSO_4$ and the solvent removed under reduced pressure to give a 9:1 mixture of 3-bromo-5-nitroquinoline and 3-bromo-8-nitroquinoline. Recrystallization from ethyl acetate afforded 3-bromo-5-nitroquinoline. Yield: 8.8 g (72%) of yellow solid. ^{1}H NMR (400 MHz, $CDCl_3$): ∂ = 9.26 (dd, 1H, J= 2.1 Hz, 0.7 Hz), 9.04 (d, 1H, J= 6.4 Hz), 8.44 (m, 2H), 7.86 (t, 1H, J= 8 Hz).

3-butyl-5-aminoquinoline (8)

3-bromo-5-nitroquinoline (1.1 g, 4.3 mmol), $PdCl_2$(dppf) (630 mg, 0.86 mmol) and LiCl (360 mg, 8.6 mmol) were stirred in DMF (20 ml) for 10 min. Tetrabutyltin (6 g, 17.2 mmol) was added dropwise to the reaction mixture, which then was refluxed under argon for 24 h. The solvent was removed under reduced pressure. Column chromatography through silica in pentane elutes unreacted tetrabutyltin, and 1:1 DCM:EtOAc elutes the product. Yield: 340 mg (39%) of brown oil which formed needle shaped crystals in the freezer, that were adequate for X-Ray crystallography. ^{1}H NMR (400 MHz, $CDCl_3$): ∂ = 8.72 (s, 1H), 8.08 (s, 1H), 7.65 (d, 1H, J=8Hz), 7.49 (t, 1H, J=8Hz), 6.84 (d, 1H, J=8Hz), 4.27 (broad s, 2H), 2.81 (t, 2H, J=8Hz) 1.69 (m, 2H) , 1.38 (m, 2H), 0.94 (t, 3H, J=7Hz) ppm; MS (m/z (%)): 202.2 (100, $[M+2H]^{+),}$ 201.2 (15, $[M+H]^+$).

N,N'-bis-(4-butylanthraquinonyl)-1,6-diaminophenazine (pre737)

1,6-diaminophenazine **(3)** (200 mg, 0.96 mmol), $Pd(dba)_2$ (150 mg, 0.26 mmol), dppf (450 mg, 0.81 mmol), sodium ^{t}butoxide (200 mg, 2.0 mmol), LiCl (160 mg, 3.8 mmol) were stirred in toluene (10ml) at 100^0 C for 10 min under argon. Then a suspension of **7** (790 mg, 1.92 mmol) in toluene (10 ml) was added dropwise. The deep red mixture was refluxed overnight under argon, cooled and chromatographed through silica in chloroform to elute first a trace amount unreacted **7**, followed by **pre737** and finally unreacted amine **3**. **pre737** was recrystallised from butanol. Yield: 280 mg (40%) of deep red crystals; ^{1}H NMR (400 MHz, $CDCl_3$): ∂ = 11.04 (broad s, 2H), 8.28 (m, 2H), 8.21 (m, 4H), 7.96 (d, 2H, J=8Hz), 7.79 (d, 2H, J= 8Hz), 7.73 (m, 4H), 7.62 (t, 2H, J= 8Hz), 6.59 (d, 2H, J=8Hz), 2.73 (t, 4H, J=8Hz), 1.63 (m, 4H), 1.21 (m, 4H), 0.78 (t, 6H, J=7Hz) ppm.

3,15-di-butyl-diceramidonino[3,4-b:3',4'-e]pyrazine (737)

pre737 (100 mg, 0.143 mmol) was heated in 70% H_2SO_4 (10 ml) at 130^0 C for 8 min with vigorous stirring. The color of the mixture changed from brown to deep red. The hot mixture was poured onto

crushed ice and the precipitate was filtered off, washed with 5% aqueous NaOH, dried under reduced pressure, chromatographed through silica in 1:1 chloroform:EtOAc and crystallised from butanol. Yield: 50 mg (53%) of brown powder; ^{1}H NMR (400 MHz, $CDCl_3$): ∂ = 9.01 (d, 2H, J=9Hz), 8.78 (d, 2H, J=7Hz), 8.62 (d, 2H, J=8Hz), 8.56 (d, 2H, J=8Hz), 8.49 (d, 2H, J=9Hz), 8.00 (d, 2H, J=7Hz), 7.89 (t, 2H, J=8Hz), 7.76 (t, 2H, J=8Hz), 3.87 (t, 4H, J=8Hz), 2.05 (m, 4H), 1.69 (m, 4H), 1.17 (t, 6H, J=7Hz) ppm. ^{13}C NMR (100 MHz, $CDCl_3$): ∂ = 182.7, 152.0, 147.2, 145.2, 144.8, 143.6, 134.8, 134.2, 133.9, 132.7, 131.1 (×2), 130.4, 129.9, 129.5, 129.4, 128.9, 126.3, 123.6, 122.9, 33.3, 32.0, 23.2, 14.2 ppm. UV-vis. ($CHCl_3$): λ_{max} (rel. intensity) = 382.0 (1.00); 433.0 (0.47); 456.0 (0.46); 480.0 nm (0.30). MS (m/z (%)): 699.2 (100, $[M+H]^+$).

N,N'-bis-(4-butylanthraquinonyl)-1,9-diaminophenazine (pre747)

Coupling between 1,9-diaminophenazine **4** (250 mg, 1.2 mmol) and **7** (990 mg, 2.4 mmol) leads to **pre747** following the above procedure with $Pd(dba)_2$ (150 mg, 0.26 mmol, 10mol%), dppf (450 mg, 0.81 mmol), sodium ^{t}butoxide (250 mg, 2.5 mmol) and LiCl (200 mg, 4.75 mmol) in toluene (20 ml). Yield: 460 mg (52%) of deep red powder; ^{1}H NMR (400 MHz, $CDCl_3$): ∂ = 11.16 (broad s, 2H), 8.16 (d, 4H, J=7 Hz), 8.12 (d, 2H, J=8Hz), 7.73 (t, 4H, J=7Hz), 7.64 (t, 4H, J=8Hz), 7.56 (t, 2H, J=8Hz), 6.66 (d, 2H, J=7Hz), 2.73 (t, 4H, J=8Hz), 1.65 (m, 4H), 1.22 (m, 4H), 0.79 (t, 6H, J=7Hz) ppm.

3,19-di-butyl-diceramidonino[3,4-b:4',3'-e]pyrazine (747)

pre747 (440 mg, 0.598 mmol) was heated in 70% H_2SO_4 (15ml) at 130^0 C for 8 min with vigorous stirring. The color changed from dark yellow via deep green to deep red. The mixture was worked up as described for **737**. Yield: 170 mg (41%) of brown powder; ^{1}H NMR (400 MHz, $CDCl_3$): ∂ = 8.92 (d, 2H, J=9Hz), 8.79 (d, 2H, J=7Hz), 8.51 (d, 2H, J=7Hz), 8.45 (d, 2H, J=7Hz), 8.10 (d, 2H, J=9Hz), 8.04 (d, 2H, J=7Hz), 7.78 (t, 2H, J=7Hz), 7.62 (t, 2H, J=7Hz), 4.12 (t, 4H, J=7 Hz), 2.12 (m, 4H), 1.54 (m, 4H), 1.00 (t, 6H, J=7Hz) ppm. ^{13}C NMR (100MHz, $CDCl_3$) : ∂ = 182.9; 152.0; 147.7; 145.6; 145.4; 142.7; 134.9; 134.1; 133.9; 132.7; 131.1; 130.8; 130.6; 130.3; 129.6; 128.8; 128.5; 126.3; 123.4; 122.8; 32.9; 31.4; 22.5; 14.5 ppm. UV-vis. ($CHCl_3$): λ_{max} (rel. intensity) = 385.0 nm (0.96), 439.0 nm (0.52), 464.0 nm (0.54); shoulder at 477.0 nm (0.49). MS (m/z (%)): 699.2 (65, $[M+H]^+$); 700.2 (50, $[M+2H]^+$);721.2 (100, $[M+Na]^+$); 722.2 (70, $[M+Na+H]^+$).

1,5-bis-(3-butylquinolin-5-ylamino)-9,10-anthraquinone (pre868)

3-butyl-5-aminoquinoline **8** (500mg, 2.5 mmol), $Pd(dba)_2$ (260 mg, 0.45 mmol, 20mol%), dppf (810 mg, 1.46 mmol), sodium ^{t}butoxide (260 mg, 2.7 mmol) and LiCl (260 mg, 6.1 mmol) were stirred in toluene (10 ml) at 100^0 C for 10 min under argon. Then a suspension of **6** (480 mg, 0.96 mmol) in toluene (10 ml) was added dropwise. The deep violet mixture was refluxed overnight and then

separated by column chromatography through silica. Chloroform elutes traces of unreacted **6**, and 1:1 chloroform:EtOAc elutes first a red trace impurity (presumably a monocyclised intermediate) and then **pre868**, which is recrystallised from butanol. Yield: 232 mg (40%) of deep red powder; ^{1}H NMR (400 MHz, $CDCl_3$): ∂ = 11.64 (broad s, 2H), 8.83 (s, 2H), 8.17 (s, 2H), 8.04 (d, 2H, J=8 Hz), 7.80 (d, 2H, J=8 Hz), 7.70 (t, 2H, J= 8Hz), 7.60 (d, 2H, J=8 Hz), 7.47 (t, 2H, J=8Hz), 7.13 (d, 2H, J=8 Hz), 2.79 (t, 4H, J=8Hz), 1.66 (m, 4H), 1.38 (m, 4H), 0.93 (t, 6H, J=7 Hz) ppm.

2,12-dibutyl-4,10,14,20-tetraaza-dinaphtho[2,1-a:2',1'-j]perylene (868)

pre868 (150 mg, 0.248 mmol) was heated in 70% sulfuric acid at 170^0 C for 30 min with vigorous stirring. The hot mixture was poured onto ice and the precipitate was filtered off and washed with 5% aqueous NaOH, dried in air, purified by column chromatography through silica in chloroform and recrystallised from methanol. Yield: 90 mg (64%) of red powder. Single crystals for X-Ray crystallography were made by slow evaporation of solvent of a chloroform solution. ^{1}H NMR (400 MHz, $CDCl_3$) : ∂ = 9.55 (s, 2H), 8.92(s,2H), 8.72 (d, 2H, J=9Hz), 8.42 (m, 4H), 8.05 (d, 2H, J=8Hz), 7.99(t, 2H, J=8Hz), 2.96 (t, 4H, J=8Hz), 1.84 (m, 4H), 1.51 (m, 4H), 1.02 (t, 6H, J=7Hz) ppm. ^{13}C NMR (100MHz, $CDCl_3$) : ∂ = 152.8, 148.6, 148.2, 147.0, 137.1, 135.5, 132.6, 131.2, 130.1, 130.1, 129.5, 128.7, 127.2, 126.8, 123.5, 121.0, 33.8, 33.4, 22.6, 14.1 ppm. UV-vis. ($CHCl_3$): λ_{max} (rel. intensity) = 338.0 nm (0.92); 469.0 nm (0.21); 499.0 nm (0.48); 535.0 nm (0.66). MS (m/z (%)):- 568.2 (40, $[M]^+$); 569.2 (100, $[M+H]^+$); 570.2(80, $[M+2H]^+$).

1-(quinolin-8-ylamino)-4-butylanthraquinone (9)

8-aminoquinoline (720 mg, 5 mmol), $Pd(dba)_2$ (100 mg, 0.16 mmol, 10mol%), dppf (300 mg, 0.54 mmol), sodium-^{t}butoxide (480 mg, 5 mmol) and LiCl (70 mg, 1.6 mmol) were stirred in toluene (10 ml) at 100^0 C for 10 min under argon. Then a suspension of 4-butyl-1-trifluoromethanesulfonyloxy anthraquinone **7** (650 mg, 1.6 mmol) in toluene (10ml) was added dropwise to the reaction mixture. The violet mixture was refluxed overnight. After cooling to room temperature, the mixture was separated by column chromatography through silica with chloroform which elutes a trace of unreacted **7** first, followed by the product. The solvent was evaporated under reduced pressure and dried and the product was crystallized from methanol. Yield: 370 mg (57%) of red powder. ^{1}H NMR (400 MHz, $CDCl_3$): ∂ = 11.00 (broad s, 1H), 9.04 (dd, 1H, J= 2Hz, 5Hz), 8.24 (m, 2H), 8.15 (d, 1H, J= 8Hz), 8.12 (t, 1H, J= 8Hz), 7.71 (m, 3H), 7.48 (dd, 1H, J= 4Hz, 8Hz), 7.28 (d, 2H, J=5Hz), 6.59 (t, 1H, J= 5Hz), 2.64 (t, 2H J=7Hz), 1.57 (m, 2H), 1,14 (m, 2H), 0.73 (t, 3H, J= 7Hz) ppm.

8-butyl-pyridino[3,2-c]ceramidonine (10)

9 (100 mg, 0.246 mmol) was heated in 70% H_2SO_4 (10 ml) at 130^0 C for 8 min with vigorous stirring. The colour of the reaction mixture changes from brown to orange. The hot mixture was poured onto crushed ice and the precipitate was filtered off and washed with 5% aqueous NaOH solution. It was dried in reduced pressure and chromatographed through silica with 1:1 chloroform:EtOAc and the solvent was evaporated under reduced pressure. Yield: 48 mg (50%) of brown sticky oil; ^{1}H NMR (400 MHz, $CDCl_3$):- ∂= 9.30 (m, 1H), 8.72 (d, 1H, J= 8Hz), 8.65 (d, 1H, J= 10Hz), 8.57 (d, 1H, J= 8Hz), 8.46 (d, 1H, J= 8Hz), 8.28 (d, 1H, J= 8Hz), 7.93 (d, 1H, J= 7Hz), 7.80 (m, 2H), 7.70 (m, 2H), 3.85 (t, 2H, J= 7Hz), 1.97 (m, 2H), 1.58 (m, 2H), 1.03 (t, 3H, J= 7Hz) ppm.

1,5-bis-(p-butylphenylamino)-anthraquinone (11)

4-*n*butylaniline (2.5 ml, 2.36 g, 15.8 mmol, large excess), $Pd(dba)_2$ (100 mg, 0.16 mmol, 10 mol%), dppf (300 mg, 0.54 mmol), sodium-*t*butoxide (480 mg, 5 mmol) and LiCl (70 mg, 1.6 mmol) were stirred in toluene (10 ml) at 100^0 C for 10 min under argon. Then a suspension of 1,5-bis-(trifluoromethanesulfonyloxy)-anthraquinone **6** (610 mg, 1.6 mmol) in toluene (10 ml) was added drop wise to the reaction mixture. The deep red mixture was refluxed for 4 h under argon atmosphere. After cooling to room temperature, the mixture was separated by column chromatography through silica with chloroform which elutes a trace amount of unreacted **6** first, followed by the product as wine red solution. The solvent was evaporated under reduced pressure and dried and the product was crystallized from methanol. Yield: 510 mg (63%) of brick-red crystals. ^{1}H NMR (400 MHz, $CDCl_3$):- ∂= 11.31 (broad s, 2H), 7.67 (d, 2H, J= 8Hz), 7.46 (t, 2H, J= 8Hz), 7.39 (d, 2H, J= 8Hz), 7.21 (s, 8H), 2.61 (t, 4H, J= 7Hz), 1.62 (m, 4H), 1,36 (m, 4H), 0.94 (t, 6H, J= 7Hz) ppm.

3,11-dibutyl-8,16-diaza-dibenzo[a,j]perylene (12)

1,5-bis-(p-butylphenylamino)-anthraquinone **11** (400 mg, 0.8 mmol) was heated in 70% sulfuric acid (30 ml of a solution prepared by adding 22ml of concentrated sulphuric acid to 8 ml of water) at 170^0 C for 30 min with vigorous stirring. The hot mixture was poured onto crushed ice and the precipitate was filtered off and washed with 5% aqueous sodium hydroxide solution, dried in air and purified by column chromatography through silica in chloroform followed by recrystallisation from methanol. Yield: 340 mg (90%) of red crystals. ^{1}H NMR (400 MHz, $CDCl_3$): ∂ = 8.53 (s, 2H), 8.43 (d, 2H, J= 7Hz), 8.25 (dd, 4H, J= 8Hz, 11Hz), 7.92 (t, 2H, J= 8Hz), 7.69 (d, 2H, J= 8Hz), 2.89 (t, 4H, J= 7Hz), 1.75 (m, 4H), 1.44 (m, 4H), 0.97 (t, 3H, J= 7Hz) ppm.

1,4-bis-(p-butylphenylamino)-anthraquinone (13)

4-^{n}butylaniline (2.5 ml, 2.36 g, 15.8 mmol, large excess), $Pd(dba)_2$ (100 mg, 0.16 mmol, 10 mol%), dppf (300 mg, 0.54 mmol), sodium-^{t}butoxide (480 mg, 5 mmol) and LiCl (70 mg, 1.6 mmol) were stirred in toluene (10 ml) at 100^0 C for 10 min under argon. Then a solution of 1,4-bis-(trifluoromethanesulfonyloxy)-anthraquinone **5** (610 mg, 1.6 mmol) in toluene (10 ml) was added dropwise to the reaction mixture. The deep red mixture was refluxed for 4 h under argon atmosphere. After cooling to room temperature, the mixture was separated by column chromatography through silica in chloroform which elutes a trace amount of unreacted **5** first, followed the product as wine red solution. The solvent was evaporated under reduced pressure and dried and the product was crystallised from methanol. Yield: 480 mg (60%) of red powder.

^{1}H NMR (400 MHz, $CDCl_3$): ∂ = 12.23 (broad s, 2H), 8.37 (dd, 2H, J= 3Hz, 6Hz), 7.73 (dd, 2H, J= 3Hz, 6Hz), 7.44 (s, 2H), 7.17 (s, 8H), 2.60 (t, 4H, J= 7Hz), 1.60 (m, 4H), 1.35 (m, 4H), 0.93 (t, 6H, J= 7Hz) ppm.

2-butyl-8-(p-butylphenylamino)-ceramidonine (14)

1,4-bis-(p-butylphenylamino)-anthraquinone **13** (400 mg, 0.8 mmol) was heated in 10 mL 70% sulphuric acid at 170°C for 30 min with vigorous stirring. The hot mixture was poured onto crushed ice and the precipitate was filtered off and washed with 5% aqueous sodium hydroxide solution, dried in air and purified by column chromatography through silica in chloroform. The solvent was evaporated under reduced pressure. Yield: 290 mg (76%) of red powder. ^{1}H NMR (400 MHz, $CDCl_3$): ∂ = 14.06 (broad s, 1H), 8.81 (m, 2H), 8.67 (s, 1H), 8.23 (m, 2H), 7.84 (t, 1H, J= 7Hz), 7.74 (m, 2H), 7.63 (d, 1H, J= 8Hz), 7.31 (m, 4H), 2.92 (t, 2H, J= 7Hz), 2.67 (t, 2H, J= 7Hz), 1.77 (m, 2H), 1.65 (m, 2H), 1.47 (m, 2H), 1.41 (m, 2H), 0.98 (t, 3H, J= 7Hz), 0.96 (t, 3H, J= 7Hz) ppm.

1, 3, 5, 7-tetrahydroxy-anthraquinone (anthrachrysone, 15):

3,5-dihydroxybenzoic acid (55g, 0.36 mol) was dissolved into 120 ml of conc. H_2SO_4 and heated at 130^0 C for 1 h. The deep red solution was then kept at room temperature for 1 d. The precipitate was filtered off and washed with water and then thrice with methanol. The crude product was dried and used in the next step without further purification. Yield: 15g (31%) of greenish solid. ^{1}H NMR (400 MHz, DMSO-d): ∂ = 12.73 (s, 1H), 11.43 (broad s, 1H), 7.18 (s, 1H), 6.60 (s, 1H).

3,7-bis-(2-ethylhexyloxy)-1,5-dihydroxyanthraquinone (16)

1, 3, 5, 7- tetrahydroxy anthraquinone **15** (10.9 g, 0.04 mol), 2-ethylhexylbromide (15.4 g, 0.08 mol), NaOH (6.4 g, 0.08 mol) in 20 ml water and tetra-*n*-butylammonium bromide (TBAB) (19 g, 0.06 mol) was taken in 100 ml of DMSO and heated at 80°C for 24 h under argon atmosphere. Then the mixture

was cooled to room temperature and poured into 300 ml of chloroform and extracted with water (5×500 ml) 5 times. The organic phase was collected, dried over $MgSO_4$ and concentrated. Column chromatography in $CHCl_3$ yielded 3,7-bis-(2-ethylhexyloxy)-1,5-dihydroxyanthraquinone. It was crystallised from butanol. Yield: 8.6 g (43%) of yellow solid.

3,7-bis-(2-ethylhexyloxy)-1,5-bis-(trifluoromethanesulfonyloxy)-anthraquinone (17)

Pyridine (10 ml) was added at 0°C to a suspension of 3,7-bis-(2-ethylhexyloxy)-1,5-dihydroxyanthraquinone **16** (4.72 g, 10 mmol) in 50 ml 1:1 dichloromethane (DCM) : chloroform and stirred at 0°C for 15 min. Then trifluoromethanesulfonic anhydride (3.7 ml, 22 mmol) was addeddrop wise at 0° C and stirring was continued at room temperature for 24 h. The reaction mixture was diluted with 100 ml of chloroform and washed with brine. The organic phase was concentrated and purified by column chromatography through silica with chloroform. Yield: 6.8 g (89%) of pale yellow solid. ^{1}H-NMR (400 MHz, $CDCl_3$): ∂ = 7.90 (s, 1H), 7.06 (s, 1H), 4.06 (d, 2H, J= 7Hz), 1.80 (m, 1H), 1.50 (m, 9H), 1.32 (m, 6H).

3,7-bis-(2-ethylhexyloxy)-1,5-bis-(phenylamino)-anthraquinone (18)

4-^{n}butylaniline (2.5 ml, 2.36 g, 15.8 mmol, large excess), $Pd(dba)_2$ (100 mg, 0.16 mmol, 10mol%), dppf (300 mg, 0.54 mmol), sodium-^{t}butoxide (480 mg, 5 mmol) and LiCl (70 mg, 1.6 mmol) were stirred in toluene (10 ml) at 100°C for 10 min under argon. Then a suspension of 3,7-bis-(2-ethylhexyloxy)-1,5-bis-(trifluoromethanesulfonyloxy)-anthraquinone **17** (1.2 g, 1.6 mmol) in toluene (10 ml) was added dropwise to the reaction mixture. The deep red mixture was refluxed for 4 h under argon atmosphere. After cooling to room temperature, the mixture was separated by column chromatography through silica in chloroform which elutes a trace amount of unreacted **17** first, followed by the product **18** as wine red solution. The solvent was evaporated under reduced pressure and dried and the product was crystallised from methanol. Yield: 800 mg (80%) of red solid.

2.9. Crystallographic data.

868: Table 1. Crystal data and structure refinement for ij_l_ps3_0m.

Identification code	ij_l_ps3_0m
Empirical formula	C40 H32 N4
Formula weight	568.70
Temperature	100(2) K
Wavelength	0.71073 A

Crystal system, space group Triclinic, P-1

Unit cell dimensions a = 9.1783(17) A alpha = 108.315(12) deg.

b = 11.032(2) A beta = 90.603(10) deg.

c = 14.830(3) A gamma = 100.772(9) deg.

Volume 1396.6(4) A^3

Z, Calculated density 2, 1.352 Mg/m^3

Absorption coefficient 0.080 mm^-1

F(000) 600

Crystal size 0.40 x 0.10 x 0.10 mm

Theta range for data collection 2.81 to 27.61 deg.

Limiting indices -12<=h<=11, -10<=k<=14, -20<=l<=19

Reflections collected / unique 11287 / 6332 [R(int) = 0.0466]

Completeness to theta = ACTA 50 ACTA 50 %

Absorption correction Empirical

Max. and min. transmission 0.9920 and 0.9687

Refinement method Full-matrix least-squares on F^2

Data / restraints / parameters 6332 / 0 / 399

Goodness-of-fit on F^2 0.984

Final R indices [I>2sigma(I)] R1 = 0.0721, wR2 = 0.1831

R indices (all data) R1 = 0.1629, wR2 = 0.2308

Largest diff. peak and hole 0.335 and -0.392 e.A^-3

2.10. References

[1] A. H. Cook, W. Waddington, *J. Chem. Soc.*, 402-405, 1945.

[2] D. W. Rangnekar, S. V. Sunthankar, *Indian J. Technology*, **12**, 548, 1974.

[3] H. Otomasu, *Chem. Pharm. Bull.*, **6**, 77, 1958.

[4] P. Huszthy, E. Samu, B. Vermes, G. Mezey-Vandor, M. Nogradi, J. S. Bradshaw, R. M. Lzatt, *Tetrahedron*, **55**, 1491-1504, 1999.

[5] M. S. Taylor, T. M. Swager, *Angew. Chem. Int. Ed.*, **46**, 8480, 2007.

[6] X. Lu, F. Tian, N. Wang, Q. Zhang, *Org. Lett.*, **4**, 4313, 2002.

[7] R. Gletier, B. Esser, S. C. Kornmayer, *Acc. Chem. Res.*, **42**, 1108, 2009.

[8] M. Matsuoka, T. Takei, I. Nakamura, K. Yoshida, T. Kitao, *Bull. Chem. Soc. Jpn.*, **54**, 2225, 1981.

[9] J. D. Crowley, I. M. Steele, B. Bosnich, *Chem. Eur. J.*, **12**, 8935, 2006.

[10] M. Viaud, P. Jamoneau, L. Savelon, G. Guillaumet, *Heterocycles*, **41**, 2799,. 1995

[11] R. Sanz, V. Guilarte, A. Pérez, *Tetrahedron Lett.*, **50**, 4423, 2009.

[12] J. Muzart, *Tetrahedron*, **65**, 8313-8323, 2009.

[13] S. Doherty, E. G. Robbins, I. Pal, C. R. Newman, C. Hardacre, D. Rooney, D. A. Mooney, *Tetrahedron (Asymmetry)*, **14**, 1517, 2003.

[14] J. A. Joule, K. Mills, G. F. Smith, *Heterocyclic Chemistry*, 3rd ed., Stanley Thornes Ltd., pp. 120-145, 1995.

[15] L. James, *Tetrahedron*, **40**, 1433, 1984.

[16] A. J. Paine, *J. Am. Chem. Soc.*, **109**, 1496, 1987.

[17] J. Louie, M. S. Driver, B. C. Hamann, J. F. Hartwig, *J. Org. Chem.*, **62**, 1268, 1997.

[18] G. M. Badger, R. Pettit, *J. Chem. Soc.*, 1874-1877, **1952**.

[19] F. B. Mallory, K. E. Butler, A. C. Evans, C. W. Mallory, *Tetrahedron Lett*., **37**, 7173, 1996.

[20] F. B. Mallory, K. E. Butler, A. C. Evans, E. J. Brondyke, C. W. Mallory, C. Yang, A. Ellenstein, *J. Am. Chem. Soc.*, **119**, 2119, 1997.

[21] *Methoden der organischen Chemie (Houben-Weyl)*, 4th edition, G. Thieme Verlag, Stuttgart **1958**

[22] E. Clar, *Polycyclic Hydrocarbons*, Academic Press & Springer Verlag, 1964.

[23] P.-M. Allemand, A. Koch, F. Wudl, Y. Rubin, F. Diederich, M. M. Alvarez, S. J. Anz, R. L. Whetten, *J. Am. Chem. Soc.*, **113**, 1050, 1991.

Chapter 3

Oxidative cyclisations of 2,3-diarylacrylates

The cyclisation of esters of Perkin condensation products by oxidation with 2,3-dichloro-5,6-dicyanobenzoquinone (DDQ) in the presence of $MeSO_3H$ is examined as a three-step approach from arylacetic acids and aromatic aldehydes to functionalised condensed arenes. The method is found to be limited to systems where one or both of the two aryl moieties are more reactive than phenyl, such as 1-naphthyl or 3-thienyl. Alkoxycarbonyl derivatives of picene, benzo[c]chrysene, three isomeric phenanthrothiophenes, a naphthothiophene and a benzodithiophene are obtained. The extension of this approach to multiple cyclisations and thus to extended ribbons appears to be hindered by the deactivating influence of multiple alkoxycarbonyl substituents except for cases involving highly active thienylacetic acid precursors, where conjugated polymers made of short ribbon fragments linked by thiophene-thiophene single bonds appear envisageable.

3.1. DDQ/$MeSO_3H$ as an oxidation system for Scholl-type cyclisations

Oxidative dehydrocyclisations are a versatile approach to condensed polycyclic arenes. Biaryl couplings with $AlCl_3$ were first reported by Scholl and co-workers one century ago [1, 2], but their extensive use for intramolecular cyclisations has been pioneered by Müllen and co-workers only in the last two decades. A particularly efficient implementation of this reaction is the oxidation of branched oligophenyl networks with $FeCl_3$, which leads to a variety of extended graphene fragments in high yields by multiple simultaneous ring closures.[3, 4] Similar results have also been obtained with other oxidants such as phenyliodine(III) bis(trifluoroacetate) (PIFA) or $MoCl_5$.[5] Very recently, Rathore and co-workers proposed an alternative oxidation system based on the combination of a quinone oxidant, 2,3-dichloro-5,6-dicyano-*p*-benzoquinone (DDQ), with methanesulfonic acid in DCM.[6] Quinone oxidants such as DDQ or chloranil are proficient tools to aromatize saturated or partially saturated cycles such as obtained by Diels-Alder reactions at high temperature [7, 8, 9, 10] whilst being tolerant to substituents such as ester, imide or anhydride groups, but are inefficient for inducing Scholl-type cyclisations. The novel combination with an acid such anhydrous methanesulfonic acid though renders DDQ surprisingly active for such cyclisations even at room temperature or below. It finds its limit at an oxidation potential of *c.* E_{ox} = 1.7V vs. SCE, such that hexa(4-*tert*-butylphenyl)benzene with E_{ox} =

1.6V can be efficiently hexacyclised to the corresponding hexa-*tert*-butyl-hexabenzocoronene, whilst unsubstituted hexaphenylbenzene, with a slightly higher E_{ox} of 1.8V, does not react.[6] Similarly, tetraphenylethylene (E_{ox} =1.36V) reacts twice via the less reactive 9-10-diphenylphenanthrene ((E_{ox} =1.59V) to slowly give the corresponding dibenzochrysene, whilst the reaction of tetra-(4-bromophenyl)ethylene ((E_{ox} =1.51V) does not go beyond the bis(bromophenyl)phenanthrene (E_{ox} =1.80V).[11] In these examples, the lower oxidation potentials and higher reactivities of oligo-aryl-substituted ethylenes compared to oligo-aryl-substituted benzenes points to stilbenes as better substrates than *o*-terphenyls.

Stilbene-type precursors, including ester-substituted ones, can also be transformed into phenanthrene-type arenes by oxidative photocyclisation, but photocyclisations of stilbenes often suffer from competing photochemical [2+2] cycloadditions either between two stilbenes or between the phenanthrene product and the stilbene substrate, and are thus generally conducted in high dilution.[12]

3.2. 2,3-Diarylacrylates by Perkin condensation

A particularly versatile access route to cyclisable, carboxy-substituted precursors to polycyclic arenes is the Perkin reaction of an aromatic aldehyde with an arylacetic acid, which yields α-aryl-*trans*-cinnamic acids (= alkoxycarbonyl-*cis*-stilbenes) [13, 14, 15] with the two aryl moieties in the appropriate *cis*-configuration for oxidative cyclisation to 9-carboxy-phenanthrene-type arenes.

As our group has a long-standing interest in carboxy-substituted polycyclic arenes and their esters and imides because carboxylic substitution is an efficient lever for the tuning of electronic properties and often leads to liquid crystalline self-assembly [10, 16, 17, 18, 19, 20, 21, 22] we wondered whether the use of DDQ/H^+ would allow the conduct of Scholl-type oxidative cyclisations in the presence of carboxylic ester substituents on stilbene-type substrates. Oxidative ring closures of stilbenecarboxylic esters with $FeCl_3$ or VOF_3 as oxidant are only reported for systems where the aromatic residues are activated by several electron-donating alkoxy substituents [23, 24], except for the lone substituent-free case of the VOF_3-induced cyclisation of methyl *trans*-2,3-bis-(1-naphthyl)-acrylate to methyl picene-14-carboxylate in 47% yield.[25]

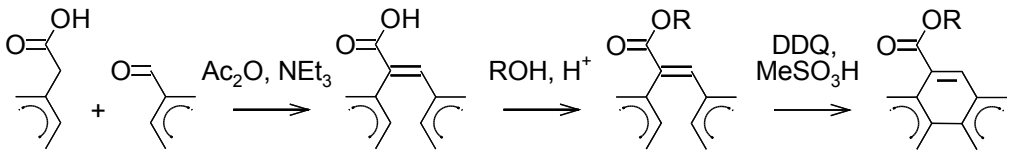

Fig. 1 Three-step access to phenanthrene-type arenecarboxylates via 1. Perkin condensation of an arylacetic acid with an arenealdehyde, 2. esterification and 3. oxidative cyclisation.

3.3. A systematic study of DDQ cyclisations of 2,3-diarylacrylates

To investigate the potential of the DDQ/H^+ oxidation on esterified Perkin products with no activating substituents, we chose, as set a of varied reactivities aryl groups, the four moieties phenyl, 1-naphthyl, 2-naphthyl and 3-thienyl, and prepared the sixteen corresponding methyl or butyl *trans*-2,3-diarylacrylates to test their ability to cyclise to the corresponding kata-annellated arenecarboxylic esters **1**-**16**. The four dinaphtyl acrylates (supposedly yielding the least soluble cyclisation products), were made as butyl esters, whilst of the twelve other acrylic acids, the methyl esters were made to optimise crystallinity.

Perkin condensations are usually conducted in refluxing acetic anhydride (bp. 140° C), which acts simultaneously as a solvent and activator of the arylacetic acid via mixed anhydride formation. At this high reaction temperature, side products form that include decarboxylated stilbene, 1,3-diaryl-2-propanone resulting from Claisen condensation, and the Perkin condensation product of the aromatic aldehyde with acetic anhydride itself, i.e. the α-unsubstituted *trans*-cinnamic acid.[26] Buckles and Cooper showed that the reaction proceeds with good yield and that side product formation can be largely suppressed if carried out at 65° C using the arenecarboxaldehyde starting material, benzaldehyde in their case, as a solvent. We found that the Perkin condensation can conveniently be conducted under mild conditions with isolated yields around 45% (including the subsequent esterification of the crude condensation product) whilst avoiding the use of excesses of either starting material, if refluxing THF (bp. 66° C) is chosen as solvent.

The 2,3-diarylacrylates so obtained were treated with DDQ/$MeSO_3H$ in DCM at room temperature for up to three days. No cyclisations to **1**-**4** could be observed with any of the four acrylates derived from phenylacetic acid (with, as counterparts, benzaldehyde, 1- and 2-naphthaldehyde, and 3-formylthiophene), and the starting material was largely recovered. All four acrylates derived from 3-thienylacetic acid yielded the desired cyclisation products **13**-**16** in yields between 63 and 85% and the reaction was completed after 16h, except for the least reactive case based on 3-thienylacetic acid and benzaldehyde, where the reaction proceeded slowly to reach a yield of 53% of **13** after 64 h. The latter case is the only benzaldehyde-based system amongst the four tested that reacted (**1**, **5**, **9** & **13**; fig. 2).

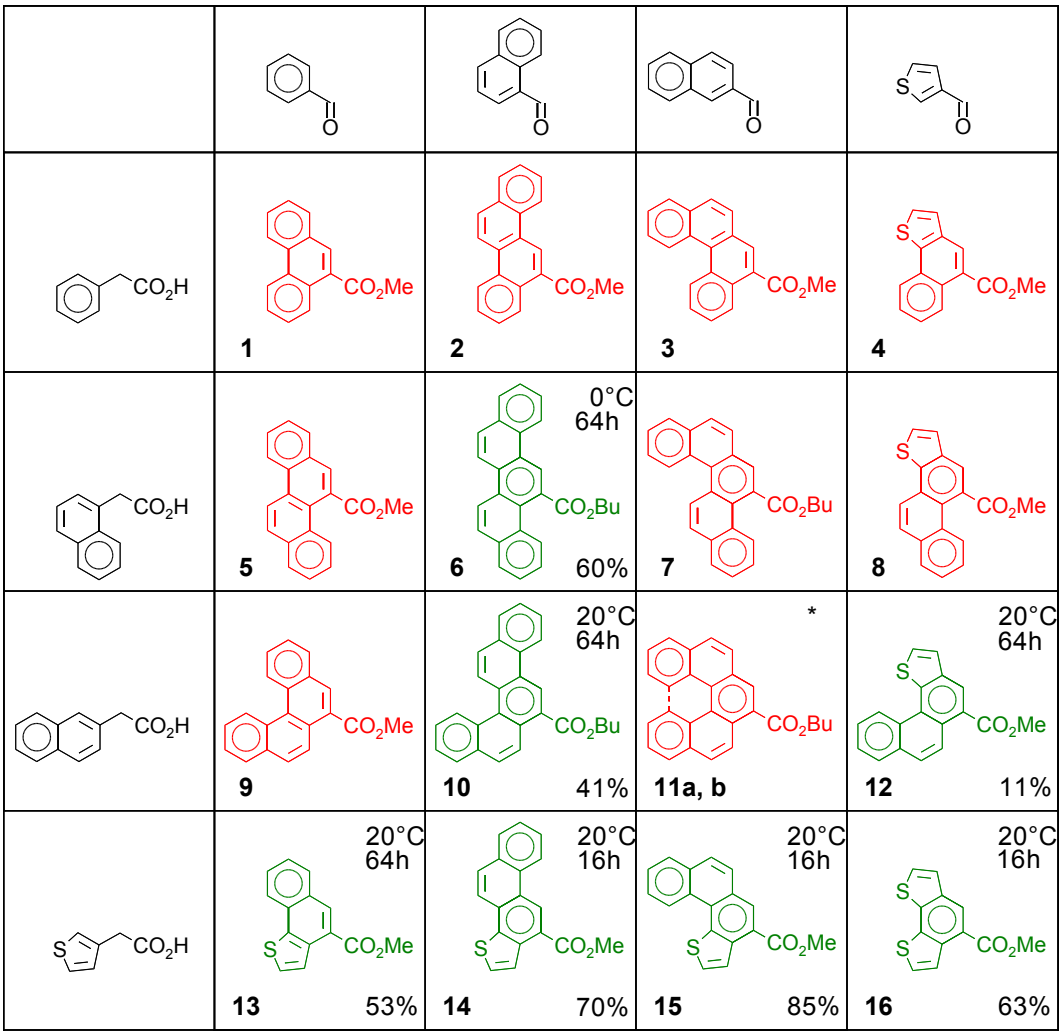

Fig. 2 Targets of oxidative cyclisations of Perkin condensation products (3mmol) with 1.2 eq. DDQ (3.6mmol, except *: 7.2mmol) and $MeSO_3H$ (30mmol, except *: 60mmol) in DCM. Black: Perkin starting materials. Green: Obtained products, with yield, reaction time, and temperature. Red: Not formed after 64h at 20°C.

Interestingly, the reactivity depends strongly on the location of the alkoxycarbonyl moiety with respect to the two aryl residues on the acrylate starting material, and reversing the substitution pattern from 2-thienyl-3-phenyl/naphthyl- to 2-phenyl/naphthyl-3-thienyl decreases the reactivity considerably: No reaction could be observed with the systems based on 3-formylthiophene and either phenyl- or 1-naphthyl-acetic acid (**4** & **8**), and only 11% yield of **12** was obtained after three days besides recovered starting ester in the case of 3-formylthiophene + 2-naphthylacetic acid. A striking difference in reactivity is also observed between 1-naphthaldehyde- and 2-naphthaldehyde-based cases when comparing the four 2,3-dinaphthylacrylates: both systems based on 1-naphthaldehyde, i.e. butyl 2-(2-naphthyl)-3-(1-naphthyl)acrylate and butyl 2,3-bis(1-naphthyl)acrylate, cyclise to **6** and **10** albeit slowly, whereas the two systems based on 2-naphthaldehyde, i.e. butyl 2-(1-naphthyl)-3-(2-

naphthyl)acrylate and butyl 2,3-bis(2-naphthyl)acrylate, do not cyclise to **7** or **11** within 64h even though in the latter case, where a further DDQ-induced oxidative ring closure of the primarily formed [5]helicene **11a** to the benzo[ghi]perylene **11b** is to be expected, we doubled the amount of oxidant used.

When we conducted the oxidative cyclisation of butyl 2,3-bis-(1-napthyl)acrylate at room temperature, cyclisation took place accompanied by loss of the alkyl group to yield a sparingly soluble product whose ^{1}H-NMR spectrum showed one aromatic hydrogen less than expected (3 instead of 4 triplets, besides 1 downfield singlet and 8 doublets). This spectrum is compatible with either a ketone formed by intramolecular Friedel-Crafts acylation or a lactone formed by a further oxidative cyclodehydrogenation. Both of these overreactions are plausible with regard to the known reactions of chrysene-6-carboxylic acid, which yields the corresponding pentagonal ketone upon dehydration in liquid HF and the corresponding intramolecular lactone upon irradiation in the presence of air and iodine.[27] The mass spectrum, with a dominant peak at 320.0836 Da corresponding to $[C_{23}H_{12}O_2]^+$, is in agreement with the lactone structure **17**. The ^{1}H-NMR spectrum of **17** shows a very downfield singlet at 9.92ppm (compared to 9.02ppm in the ester) due to the rigidly coplanar carbonyl (which is free to rotate in the butyl ester), and a doublet at 7.58 ppm, which is upfield of the triplets, indicative of a proton next to a phenolic oxygen.

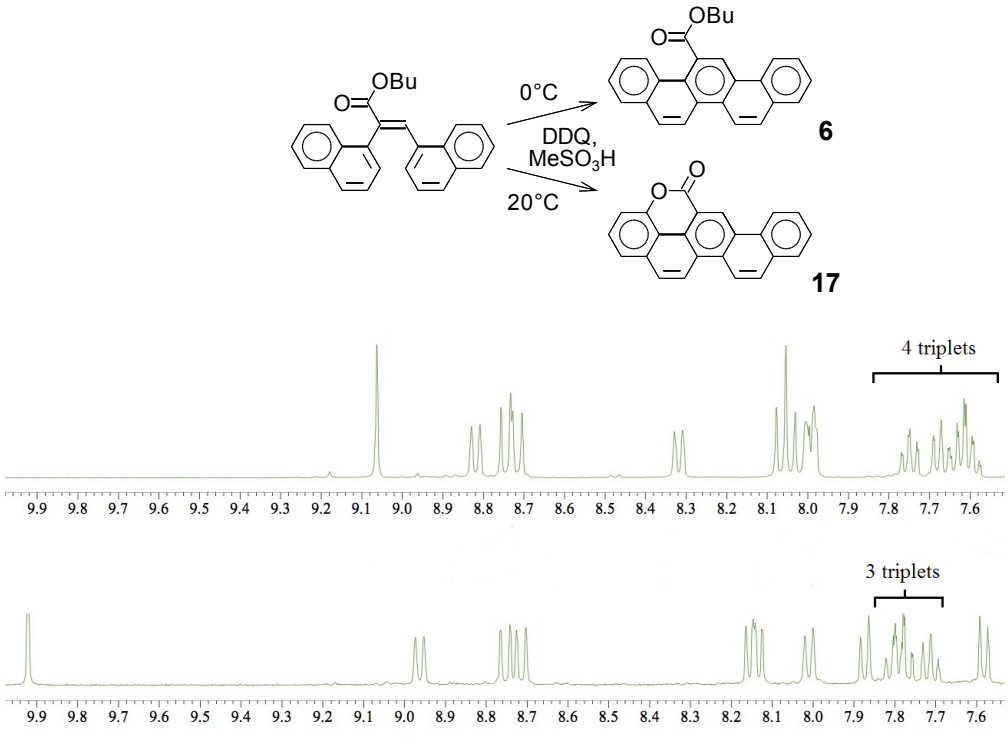

Fig. 3 Top: oxidative cyclodehydrogenation of butyl 2,3-bis-(1-naphthyl)acrylate to butyl picene-9-carboxylate (at 0°C) and to the corresponding intramolecular lactone (at 20°C). Bottom: aromatic region of the ^{1}H-NMR spectra in $CDCl_3$ of the ester (above) and the lactone (below).

To explain the variations in reactivity between the different alkyl 2,3-diaryl-acrylates, we consider that in the strongly acidic reaction medium, protonation at the ester carbonyl creates a positive charge localised in the terminal (aldehyde derived) aryl substituent of the diarylacrylate, and leads to electrophilic attack by the positively charged aldehyde-derived aryl group on the intermediate (arylacetic acid derived) aryl group. Stabilisation of the positive charge on the central aryl group is mesomerically forbidden. Reactivity is thus controlled by the ease of electrophilic attack on the intermediate aryl group, and the expected order of reactivity should be 3-thienyl (attacked in the very reactive 2-position) >> 2-naphthyl (attacked in the more reactive 1-position) > 1-naphthyl (attacked in the less reactive 2-position) >> phenyl, which concords with our observations. To tentatively explain the reactivity differences between substrates of same intermediate aryl group and different terminal aryl group – especially between the four dinaphthylacrylates –, steric effects may be considered: Whereas both in 1-naphthyl and in 2-naphthyl charge localisation in the desired position in the substituted naphthalene ring is favoured as the aromatic sextet can only be maintained if localised in the non-substituted ring of the naphthalene, a suitable orientation of the charged position close to the intermediate aryl substituent is sterically favoured in 1-naphthyl but disfavoured in 2-naphthyl.

In summary, we have found that the Scholl-analogous oxidative cyclisation of dialkyl 2,3-diarylacrylates with DDQ/$MeSO_3H$ in DCM is feasible (i) largely independently of the nature of the terminal aryl substituent if the intermediate aryl substituent is 3-thienyl, and (ii) if the terminal substituent is 1-naphthyl and the intermediate substituent is either 1- or 2-naphthyl.

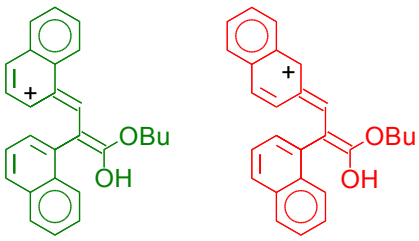

Fig. 4 Maximally conjugated and sterically least crowded conformations of protonated *trans*-2-(1-naphthyl)-3-(1-/2-naphthyl)-acrylates.

3.4. Conformational observations on crystallised cyclisation products

Butyl benzo[c]chrysene-6-carboxylate **10**, the condensation product obtained from butyl 2-(2-naphthyl)-3-(1-naphthyl)-acrylate, is the most sterically crowded cyclisation product obtained and contains a [4]helicene fragment. We obtained crystals good enough for X-ray crystallography, which allowed us to quantify the deviation from planarity in this arene system. It crystallises in racemic

crystals with two molecules of opposite helix sense in the unit cell, and the torsion angle between the a priori parallel "bay shore" C-C bonds of the first and fourth helicenic rings amounts to 37.1° and the distance of the two H-bearing carbons on opposite sides of the bay is 0.297nm, very slightly smaller than in unsubstituted [4]helicene (0.300nm).[28]

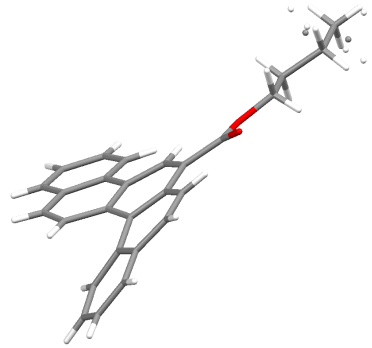

Fig. 5 Structure of crystallised butyl benzo[c]chrysene-6-carboxylate **10**.

We could further obtain a crystal structure from methyl phenanthro[1,2-b]thiophene-9-carboxylate **14**, the cyclisation product of methyl 2-(3-thienyl)-3-(1-naphthyl)-acrylate. This molecule is planar, with the carbonyl aligned in the plane of the aromatic moiety and pointing towards the thiophene side. The carbonyl thus chooses, as in the [4]helicenic structure, the same orientation towards the hydrogen on the closest neighbouring ring instead of towards the hydrogen on the same ring, even though in the thiophene case this next-ring hydrogen is further away than the same-ring hydrogen whereas in the helicene case it is closer than the same-ring hydrogen. In both molecules, the shortest C-C-bonds (i.e. with strongest double bond character) are those in meta-position to the ring-fusing bonds. It appears thus that the orientation of the carbonyl double bond is not dominated by steric effects but by a tendency towards transoid alignment with the most double-bond-like conjugated aromatic C-C bond. Conformational considerations of this type are important for the prediction of space-filling preferences and thus propensity of liquid crystalline self-assembly in arenes with several ester substituents.

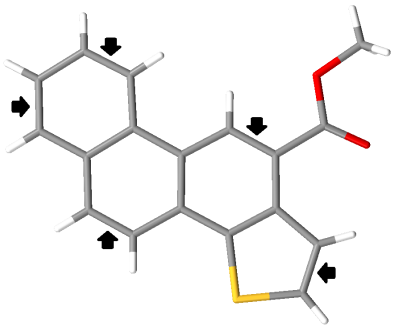

Fig. 6 Structure of crystallised methyl phenanthro[1,2-b]thiophene-9-carboxylate **14**. Arrows indicate carbon-carbon bonds of less than 0.138nm length; all others are longer than 0.140nm.

Methyl phenanthro [4,3-b] thiophene-5-methylcarboxylate **12**, the cyclisation product of methyl 2-(2-naphthyl)-3-(3-thienyl)-2-acrylate, also crystallised well enough to yield an X-ray crystal structure. It is an analogue of [4]helicene, where one of the terminal benzene rings is replaced by a thiophene ring with inward-pointing sulphur atom. Due to the comparatively smaller sterical hindrance, the torsion angle has been reduced to 8.6°. And as in the [4]helicene **10** and in isomeric **14**, the carbonyl oxygen is pointing as well towards the hydrogen on the closest neighbouring ring, not towards the same-ring hydrogen.

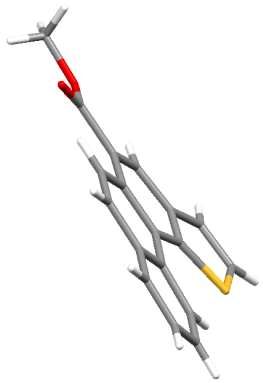

Fig. 7. Structure of crystallised phenanthro[4,3-b]thiophene-5-methylcarboxylate **12**.

3.5. Attempts towards ribbon-like structures by multiple Perkin and DDQ condensations

The good reactivity of diarylacrylates derived from 3-thienylacetic acid opens the perspective of using this methodology for the obtention of carboxy-functionalised areno-dithiophenes resulting from the combination of sufficiently reactive diformylarenes with 3-thienylacetic acid. Such arenodithiophenes would be suitable monomers for the obtention of rigidified poly(alkoxycarbonylthiophene)-analogous polymers [29] with enhanced planarity of the conjugated backbone and possibly enhanced semiconducting properties exploitable in organic electronics, where the presence of ester side chains allows both the tuning of physical properties by adjusting the size and form of the alkyl substituents, and the generation of conjugated polyelectrolytes by saponification.

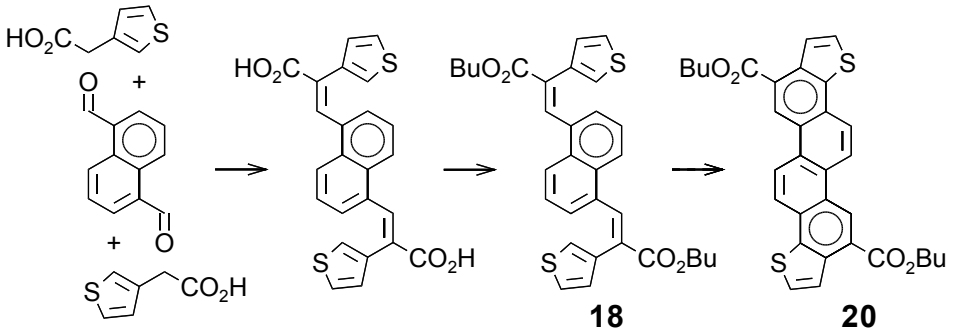

Fig.7 Approach to ester-decorated arenodithiophene polymerisation precursors, exemplified with 1,5-diformylnaphthalene.

We thus synthesised 1,5-diformylnaphthalene from commercial 1,5-dimethylnaphthalene as reported, by radical bromination followed by oxidation with *N*-methylmorpholine-*N*-oxide [30], and condensed it in a double Perkin reaction with 3-thienylacetic acid, which we attempted, after esterification to the dibutyl ester **18**, to doubly cyclise with DDQ/$MeSO_3H$ in DCM. To our chagrin, the reaction yielded a product **19** whose mass (1078.2 Da) corresponds to the double of the desired dicyclised product, minus two hydrogen atoms. The ^{1}H-NMR spectrum shows the right ratio between aliphatic and aromatic protons for a dimer of the expected chrysenodithiophene **20**. **19** was obtained both at 20 and at 0°C in reasonable yield (~50%) within 16h. Such a dimer could have been formed by oxidative dimerization at the reactive thiophene position, but four different sets of butyl chain signals and twice the expected number of different signals in the aromatic region testify of a non-symmetric dimeric structure. The ^{1}H-NMR spectrum of the symmetric dimer arising from coupling in the activated position adjacent to a sulfur atom should show 6 aromatic doublets and three aromatic singlets, whereas the product obtained shows 12 doublets, 5 singlets and one triplet. The presence of a triplet, necessarily located on a naphthalene, implies that one of the four oxidative thiophene-to-naphthalene cyclisations has not taken place in the desired way, and suggests that the corresponding thiophene unit has reacted otherwise. We prepared both the better soluble butyl derivative **19a** (from **18** in 51% yield) and the less soluble ethyl ester **19b** (from **19a**), and we obtained crystals with the former that were suitable for X-ray crystallography. The structure reveals that after double cyclisation, the active position adjacent to the sulfur attacks at the naphthalene moiety of a non-cyclised starting material or mono-cyclised intermediate, whereupon one thienyl unit of the attacked molecule strangely choses to couple with the carbon next to the attacked position to form a 7-membered ring. This scenario implies that with more dilute reaction conditions, this such unexpected dimerization should be avoidable. We were indeed able to suppress this dimerization by using an increased amount of solvent together with slow addition of the methanesulfonic acid, to successfully isolate the desired doubly cyclised monomer **20** in 50% yield.

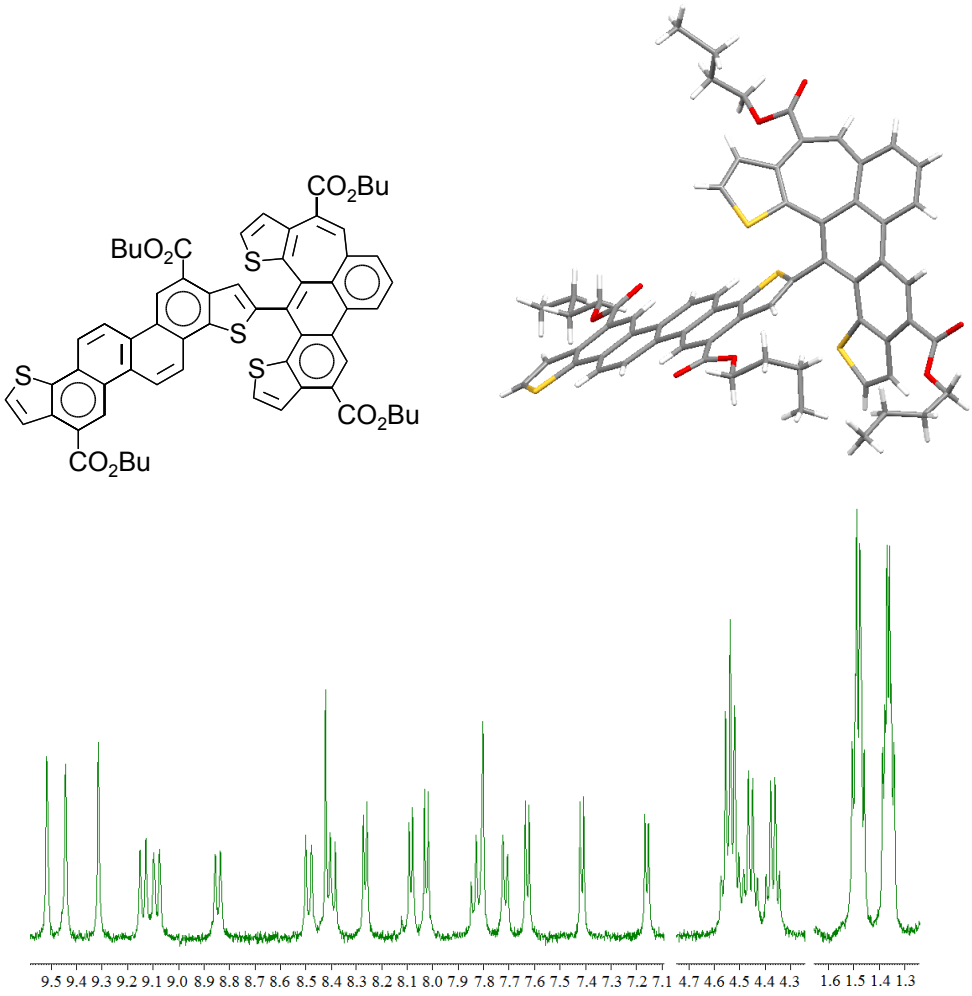

Fig.8 Top: Structure of crystallised unexpected dimer **19a** (R= Bu) formed by oxidation of **18**. Bottom: ^{1}H-NMR spectrum of the analogous ethyl ester **19b** (R= Et) in d_6-DMSO at 150°C clearly showing 5 singlets and 4 different methylene quartets. The one triplet is at the left flank of the rightmost singlet.

Having 1,5-diformylnaphthalene in hand, we also reacted it with naphthyl-1-acetic acid, but the resulting diester **21** did not even monocyclised with DDQ/$MeSO_3H$, neither at 20°C for 64h nor even at reflux for 16h. Apparently a distant second ester substituent is decisively desactivating in this case.

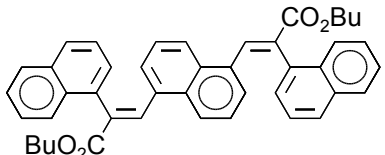

21

Fig.9 Potential precursor to [8]phenacene-dicarboxylate, synthesised from 1,5-diformylnaphthalene, that proved to be inert towards DDQ/$MeSO_3H$.

We measured the absorption spectra of the two arenodithiophenes **16** and **20** (fig. 10), as well as of the extended thienophenanthrene **14** and picene **6**. Only **6** and **20** possess chromophores long enough to

exhibit distinct absorption peaks at wavelengths greater than 350nm.

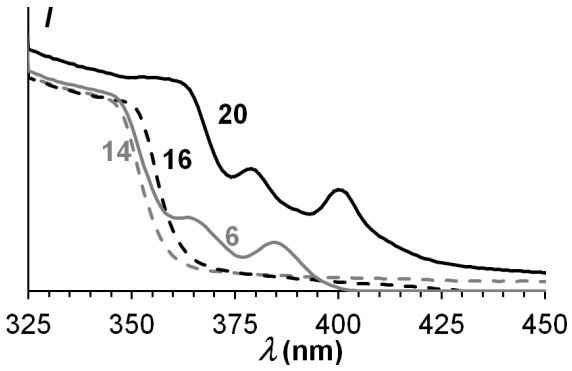

Fig.10 Absorption spectra of **6**, **14**, **16** and **20** in $CHCl_3$.

As the successful cyclisation of methyl 2,3-bis(3-thienyl)acrylate easily yielded a benzodithiophene monoester **16** with two thiophene extremities for potential polymerisation, we wondered whether the introduction of a second ester group would still allow the reaction, offering the potential of more varied substitution, *eg*. by replacement of the ester groups by an imide function after successful cyclisation. Perkin reactions have been reported also with a phenylglyoxylic acid in the place of the aromatic aldehyde, yielding diarylmaleic anhydrides [31, 32] which may be esterified prior to cyclisation attempts. As 3-thienylglyoxylic acid is not commercially available but 2-thienylglyoxylic acid is, we condensed the latter with 3-thienylacetic acid to obtain, after esterification, dimethyl 2-(2-thienyl)-3-(3-thienyl)-maleate **22**. The reaction proceeded slowly and leads to the expected product **23** in only moderate yield (34%) after 64h, accompanied by substantial amounts of side products. From one demethylated crystalline side product **24** obtained in small amounts we could obtain an X-ray structure: Surprisingly, the 3-thiophene ring there has been split open by the neighbouring carboxy group to give a thiopyranone cycle (fig. 11). We could not find any literature reference to any similar reaction. We also obtained a crystallographic structure of the expected product **23** (fig. 11), allowing us to quantify the sterically imposed out-of-plane orientation of the two carbonyl groups, which make angles of *c.*60° and *c.*30° with the aromatic plane (values differ slightly between the two molecules in the crystallographic unit cell) and are surprisingly oriented towards same sides of the plane. The aromatic moiety is perfectly planar, and due to the compensating positions of the pentagon-deforming sulphur atoms in the two thiophene rings, the two C-H bonds next to the sulphur atoms on opposite sides of the molecule make an angle of 120° with each other, indicating that a cyclic head-to-tail hexamer with six transoid thiophene-thiophene bonds could in principle form without strain.

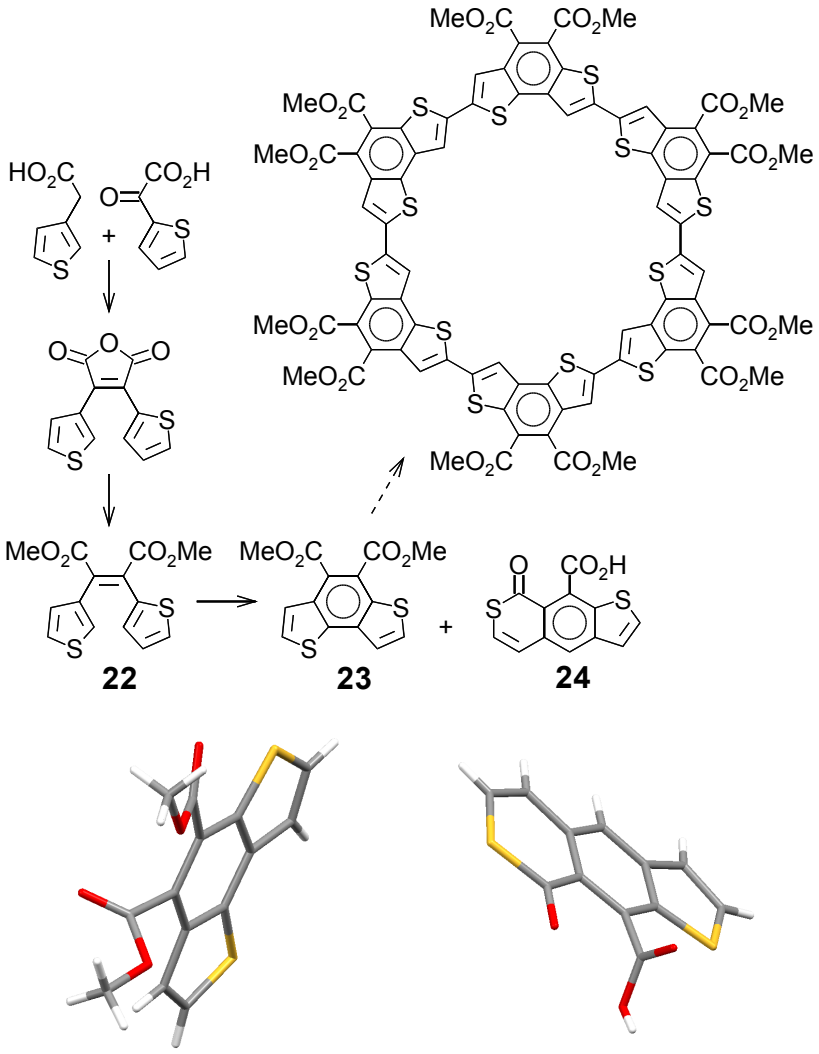

Fig.11 Synthesis of dimethyl 2-(2-thienyl)-3-(3-thienyl)-maleate **22** and cyclisation to benzodithiophene **23** and thiopyranone **24** together with their structures in crystals, and hypothetical cyclic hexamer of **23**.

3.6. Conclusion

To sum up, we found that the DDQ/$MeSO_3H$ promoted oxidative cyclisation of Perkin condensation products is of only limited efficiency on homoaromatic substrates and is unlikely to lead to extended homoaromatic ribbons unless particularly reactive bifunctional aromatic dialdehydes and aromatic diacetic acids are found. In contrast, the combination of thienylacetic acid with aromatic dialdehydes may yield interesting arenodithiophene monomers for the construction of conjugated polymers made up of short ribbon segments linked by highly planar thienyl-thienyl junctions. We obtained one such monomer based on 1,5-diformylnaphthalene, and were successful in obtaining simpler carboxysubstituted potential monomers of this type in the form of benzodithiophenes.

3.7. Experimental

Single Perkin condensations of arylacetic acids with formylarenes followed by esterification

General procedure for Perkin condensations

To a mixture of arylacetic acid (30 mmol), triethylamine (5.05 g, 50 mmol) and acetic anhydride (10.2 g, 100 mmol), the aldehyde (30 mmol) and THF (50 mL) were added. The mixture, which turned into a homogeneous solution upon heating, was stirred at reflux under exclusion of moisture for 16h. Water (50 mL) was added and reflux continued for 1 h. The mixture was concentrated under reduced pressure. The residue was dissolved in 20% aqueous KOH (200 mL) and the crude product was precipitated by acidification with concentrated hydrochloric acid. The precipitate was filtered, dried on air and esterified without further purification.

General procedure for acidic esterifications to methyl esters with sulphuric acid

To a solution in methanol (300 mL) of the crude product of the Perkin condensation, a solution of concentrated sulfuric acid in methanol (2 mL in 10 mL, caution during preparation!) was added dropwise trough a reflux condenser. The reaction mixture was refluxed for 5 h under exclusion of moisture and then concentrated at reduced pressure to a volume of 100 mL. It was kept overnight in the freezer and the ensuing precipitate was filtered and recrystallised from methanol.

General procedure for basic esterifications to methyl or butyl esters with DBU

To a solution in methanol (300 mL) (for methyl esters) or *n*-butanol (300 mL) (for butyl esters) of the crude product of the Perkin condensation, DBU (9.1 g, 60 mmol) and iodomethane (14.2 g, 100 mmol) or 1-bromobutane (13.7 g, 100 mmol) was added. The solution was stirred at 60^0 C for 4 hrs under exclusion of moisture, then concentrated at reduced pressure and chromatographed in chloroform through silica. The product was recrystallised from methanol (methyl esters) or *n*-butanol (butyl esters).

*The substrates for the successful or failed oxidative cyclisations to the cyclised esters **1** to **16** (fig. 2) are in the following designated as **pre1** to **pre16**.*

Methyl *trans*-2,3-diphenylacrylate (pre1)

Yield from phenylacetic acid and benzaldehyde after acidic esterification: 3.4 g (48%) of white powder. ^{1}H NMR (400 MHz, $CDCl_3$): ∂ = 7.84 (s, 1H), 7.36 (m, 3H), 7.17 (m, 5H), 7.02 (d, 2H, J= 7.3 Hz), 3.78 (s, 3H) ppm. ^{13}C NMR (100MHz, $CDCl_3$) : ∂ = 168.4, 140.6, 135.9, 134.7, 132.5, 130.7

(2 Carbons), 129.8 (2 Carbons), 129.1, 128.7 (2 Carbons), 128.3 (2 Carbons), 127.9, 52.5 ppm. Elemental analysis calcd (%) for $C_{16}H_{14}O_2$: C 80.65, H 5.92; found: C 80.93, H 5.63.

Methyl *trans*-2-phenyl-3-(1-naphthyl)-acrylate (pre2)

Yield from phenylacetic acid and naphthalene-1-carbaldehyde after acidic esterification: 3.4 g (39%) of grey flakes. ^{1}H NMR (400 MHz, $CDCl_3$): ∂ = 8.53 (s, 1H), 8.16 (d, 1H, J= 8.2 Hz), 7.85 (d, 1H, J= 7.8 Hz), 7.71 (d, 1H, J= 8.2 Hz), 7.55 (m, 2H), 7.23 (m, 3H), 7.16 (m, 3H), 7.00 (d, 1H, J= 7.3 Hz), 3.90 (s, 3H) ppm. ^{13}C NMR (100MHz, $CDCl_3$) : ∂ = 168.3, 139.0, 135.5, 135.0, 133.5, 132.3, 132.2, 130.3 (2 Carbons), 129.0, 128.8, 128.2 (3 Carbons), 127.7, 126.7, 126.2, 125.2, 124.3, 52.6 ppm. Elemental analysis calcd (%) for $C_{20}H_{16}O_2$: C 83.31, H 5.59; found: C 83.21, H 5.71.

Methyl *trans*-2-phenyl-3-(2-naphthyl)-acrylate (pre3)

Yield from phenylacetic acid and naphthalene-2-carbaldehyde after acidic esterification: 4.3 g (49%) of white powder. ^{1}H NMR (400 MHz, $CDCl_3$): ∂ = 8.02 (s, 1H), 7.70 (d, 1H, J= 7.8 Hz), 7.64 (broad s, 2H), 7.53 (d, 1H, J= 8.7 Hz), 7.42 (m, 5H), 7.26 (m, 2H), 6.98 (d, 1H, J= 8.7 Hz), 3.82 (s, 3H) ppm. ^{13}C NMR (100MHz, $CDCl_3$) : ∂= 168.5, 140.7, 136.0, 133.4, 133.0, 132.6, 132.3, 131.7, 130.0 (2 Carbons), 128.8 (2 Carbons), 128.6, 128.0, 127.64, 127.61, 127.1, 127.0, 126.4, 52.6 ppm. Elemental analysis calcd (%) for $C_{20}H_{16}O_2$: C 83.31, H 5.59; found: C 83.21, H 5.44.

Methyl *trans*-2-phenyl-3-(3-thienyl)-acrylate (pre4)

Yield from phenylacetic acid and thiophene-3-carbaldehyde after acidic esterification: 3.6 g (49%) of brown powder. ^{1}H NMR (400 MHz, $CDCl_3$): ∂ = 7.86 (s, 1H), 7.40 (m, 3H) 7.23 (dd, 2H, J= 2.3 Hz, 7.3 Hz), 7.08 (m, 1H), 7.05 (m, 1H), 6.44 (d, 1H, J= 4.1 Hz), 3.76 (s, 3H) ppm. ^{13}C NMR (100MHz, $CDCl_3$) : ∂ = 168.4, 136.8, 136.4, 134.5, 130.7, 129.7 (2 Carbons), 129.6, 128.8 (2 Carbons), 128.4, 128.1, 125.5, 52.4 ppm. Elemental analysis calcd (%) for $C_{14}H_{12}O_2S$: C 68.83, H 4.95; found: C 68.73, H 4.93.

Methyl *trans*-2-(1-naphthyl)-3-phenyl-acrylate (pre5)[33]

Yield from naphthyl-1-acetic acid and benzaldehyde after acidic esterification: 3.5 g (40%) of brown oil.^{1}H NMR (400 MHz, $CDCl_3$): ∂ = 8.20 (s, 1H), 7.95-7.83 (m, 3H), 7.55-7.36 (m, 4H), 7.14 (t, J=7.5Hz, 1H), 7.07 (t, J=7.5Hz, 2H), 6.98 (d, 7.5Hz, 2H), 3.74 (s, 3H) ppm.

Butyl *trans*-2,3-di-(1-naphthyl)-acrylate (pre6)

Yield from naphthyl-1-acetic acid and naphthalene-1-carbaldehyde after basic esterification: 5.2 g (46%) of white powder. ^{1}H NMR (400 MHz, $CDCl_3$): ∂ = 8.72 (s, 1H), 8.23 (d, 1H, J= 8.2 Hz), 7.84

(d, 2H, J= 8.7 Hz), 7.78 (d, 1H, J= 8.2 Hz), 7.75 (d, 1H, J= 8.0 Hz), 7.60 (m, 2H), 7.51 (d, 1H, J= 6.9 Hz), 7.41 (m, 2H), 7.28 (d, 1H, J= 7.3 Hz), 7.14 (d, 1H, J= 6.0 Hz), 6.92 (t, 1H, J= 7.8 Hz), 6.81 (d, 1H, J= 7.3 Hz), 4.18 (m, 2H), 1.56 (m, 2H), 1.13 (m, 2H), 0.78 (t, 3H, J= 7.3 Hz) ppm. ^{13}C NMR (100MHz, $CDCl_3$) : ∂ = 168.1, 139.8, 134.0, 133.9, 133.5, 133.4, 132.7, 132.1, 131.9, 129.1, 128.8, 128.6, 128.2, 127.7, 127.3, 126.7, 126.3, 126.1, 125.9, 125.6, 125.3, 125.1, 124.1, 65.2, 30.6, 19.1, 13.7 ppm. Elemental analysis calcd (%) for $C_{27}H_{24}O_2$: C 85.23, H 6.36; found: C 85.19, H 6.46.

Butyl *trans*-2-(1-naphthyl)-3-(2-naphthyl)-acrylate (pre7)

Yield from naphthyl-1-acetic acid and naphthalene-2-carbaldehyde after basic esterification: 5.0 g (44%) of white powder. ^{1}H NMR (400 MHz, $CDCl_3$): ∂ = 8.27 (s, 1H), 7.91 (dd, 2H, J= 2.8 Hz, 7.79 Hz), 7.82 (d, 1H, J= 8.2 Hz), 7.62 (m, 2H), 7.57 (d, 1H, J= 7.8 Hz), 7.47 (m, 2H), 7.36 (m, 5H), 6.81 (d, 1H, J= 8.7 Hz), 4.16 (m, 2H), 1.50 (m, 2H), 1.15 (m, 2H), 0.79 (t, 3H, J= 7.8 Hz) ppm. ^{13}C NMR (100MHz, $CDCl_3$) : ∂ = 168.3, 141.8, 134.3, 133.8, 133.4, 133.0, 132.2, 131.9, 131.4, 128.6 (2 carbons), 128.5, 128.4, 127.8, 127.5, 127.4, 127.1, 126.6, 126.4, 126.3, 126.1, 125.9, 125.3, 65.1, 30.6, 19.1, 13.7 ppm. Elemental analysis calcd (%) for $C_{27}H_{24}O_2$: C 85.23, H 6.36; found: C 85.28, H 6.45.

Methyl *trans*-2-(1-naphthyl)-3-(3-thienyl)-acrylate (pre8)

Yield from naphthyl-1-acetic acid and thiophene-3-carbaldehyde after acidic esterification: 3.7 g (43%) of pale yellow powder. ^{1}H NMR (400 MHz, $CDCl_3$): ∂ = 8.15 (s, 1H), 7.91 (m, 2H), 7.75 (d, 1H, J= 8.2 Hz), 7.50 (m, 2H), 7.40 (t, 1H, J= 7.8 Hz), 7.35 (d, 1H, 6.9 Hz), 6.98 (s, 1H), 6.96 (m, 1H), 6.23 (d, 1H, J= 5.0 Hz), 3.70 (s, 3H) ppm. ^{13}C NMR (100MHz, $CDCl_3$) : ∂ = 168.7, 136.7, 136.0, 134.2, 133.8, 131.9, 130.0, 128.7, 128.64, 128.55, 128.3, 127.3, 126.6, 126.3, 126.0, 125.6, 125.1, 52.5 ppm. Elemental analysis calcd (%) for $C_{18}H_{14}O_2S$: C 73.44, H 4.79; found: C 73.68, H 4.93.

Methyl *trans*-2-(2-naphthyl)-3-phenyl-acrylate (pre9)

Yield from naphthyl-2-acetic acid and benzaldehyde after acidic esterification: 4.2 g (48%) of white powder. ^{1}H NMR (400 MHz, $CDCl_3$): ∂ = 7.86 (s, 1H), 7.77 (m, 2H), 7.70 (d, 1H, J= 7.8 Hz), 7.65 (s, 1H), 7.40 (m, 2H), 7.23 (d, 1H, J= 8.7 Hz), 7.09 (pseudo t, 1H, J= 6.4 Hz, 6.0 Hz), 7.00 (m, 4H), 3.71 (s, 3H) ppm. ^{13}C NMR (100MHz, $CDCl_3$) : ∂ = 168.8, 141.0, 134.5, 133.5, 133.3, 132.9, 132.1, 130.7 (2 Carbons), 129.2, 128.8, 128.3 (3 Carbons), 128.1, 127.8, 127.7, 126.3, 126.1, 52.5 ppm. Elemental analysis calcd (%) for $C_{20}H_{16}O_2$: C 83.31, H 5.59; found: C 83.00, H 5.89.

Butyl *trans*-2-(2-naphthyl)-3-(1-naphthyl)-acrylate (pre10)

Yield from naphthyl-2-acetic acid and naphthalene-1-carbaldehyde after basic esterification: 5.4 g (47%) of white powder. ^{1}H NMR (400 MHz, $CDCl_3$): ∂ = 8.61 (s, 1H), 8.22 (d, 1H, J= 11.0 Hz), 7.85

(d, 1H, J= 10.5 Hz), 7.78 (d, 1H, J= 7.8 Hz), 7.73 (s, 1H), 7.67 (m, 3H), 7.61 (pseudo t, 1H, J= 6.9 Hz, 8.2 Hz), 7.54 (pseudo t, 1H, J= 4.1 Hz, 9.6 Hz), 7.43 (m, 2H), 7.25 (d, 1H, J= 6.0 Hz), 7.04 (m, 2H), 4.34 (t, 2H, J= 6.9 Hz), 1.73 (m, 2H), 1.46 (m, 2H), 0.98 (t, 3H, J= 7.3 Hz) ppm. ^{13}C NMR (100MHz, $CDCl_3$) : ∂ = 168.0, 138.7, 135.1, 133.5, 133.3, 133.1, 132.8, 132.3, 132.2, 129.6, 129.0, 128.8, 128.4 (2 Carbons), 128.2, 127.7, 127.6, 126.7, 126.20, 126.17, 126.0, 125.3, 124.3, 65.4, 30.9, 19.4, 13.9 ppm. Elemental analysis calcd (%) for $C_{27}H_{24}O_2$: C 85.23, H 6.36; found: C 85.11, H 6.47.

Butyl *trans*-2,3-di-(1-naphthyl)-acrylate (pre11)

Yield from naphthyl-2-acetic acid and naphthalene-2-carbaldehyde after basic esterification: 5.8 g (51%) of white powder. ^{1}H NMR (400 MHz, $CDCl_3$): ∂ = 8.01 (s, 1H), 7.86 (pseudo t, 2H, J= 10.5 Hz, 9.2 Hz), 7.73 (m, 3H), 7.64 (d, 1H, J= 7.3 Hz), 7.61 (d, 1H, J= 7.8 Hz), 7.41 (m, 6H), 6.96 (d, 1H, J= 8.7 Hz), 4.23 (t, 2H, J= 6.9 Hz), 1.64 (m, 2H), 1.35 (m, 2H), 0.90 (t, 3H, J= 7.3 Hz) ppm. ^{13}C NMR (100MHz, $CDCl_3$) : ∂ = 168.2, 140.6, 133.53, 133.51, 133.4, 133.1, 132.9, 132.8, 132.4, 131.8, 129.2, 128.5, 128.3, 128.2, 128.1, 127.8, 127.7, 127.6, 127.1, 126.8, 126.34, 126.27, 126.1, 65.3, 30.7, 19.3, 13.8 ppm. Elemental analysis calcd (%) for $C_{27}H_{24}O_2$: C 85.23, H 6.36; found: C 85.22, H 6.36.

Methyl *trans*-2-(2-naphthyl)-3-(3-thienyl)-acrylate (pre12)

Yield from naphthyl-2-acetic acid and thiophene-3-carbaldehyde after acidic esterification: 4.3 g (49%) of grey powder. ^{1}H NMR (400 MHz, $CDCl_3$): ∂ =7.96 (s, 1H), 7.89 (m, 2H), 7.80 (d, 1H, J= 9.2 Hz), 7.75 (s, 1H), 7.49 (m, 2H), 7.33 (d, 1H, J= 8.2 Hz), 7.12 (s, 1H), 6.97 (dd, 1H, J= 5.0 Hz, 3.2 Hz), 6.45 (d, 1H, J= 5.0 Hz), 3.77 (s, 3H) ppm. ^{13}C NMR (100MHz, $CDCl_3$) : ∂ =168.7, 136.8, 134.8, 133.9, 133.6, 133.0, 130.5, 130.0, 128.8, 128.6, 128.4, 128.3, 127.9, 127.7, 126.4, 126.3, 125.7, 52.5 ppm. Elemental analysis calcd (%) for $C_{18}H_{14}O_2S$: C 73.44, H 4.79; found: C 73.79, H 4.84.

Methyl *trans*-2-(3-thienyl)-3-phenyl-acrylate (pre13)

Yield from thienyl-3-acetic acid and benzaldehyde after acidic esterification: 3.2 g (44%) of brown solid. ^{1}H NMR (400 MHz, $CDCl_3$): ∂ = 7.83 (s, 1H), 7.31 (dd, 1H, J= 2.8 Hz, 5.0 Hz), 7.21 (m, 4H), 7.10 (m, 2H), 6.93 (dd, 1H, J= 1.4 Hz, 5.0 Hz), 3.81 (s, 3H) ppm. ^{13}C NMR (100MHz, $CDCl_3$) : ∂ = 168.1, 141.2, 135.2, 134.9, 130.3 (2 Carbons), 129.2, 129.1, 128.4 (2 Carbons), 127.4, 125.5, 125.0, 52.5 ppm. Elemental analysis calcd (%) for $C_{14}H_{12}O_2S$: C 68.83, H 4.95; found: C 68.51, H 5.07.

Methyl *trans*-2-(3-thienyl)-3-(1-naphthyl)-acrylate (pre14)

Yield from thienyl-3-acetic acid and naphthalene-1-carbaldehyde after acidic esterification: 3.6 g (41%) of white powder. ^{1}H NMR (400 MHz, $CDCl_3$): ∂ = 8.40 (s, 1H), 8.06 (d, 1H, J= 6.9 Hz), 7.85 (d, 1H, J= 8.2 Hz), 7.75 (d, 1H, J= 8.2 Hz), 7.52 (m, 2H), 7.26 (t, 1H, 8.2 Hz), 7.1 (m, 3H), 6.76 (d,

1H, J= 4.6 Hz), 3.90 (s, 3H) ppm. ^{13}C NMR (100MHz, $CDCl_3$) : ∂ = 168.0, 138.8, 134.8, 134.0, 132.8, 131.8, 129.7, 129.3, 129.0, 128.7, 127.5, 126.6, 126.2, 125.8, 125.3, 124.6, 124.3, 52.6 ppm. Elemental analysis calcd (%) for $C_{18}H_{14}O_2S$: C 73.44, H 4.79; found: C 73.84, H 4.99.

Methyl *trans*-2-(3-thienyl)-3-(2-naphthyl)-acrylate (pre15)

Yield from thienyl-3-acetic acid and naphthalene-2-carbaldehyde after acidic esterification: 4.1 g (46%) of white powder. ^{1}H NMR (400 MHz, $CDCl_3$): ∂ = 7.98 (s, 1H), 7.72 (d, 1H, J= 8.7 Hz), 7.67 (m, 2H), 7.58 (d, 1H, J= 8.7 Hz), 7.43 (m, 2H), 7.32 (dd, 1H, J= 2.7 Hz, 4.58 Hz), 7.19 (dd, 1H, J= 2.7 Hz, 1.4 Hz), 7.05 (dd, 1H, J= 1.4 Hz, 8.7 Hz), 6.95 (dd, 1H, J= 0.9 Hz, 5.0 Hz), 3.82 (s, 3H) ppm. ^{13}C NMR (100MHz, $CDCl_3$) : ∂ = 168.2, 141.3, 135.3, 133.5, 133.1, 132.5, 131.3, 129.2, 128.6, 127.7, 127.6, 127.4, 127.1, 126.7, 126.4, 125.6, 125.3, 52.6 ppm. Elemental analysis calcd (%) for $C_{18}H_{14}O_2S$: C 73.44, H 4.79; found: C 73.17, H 4.84. HRMS (m/z (%)): calcd. For $C_{18}H_{14}O_2S$ $[M]^+$ 294.0714; found 294.0700.

Methyl *trans*-2,3-di-(3-thienyl)-acrylate (pre16)

Yield from thienyl-3-acetic acid and thiophene-3-carbaldehyde after basic esterification: 3.0 g (40%) of brown needles. ^{1}H NMR (400 MHz, $CDCl_3$): ∂ = 7.86 (s, 1H), 7.37 (m, 1H), 7.18 (broad s, 2H), 7.10 (m, 1H), 6.97 (d, 1H, J= 4.6 Hz), 6.55 (d, 1H, J= 5.0 Hz), 3.78 (s, 3H) ppm. ^{13}C NMR (100MHz, $CDCl_3$) : ∂ = 168.2, 136.8, 135.8, 135.4, 129.7, 129.0, 128.1, 125.9, 125.7, 125.6, 124.7, 52.5 ppm. Elemental analysis calcd (%) for $C_{12}H_{10}O_2S_2$: C 57.57, H 4.03; found: C 57.36, H 4.21.

***trans,trans*-1,5-Bis-(2-(3-thienyl)-2-(butoxycarbonyl)-vinyl)-naphthalene (18)**

To a mixture of thienyl-3-acetic acid (8.52 g, 60 mmol), triethylamine (10.1 g, 100 mmol) and acetic anhydride (20.4 g, 200 mmol), naphthalene-1,5-di-carbaldehyde (5.53 g, 30 mmol)and THF (100 mL) were added. The mixture, which turned into a homogeneous solution upon heating, was stirred at reflux under exclusion of moisture for 16 h. The Perkin condensation product precipitated upon cooling to room temperature and was filtered off after 5 h, washed with water, dried on air and dissolved in butanol (500 mL). DBU (9.1 g, 60 mmol) and 1-bromobutane (13.7 g, 100 mmol) were added and the solution was stirred at 60^0 C for 4 hrs under exclusion of moisture, then concentrated at reduced pressure chromatographed in chloroform through silica. The product was recrystallised from butanol. Yield: 9.0 g (55%) of pale yellow powder. ^{1}H NMR (400 MHz, $CDCl_3$): ∂ = 8.32 (s, 1H), 7.95 (d, 1H, J= 8.3 Hz), 7.29 (t, 1H, J= 7.3 Hz), 7.12 (m, 3H), 6.73 (d, 1H, J= 4.6 Hz), 4.30 (t, 2H, J= 6.9 Hz), 1.73 (m, 2H), 1.44 (m, 2H), 0.97 (t, 3H, J= 7.3 Hz) ppm. ^{13}C NMR (100MHz, $CDCl_3$) : ∂ = 167.6, 138.3, 134.6, 133.6, 131.7, 130.4, 129.2, 127.6, 125.8 (x2), 125.1, 124.4, 65.4, 34.8, 19.3, 13.9.

***trans,trans*-1,5-Bis-(2-(1-naphthyl)-2-(butoxycarbonyl)-vinyl)-naphthalene (21)** was synthesised following the procedure for **18** using naphthyl-1-acetic acid (11.17 g, 60 mmol) instead of thienyl-3-acetic acid. Yield: 9.3 g (58%) of white powder. ^{1}H NMR (400 MHz, $CDCl_3$): ∂ = 8.67 (s, 1H), 8.00 (d, 1H, J= 8.2 Hz), 7.84 (d, 1H, J= 8.2 Hz), 7.80 (d, 1H, J= 8.2 Hz), 7.76 (d, 1H, J= 8.2 Hz), 7.47 (d, 1H, J= 6.9 Hz), 7.40 (broad s, 1H), 7.27 (broad s, 1H), 7.05 (broad s, 1H), 7.01 (d, 1H, J= 7.8 Hz), 6.87 (d, 1H, J= 7.3 Hz), 4.15 (m, 2H), 1.47 (m, 2H), 1.10 (m, 2H), 0.75 (t, 3H, J= 7.8 Hz) ppm. ^{13}C NMR (100MHz, $CDCl_3$) : ∂ = 168.0, 139.8 (2 Carbons), 133.7, 133.5, 132.7, 132.6, 132.9, 128.6, 128.2, 127.7, 127.4, 126.3, 125.9, 125.7, 125.5, 125.2, 125.0, 65.2, 30.6, 19.1, 13.8 ppm. HRMS (m/z (%)): calcd. For $C_{44}H_{40}O_4$ $[M]^+$, 632.2926; found 632.2904.

Dimethyl 2-(2-thienyl)-3-(3-thienyl)-maleate (22)

To a mixture of thienyl-3-acetic acid (4.26 g, 30 mmol), triethylamine (5.05 g, 50 mmol) and acetic anhydride (10.2 g, 100 mmol), thienyl-2-glyoxylic acid (4.70 g, 30 mmol) and THF (50 mL) were added. The mixture, which turned into a homogeneous solution upon heating, was stirred at reflux under exclusion of moisture for 2 h. Water (50 mL) was added and reflux continued for 1 h. The mixture was concentrated under reduced pressure. The residue was dissolved in 20% aqueous KOH (200 mL) and the crude product was precipitated by acidification with concentrated hydrochloric acid. The precipitate was filtered, dried on air and dissolved in methanol. DBU (13.7 g, 90 mmol) and methyl iodide (15.6 g, 120 mmol) was added. The solution was stirred at room temperature for 3d, concentrated at reduced pressure and chromatographed through silica with chloroform as eluent. The product was recrystallized from methanol. Yield: 5.6 g (61%) of yellow needles. ^{1}H NMR (400 MHz, $CDCl_3$): ∂ = 7.34 (dd, 1H, J= 3.2 Hz, 5.0 Hz), 7.31 (d, 1H, J= 5.0 Hz), 7.25 (d, 1H, J= 3.2 Hz), 7.03 (d, 1H, J= 5.0 Hz), 6.93 (dd, 1H, J= 3.7 Hz, 5.0 Hz), 6.85 (d, 1H, J= 5.0 Hz), 3.93 (s, 3H), 3.76 (s, 3H) ppm. ^{13}C NMR (100MHz, $CDCl_3$) : ∂ = 168.2, 167.1, 136.3, 136.2, 133.8, 131.5, 130.6, 128.5, 127.0 (2 Carbons), 126.7, 126.4, 125.6, 52.9, 52.7 ppm. Elemental analysis calcd (%) for $C_{14}H_{12}O_4S_2$: C 54.53, H 3.92; found: C 54.18, H 3.86.

Oxidative ring closures

General procedure

Except when stated otherwise, all cyclodehydrogenation reactions with DDQ were performed under argon atmosphere in septum-sealed 50 ml round bottom flasks. To the ester substrate (3mmol) and 1.2 equivalents of DDQ (820 mg, 3.6 mmol), methanesulfonic acid (3 ml, ~10 equiv.) and anhydrous dichloromethane (30 ml) were added at 0°C with stirring. The dark green solution was stirred at room

temperature (0°C for **6**). The progress of the reaction was monitored by TLC. After the completion of reaction, the reaction mixture was quenched with 10% $NaHCO_3$ solution (100 ml). The dichloromethane layer was separated, washed with water and brine solution, dried over anhydrous Na_2SO_4 and filtered. The solvent was removed under reduced pressure and the crude product was chromatographed through silica in DCM and recrystallised from methanol (methyl esters) or butanol (butyl esters).

Butyl picene-13-carboxylate (6)

Reaction time: 64 h at 0° C. Yield: 680 mg (60%) of white powder. ^{1}H NMR (400 MHz, $CDCl_3$): ∂ = 9.06 (s, 1H), 8.82 (d, 1H, J= 8.7 Hz), 8.75 (d, 1H, J= 9.6 Hz), 8.72 (d, 1H, J= 9.2 Hz), 8.32 (d, 1H, J= 8.2 Hz), 8.07 (t, 2H, J= 9.2 Hz), 7.99 (m, 2H), 7.75 (m, 1H), 7.63 (m, 3H), 4.47 (t, 2H, J= 6.9 Hz), 1.69 (m, 2H), 1.31 (m, 2H), 0.89 (t, 3H, J= 7.8 Hz) ppm. ^{13}C NMR (100MHz, $CDCl_3$) : ∂ = 172.6, 132.7, 132.1, 130.5, 129.9 (2 Carbons), 129.5, 129.4, 129.2, 128.6 (2 Carbons), 128.4, 127.5, 127.3, 127.1, 127.0, 126.7, 126.0, 125.9, 124.0, 123.3, 121.3 (2 Carbons), 65.9, 30.5, 19.2, 13.7 ppm. Elemental analysis calcd (%) for $C_{27}H_{22}O_2$: C 85.69, H 5.86; found: C 85.49, H 6.12. MS (m/z (%)): 378.2 (100, $[M]^+$); 379.2 (30, $[M+H]^+$); 380.2 (5, $[M+2H]^+$); HRMS (m/z (%)): calcd. for $C_{27}H_{22}O_2Na^+$ $[M+Na]^+$, 401.1512; found, 401.1521.

Reaction at 20°C for 64h yields lactone **17**: Yield: 410 mg (43%) of white powder. ^{1}H NMR (400 MHz, $CDCl_3$): ∂ = 9.92 (s, 1H), 8.96 (d, 1H, J= 8.2 Hz), 8.75 (d, 1H, J= 9.2 Hz), 8.71 (d, 1H, J= 9.2 Hz), 8.15 (dd, 2H, J= 7.3 Hz, 9.2 Hz), 8.01 (d, 1H, J= 7.8 Hz), 7.87 (d, 1H, J= 8.2 Hz), 7.80 (m, 2H), 7.71 (Pseudo t, 1H, J= 7.8 Hz, 7.3 Hz), 7.58 (d, 1H, J= 7.8 Hz). HRMS (m/z (%)): calcd. for $C_{23}H_{12}O_2$ $[M]^+$, 320.0837; found, 320.0836.

Butyl benzo[c]chrysene-6-carboxylate (10)

Reaction time: 64 h at 20° C. Yield: 465 mg (41%) of white powder. ^{1}H NMR (400 MHz, $CDCl_3$): ∂ = 9.44 (s, 1H), 8.95 (d, 1H, J= 9.6 Hz), 8.93 (d, 1H, J= 9.2 Hz), 8.85 (d, 1H, J= 9.2 Hz), 8.84 (d, 1H, J= 8.2 Hz), 8.03 (m, 3H), 7.96 (d, 1H, J= 9.2 Hz), 7.77 (t, 1H, J= 8.2 Hz), 7.70 (d, 1H, J= 6.9 Hz), 7.66 (d, 1H, J= 9.6 Hz), 7.65 (dd, 1H, J= 1.4 Hz, 3.2 Hz), 4.54 (t, 2H, J= 6.9 Hz), 1.92 (m, 2H), 1.61 (m, 2H), 1.07 (t, 3H, J= 7.3 Hz) ppm. ^{13}C NMR (100MHz, $CDCl_3$) : ∂= 168.4, 133.3, 131.7, 130.7, 130.6, 129.9, 129.2, 129.0, 128.7, 128.4, 128.33, 128.26 (2 Carbons), 128.2, 127.3, 127.1, 126.64 (2 Carbons), 126.60, 125.9, 125.7, 123.6, 123.3, 65.5, 31.0, 19.6, 14.0 ppm. Elemental analysis calcd (%) for $C_{27}H_{22}O_2$: C 85.69, H 5.86 found: C 85.71, H 5.83.

Methyl phenanthro[4,3-b]thiophene-5-carboxylate (12)

Reaction time: 64 h at 20° C. Yield: 100 mg (11%) of white powder. ^{1}H NMR (400 MHz, $CDCl_3$): ∂ = 9.22 (d, 1H, J= 8.2 Hz), 8.89 (d, 1H, J= 9.2 Hz), 8.64 (s, 1H), 8.01 (d, 1H, J= 7.8 Hz), 7.92 (d, 1H, J= 9.2 Hz), 7.82 (t, 1H, J= 8.7 Hz), 7.69 (m, 2H), 7.59 (d, 1H, J= 5.5 Hz), 4.05 (s, 3H) ppm. ^{13}C NMR (100MHz, $CDCl_3$) : ∂= 168.8, 138.6, 137.8, 132.5, 129.4, 129.0, 128.6, 127.9, 127.1 (2 Carbons), 127.0, 126.7, 126,4, 126.1, 125.9, 125.1, 124.6, 52.5 ppm. Elemental analysis calcd (%) for $C_{18}H_{12}O_2S$: C 73.95, H 4.14; found: C 73.91, H 4.11.

Methyl naphtho[1,2-b]thiophene-4-carboxylate (13)

Reaction time: 64 h at 20° C. Yield: 385 mg (53%) of red powder. ^{1}H NMR (400 MHz, $CDCl_3$): ∂ = 8.56 (s, 1H), 8,32 (d, 1H, J= 5.5 Hz), 8.15 (d, 1H, J= 8.2 Hz), 8.00 (d, 1H, J= 7.3 Hz), 7.67 (pseudo t, 1H, J= 8.2 Hz, 6.9 Hz), 7.60 (d, 1H, J= 5.5 Hz), 7.56 (pseudo t, 1H, J= 6.9 Hz, 8.2 Hz), 4.03 (s, 3H) ppm. ^{13}C NMR (100MHz, $CDCl_3$) : ∂ = 167.4, 131.1, 130.6, 130.4, 130.3, 129.6, 129.2, 128.6, 126.3, 126.0, 125.9, 123.7, 123.4, 52.3 ppm. Elemental analysis calcd (%) for $C_{14}H_{10}O_2S$: C 69.40, H 4.16; found: C 69.08, H 3.97.

Methyl phenanthro[1,2-b]thiophene-9-carboxylate (14)

Reaction time: 16 h at 20° C. Yield: 620 mg (70%) of white needles. ^{1}H NMR (400 MHz, $CDCl_3$): ∂ = 9.39 (s, 1H), 8.77 (d, 1H, J= 8.2 Hz), 8.35 (d, 1H, J= 5.5 Hz), 8.03 (d, 1H, J= 8.7 Hz), 7.92 (m, 2H), 7.71 (pseudo t, 1H), 7.64 (d, 1H, J= 5.5 Hz), 7.61 (pseudo t, 1H), 4.07 (s, 3H) ppm. ^{13}C NMR (100MHz, $CDCl_3$) : ∂ = 167.5, 140.2, 136.2, 131.9, 131.1, 130.4, 130.0, 129.1, 127.7, 127.0, 126.8, 125.9, 125.9, 124.5, 123.2, 123.0, 122.6, 52.3 ppm. Elemental analysis calcd (%) for $C_{18}H_{12}O_2S$: C 73.95, H 4.14; found: C 73.59, H 4.30. MS (m/z (%)): 291.9 (100, $[M]^+$); 292.9 (60, $[M+H]^+$); 293.9 (20, $[M+2H]^+$)

Methyl phenanthro[4,3-b]thiophene-4-carboxylate (15)

Reaction time: 16 h at 20° C. Yield: 750 mg (85%) of white powder. ^{1}H NMR (400 MHz, $CDCl_3$): ∂ = 9.32 (d, 1H, J= 8.2 Hz), 8.68 (s, 1H), 8.57 (d, 1H, J= 5.5 Hz), 8.03 (d, 1H, J= 8.2 Hz), 7.94 (d, 1H, J= 8.7 Hz), 7.84 (m, 3H), 7.73 (t, 1H, J= 6.9 Hz), 4.07 (s, 3H) ppm. ^{13}C NMR (100MHz, $CDCl_3$) : ∂ = 167.3, 137.5, 136.8, 134.0, 130.8, 129.6, 129.3, 129.2, 129.0, 128.2, 127.5, 127.4 (2 Carbons), 127.3, 126.5, 124.9, 123.5, 52.4 ppm. Elemental analysis calcd (%) for $C_{18}H_{12}O_2S$: C 73.95, H 4.14; found: C 74.00, H 4.53.

Methyl benzo[2,1-b : 3,4-b']dithiophene-5-carboxylate (16)

Reaction time: 16 h at 20° C. Yield: 470 mg (63%) of brown solid. ^{1}H NMR (400 MHz, $CDCl_3$): ∂ = 8.56 (s, 1H), 8.31 (d, 1H, J= 5.5 Hz), 7.53 (d, 1H, J= 5.5 Hz), 7.48 (d, 1H, J= 5.0 Hz), 7.44 (d, 1H, J= 5.5 Hz), 4.01 (s, 3H) ppm. ^{13}C NMR (100MHz, $CDCl_3$) : ∂ = 167.5, 138.2, 136.2, 135.7, 134.9, 125.9, 125.8, 125.4, 125.3, 124.5, 122.1, 52.2 ppm. Elemental analysis calcd (%) for $C_{12}H_8O_2S_2$: C 58.04, H 3.25; found: C 57.78, H 3.59.

Unexpected dimeric cyclisation product 19a

Raection time: 64 h at 20° C. Yield (from **18**): 825 mg (51%). ^{1}H NMR (400 MHz, $CDCl_3$): ∂ = 9.57 (s, 1H), 9.50 (s, 1H), 9.38 (s, 1H), 9.03 (d, 1H, J= 9.2 Hz), 8.95 (d, 1H, J= 6.9 Hz), 8.76 (d, 1H, J= 8.2 Hz), 8.49 (s, 1H), 8.42 (d, 1H, J= 9.2 Hz), 8.36 (m, 2H), 8.20 (d, 1H, J= 6.0 Hz), 7.89 (s, 1H), 7.70 (m, 2H), 7.57 (d, 1H, J= 7.3 Hz), 7.31 (d, 1H, J= 3.2 Hz), 7.21 (d, 1H, J= 5.5 Hz), 7.15 (d, 1H, J= 5.0 Hz), 4.54 (m, 4H), 4.40 (broad m, 4H), 1.91 (m, 4H), 1.77 (m, 4H), 1.54 (m, 4H), 1.50 (m, 4H), 0.95 (m, 12H) ppm. ^{13}C NMR (100MHz, $CDCl_3$): ∂ = 172.6, 138.9, 132.7, 132.1, 132.2, 130.5, 129.93, 129.87, 129.52, 129.46 (2 Carbons), 129.2, 128.7, 128.6, 128.4, 127.5, 127.44, 127.35, 127.2, 127.1, 127.0, 126.8, 126.1, 126.0, 125.9, 124.4, 124.0, 123.5, 123.3, 121.4 (2 Carbons), 66.1, 66.0, 30.6, 30.5, 19.34, 19.25, 13.83, 13.75 ppm. Elemental analysis calcd (%) for $C_{64}H_{54}O_8S_4$: C 71.22, H 5.04; found: C 70.84, H 5.16. MS (m/z (%)): 1078.2 (100, $[M]^+$); 1080.2 (80, $[M+2H]^+$); 1082.2(20, $[M+4H]^+$).

Tetraethyl ester 19b

100 mg of **18b** was refluxed with methanol (50 ml) and KOH (1 g) for 5 h. 300 ml of water was added and the solution was acidified with conc. HCl. Tthe precipitate was filtered and dried in air. Then it was refluxed with ethanol (100 mL) and H_2SO_4 (2 mL) for 10 h. The solution was put in the freezer, where the product crystallised. It was filtered, washed with EtOH and dried in air. Yield: 50 mg (56%) of yellow powder. ^{1}H NMR (400 MHz, DMSO-d_6 at 150^0 C): ∂ = 9.52 (s, 1H), 9.44 (s, 1H), 9.32 (s, 1H), 9.14 (d, 1H, J= 9.2 Hz), 9.09 (d, 1H, J= 9.6 Hz), 8.85 (d, 1H, J= 8.2 Hz), 8.49 (d, 1H, J= 8.7 Hz), 8.42 (s, 1H), 8.39 (d, 1H, J= 8.7 Hz), 8.26 (d, 1H, J= 5.5 Hz), 8.08 (d, 1H, J= 5.5 Hz), 8.03 (d, 1H, J= 5.5 Hz), 7.84 (t, 1H, J= 7.8 Hz), 7.80 (s, 1H), 7.72 (d, 1H, J= 7.3 Hz), 7.63 (d, 1H, J= 6.0 Hz), 7.41 (d, 1H, J= 5.5 Hz), 7.16 (d, 1H, J= 5.5 Hz), 4.54 (m, 2H), 4.47 (m, 2H), 4.36 (m, 2H), 1.49 (m, 6H), 1.37 (m, 6H) ppm.

Dibutyl chryseno[1,2-b : 7,8-b']dihiophene-3,9-dicarboxylate (20)

Reaction time: 64 h at 20° C. 250 mg (0.459 mmol) of **18** was used with 255 mg (1.1 mmol) of DDQ, 300 mL of DCM and 3 mL of methanesulfonic acid (added after addition of DCM). Yield: 123 mg (50%) of yellow powder. ^{1}H NMR (400 MHz, $CDCl_3$): ∂ = 9.50 (s, 1H), 8.99 (d, 1H, J= 9.2 Hz), 8.37

(m, 2H), 7.70 (d, 1H, J= 5.5 Hz), 4.53 (t, 2H, J= 6.9), 1.93 (m, 2H), 1.60 (m, 2H), 1.07 (t, 3H, J= 7.3 Hz) ppm. ^{13}C NMR (100MHz, $CDCl_3$) : ∂= 167.1, 136.1, 129.8, 129.5, 127.1, 126.3, 126.1, 126.0, 124.9, 124.7, 124.2, 124.0, 65.5, 31.0, 19.6, 14.0 ppm. HRMS (m/z (%)): calcd. for $C_{32}H_{28}O_4S_2$ $[M]^+$, 540.1429; found, 540.1453. Elemental analysis calcd (%) for $C_{32}H_{28}O_4S_2$: C 71.08, H 5.22, found: C 70.89, H 5.20.

Dimethyl benzo[1,2-b : 3,4-b']dithiophene-1,5-dicarboxylate (23) and **thieno[3,2-g]-1H-2-benzothiopyran-1-one-10-carboxylic acid (24)**

23: Yield (from **22**): 310 mg (34%) of brown needles (the compound was separated from **24** by column chromatography through silica in DCM as eluent). ^{1}H NMR (400 MHz, $CDCl_3$): ∂ = 7.77 (d, 1H, J= 5.5 Hz), 7.59 (d, 1H, J= 5.5 Hz), 7.56 (d, 1H, J= 5.5 Hz), 7.47 (d, 1H, J= 5.5 Hz), 3.99 (s, 3H), 3.98 (s, 3H) ppm. ^{13}C NMR (100MHz, $CDCl_3$) : ∂= 168.8, 166.3, 138.7, 135.2, 135.0, 134.3, 132.1, 127.6, 126.6, 123.7, 121.0, 120.1, 53.0, 52.9 ppm.

24: Yield: 80 mg (10%) of yellow needles. ^{1}H NMR (400 MHz, DMSO-d_6): ∂ = 8.34 (s, 1H), 8.19 (d, 1H, J= 5.5 Hz), 7.65 (d, 1H, J= 5.5 Hz), 7.52 (d, 1H, J= 9.6 Hz), 7.43 (d, 1H, J= 6.9 Hz) ppm. ^{13}C NMR (100MHz, DMSO-d_6) : ∂ = 185.3, 169.6, 144.2, 138.1, 135.6, 134.7, 129.8, 126.1, 124.6, 124.2, 122.9, 120.5 ppm. HRMS (m/z (%)): calcd. for $C_{12}H_6O_3S_2$ $[M]^+$, 261.9724; found, 261.9716.

3.8. Crystallographic data.

10: Table 1. Crystal data and structure refinement for 10.

Identification code	compound_10
Empirical formula	C27 H22 O2
Formula weight	378.45
Temperature	120(2) K
Wavelength	0.71073 A
Crystal system, space group	Monoclinic, Pc
Unit cell dimensions	a = 10.093(3) A alpha = 90 deg.
	b = 12.737(4) A beta = 90.795(11) deg.
	c = 7.613(2) A gamma = 90 deg.
Volume	978.6(5) A^3
Z, Calculated density	2, 1.284 Mg/m^3
Absorption coefficient	0.080 mm^-1
F(000)	400
Crystal size	0.33 x 0.12 x 0.06 mm

Theta range for data collection 1.60 to 25.39 deg.
Limiting indices -11<=h<=12, -15<=k<=15, -9<=l<=7
Reflections collected / unique 17013 / 2899 [R(int) = 0.0438]
Completeness to theta = 25.39 97.0 %
Absorption correction Semi-empirical from equivalents
Max. and min. transmission 0.9952 and 0.9742
Refinement method Full-matrix least-squares on F^2
Data / restraints / parameters 2899 / 2 / 282
Goodness-of-fit on F^2 1.051
Final R indices [I>2sigma(I)] R1 = 0.0431, wR2 = 0.1112
R indices (all data) R1 = 0.0486, wR2 = 0.1156
Absolute structure parameter ?
Largest diff. peak and hole 0.150 and -0.148 e.A^-3

12: Table 1. Crystal data and structure refinement for 12.

Identification code compound_12
Empirical formula C18 H12 O2 S
Formula weight 292.34
Temperature 120(2) K
Wavelength 0.71073 A
Crystal system, space group Orthorhombic, Pca2(1)
Unit cell dimensions a = 21.472(2) A alpha = 90 deg.
b = 3.9116(3) A beta = 90 deg.
c = 15.4115(15) A gamma = 90 deg.
Volume 1294.4(2) A^3
Z, Calculated density 4, 1.500 Mg/m^3
Absorption coefficient 0.251 mm^-1
F(000) 608
Crystal size 0.25 x 0.08 x 0.06 mm
Theta range for data collection 1.90 to 28.65 deg.
Limiting indices -28<=h<=28, -4<=k<=5, -20<=l<=20
Reflections collected / unique 20545 / 3302 [R(int) = 0.0514]
Completeness to theta = 28.65 99.3 %
Absorption correction Semi-empirical from equivalents

Max. and min. transmission	0.9851 and 0.9400
Refinement method	Full-matrix least-squares on F^2
Data / restraints / parameters	3302 / 1 / 192
Goodness-of-fit on F^2	0.981
Final R indices [I>2sigma(I)]	R1 = 0.0376, wR2 = 0.0934
R indices (all data)	R1 = 0.0473, wR2 = 0.0998
Absolute structure parameter	0.01(9)
Largest diff. peak and hole	0.298 and -0.383 e.A^-3

Table 2. Atomic coordinates (x 10^4) and equivalent isotropic displacement parameters (A^2 x 10^3) for 12.
U(eq) is defined as one third of the trace of the orthogonalized Uij tensor.

	x	y	z	U(eq)
S(1)	6780(1)	135(1)	7282(1)	26(1)
C(3)	7103(1)	-3429(6)	3879(2)	31(1)
C(4)	6499(1)	-2544(6)	3706(2)	28(1)
C(5)	6118(1)	-1052(6)	4350(1)	25(1)
C(7)	5494(1)	-96(6)	4147(2)	28(1)
C(8)	5118(1)	1337(6)	4743(2)	27(1)
C(9)	5323(1)	1980(5)	5611(1)	21(1)
C(14)	4916(1)	3579(5)	6232(1)	22(1)
C(17)	4268(1)	4648(6)	6010(2)	26(1)

O(2)	3993(1)	6265(5)	6678(1)	37(1)
C(2)	7346(1)	-2812(6)	4708(2)	33(1)
C(1)	6978(1)	-1390(6)	5341(2)	29(1)
C(6)	6350(1)	-487(5)	5196(1)	22(1)
C(10)	5943(1)	979(5)	5850(1)	20(1)
C(11)	6109(1)	1417(5)	6739(1)	20(1)
C(15)	6505(1)	1573(6)	8270(2)	29(1)
C(16)	5938(1)	3001(6)	8208(1)	27(1)
C(12)	5700(1)	2928(5)	7339(2)	23(1)
C(13)	5115(1)	4070(6)	7072(1)	25(1)
O(1)	3988(1)	4153(7)	5352(1)	58(1)
C(18)	3358(1)	7288(7)	6547(2)	38(1)

Table 3. Bond lengths [A] and angles [deg] for 12.

S(1)-C(15)	1.726(2)
S(1)-C(11)	1.740(2)
C(3)-C(4)	1.370(3)
C(3)-C(2)	1.400(3)

C(3)-H(3)	0.9500
C(4)-C(5)	1.412(3)
C(4)-H(4)	0.9500
C(5)-C(6)	1.413(3)
C(5)-C(7)	1.425(3)
C(7)-C(8)	1.345(3)
C(7)-H(7)	0.9500
C(8)-C(9)	1.431(3)
C(8)-H(8)	0.9500
C(9)-C(10)	1.435(3)
C(9)-C(14)	1.439(3)
C(14)-C(13)	1.376(3)
C(14)-C(17)	1.493(3)
C(17)-O(1)	1.194(3)
C(17)-O(2)	1.344(3)
O(2)-C(18)	1.436(3)
C(2)-C(1)	1.374(3)
C(2)-H(2)	0.9500

C(1)-C(6)	1.412(3)
C(1)-H(1)	0.9500
C(6)-C(10)	1.453(3)
C(10)-C(11)	1.425(3)
C(11)-C(12)	1.407(3)
C(15)-C(16)	1.343(3)
C(15)-H(15)	0.9500
C(16)-C(12)	1.434(3)
C(16)-H(16)	0.9500
C(12)-C(13)	1.396(3)
C(13)-H(13)	0.9500
C(18)-H(18A)	0.9800
C(18)-H(18B)	0.9800
C(18)-H(18C)	0.9800
C(15)-S(1)-C(11)	92.73(10)
C(4)-C(3)-C(2)	119.1(2)

C(4)-C(3)-H(3)	120.5
C(2)-C(3)-H(3)	120.5
C(3)-C(4)-C(5)	121.2(2)
C(3)-C(4)-H(4)	119.4
C(5)-C(4)-H(4)	119.4
C(4)-C(5)-C(6)	120.5(2)
C(4)-C(5)-C(7)	119.9(2)
C(6)-C(5)-C(7)	119.5(2)
C(8)-C(7)-C(5)	121.6(2)
C(8)-C(7)-H(7)	119.2
C(5)-C(7)-H(7)	119.2
C(7)-C(8)-C(9)	121.80(19)
C(7)-C(8)-H(8)	119.1
C(9)-C(8)-H(8)	119.1
C(8)-C(9)-C(10)	118.55(18)
C(8)-C(9)-C(14)	120.77(18)
C(10)-C(9)-C(14)	120.68(18)
C(13)-C(14)-C(9)	119.87(18)

C(13)-C(14)-C(17)	117.7(2)
C(9)-C(14)-C(17)	122.36(19)
O(1)-C(17)-O(2)	120.5(2)
O(1)-C(17)-C(14)	128.1(2)
O(2)-C(17)-C(14)	111.37(19)
C(17)-O(2)-C(18)	116.09(19)
C(1)-C(2)-C(3)	120.3(2)
C(1)-C(2)-H(2)	119.9
C(3)-C(2)-H(2)	119.9
C(2)-C(1)-C(6)	122.5(2)
C(2)-C(1)-H(1)	118.7
C(6)-C(1)-H(1)	118.7
C(1)-C(6)-C(5)	116.38(19)
C(1)-C(6)-C(10)	124.26(19)
C(5)-C(6)-C(10)	119.35(18)
C(11)-C(10)-C(9)	116.57(18)
C(11)-C(10)-C(6)	124.28(18)

C(9)-C(10)-C(6)	119.12(18)
C(12)-C(11)-C(10)	121.71(18)
C(12)-C(11)-S(1)	108.74(16)
C(10)-C(11)-S(1)	129.48(16)
C(16)-C(15)-S(1)	112.54(17)
C(16)-C(15)-H(15)	123.7
S(1)-C(15)-H(15)	123.7
C(15)-C(16)-C(12)	112.4(2)
C(15)-C(16)-H(16)	123.8
C(12)-C(16)-H(16)	123.8
C(13)-C(12)-C(11)	120.2(2)
C(13)-C(12)-C(16)	126.2(2)
C(11)-C(12)-C(16)	113.58(18)
C(14)-C(13)-C(12)	120.79(19)
C(14)-C(13)-H(13)	119.6
C(12)-C(13)-H(13)	119.6
O(2)-C(18)-H(18A)	109.5
O(2)-C(18)-H(18B)	109.5

H(18A)-C(18)-H(18B) 109.5

O(2)-C(18)-H(18C) 109.5

H(18A)-C(18)-H(18C) 109.5

H(18B)-C(18)-H(18C) 109.5

Symmetry transformations used to generate equivalent atoms:

Table 4. Anisotropic displacement parameters (A^2 x 10^3) for 12.
The anisotropic displacement factor exponent takes the form:
-2 pi^2 [h^2 a*^2 U11 + ... + 2 h k a* b* U12]

	U11	U22	U33	U23	U13	U12
S(1)	18(1)	35(1)	25(1)	0(1)	-3(1)	2(1)
C(3)	27(1)	33(1)	33(1)	-4(1)	9(1)	0(1)
C(4)	31(1)	30(1)	24(1)	-4(1)	4(1)	-4(1)
C(5)	25(1)	23(1)	26(1)	1(1)	3(1)	-3(1)
C(7)	27(1)	37(1)	21(1)	-1(1)	-4(1)	-1(1)
C(8)	23(1)	31(1)	27(1)	3(1)	-6(1)	-1(1)
C(9)	17(1)	24(1)	23(1)	4(1)	0(1)	0(1)
C(14)	18(1)	23(1)	26(1)	3(1)	0(1)	-1(1)
C(17)	20(1)	32(1)	27(1)	5(1)	3(1)	3(1)

O(2)	21(1)	53(1)	38(1)	-9(1)	-2(1)	12(1)
C(2)	21(1)	39(1)	38(1)	2(1)	3(1)	3(1)
C(1)	22(1)	37(1)	28(1)	-1(1)	1(1)	-2(1)
C(6)	19(1)	24(1)	24(1)	2(1)	4(1)	-4(1)
C(10)	16(1)	21(1)	23(1)	3(1)	0(1)	-4(1)
C(11)	14(1)	22(1)	25(1)	0(1)	-1(1)	-2(1)
C(15)	28(1)	35(1)	23(1)	2(1)	-4(1)	-4(1)
C(16)	23(1)	33(1)	23(1)	0(1)	0(1)	-3(1)
C(12)	20(1)	27(1)	21(1)	0(1)	0(1)	-3(1)
C(13)	19(1)	30(1)	26(1)	-1(1)	5(1)	1(1)
O(1)	29(1)	110(2)	35(1)	-14(1)	-7(1)	24(1)
C(18)	19(1)	44(2)	51(2)	-2(1)	2(1)	10(1)

14: Table 1. Crystal data and structure refinement for 14.

Identification code	compound_14
Empirical formula	C18 H12 O2 S
Formula weight	292.34
Temperature	100(2) K
Wavelength	0.71073 A
Crystal system, space group	Monoclinic, P21/c

Unit cell dimensions a = 15.7299(7) A alpha = 90 deg.
b = 6.1083(2) A beta = 118.368(2) deg.
c = 15.8294(6) A gamma = 90 deg.

Volume 1338.29(9) A^3

Z, Calculated density 4, 1.451 Mg/m^3

Absorption coefficient 0.243 mm^-1

F(000) 608

Crystal size 0.20 x 0.10 x 0.10 mm

Theta range for data collection 1.47 to 27.44 deg.

Limiting indices -20<=h<=20, -7<=k<=6, -20<=l<=19

Reflections collected / unique 12588 / 3036 [R(int) = 0.0445]

Completeness to theta = 27.44 99.8 %

Absorption correction Semi-empirical from equivalents

Max. and min. transmission 0.9762 and 0.9531

Refinement method Full-matrix least-squares on F^2

Data / restraints / parameters 3036 / 0 / 191

Goodness-of-fit on F^2 1.055

Final R indices [I>2sigma(I)] R1 = 0.0423, wR2 = 0.0987

R indices (all data) R1 = 0.0644, wR2 = 0.1211

Largest diff. peak and hole 0.393 and -0.317 e.A^-3

Table 2. Atomic coordinates (x 10^4) and equivalent isotropic displacement parameters (A^2 x 10^3) for 14.
U(eq) is defined as one third of the trace of the orthogonalized Uij tensor.

	x	y	z	U(eq)
S(1)	8057(1)	-89(1)	6626(1)	21(1)
O(1)	8573(1)	6584(2)	3903(1)	18(1)
O(2)	9461(1)	6592(3)	5508(1)	23(1)

C(1)	9117(2)	8459(3)	3871(2)	20(1)
C(2)	8830(2)	5793(3)	4781(2)	16(1)
C(3)	8254(1)	3814(3)	4739(1)	15(1)
C(4)	7661(1)	2862(3)	3872(2)	15(1)
C(5)	7134(1)	922(3)	3780(2)	15(1)
C(6)	6567(1)	-152(3)	2864(2)	15(1)
C(7)	6469(2)	694(4)	1993(2)	17(1)
C(8)	5961(2)	-416(4)	1143(2)	21(1)
C(9)	5521(2)	-2427(4)	1119(2)	22(1)
C(11)	6104(1)	-2174(3)	2833(2)	17(1)
C(12)	6177(2)	-3061(4)	3701(2)	20(1)
C(13)	6705(2)	-2065(3)	4550(2)	19(1)
C(14)	7210(2)	-78(3)	4619(2)	16(1)
C(15)	7821(2)	929(3)	5512(2)	16(1)
C(16)	8343(2)	2854(3)	5598(2)	16(1)
C(17)	8915(2)	3472(4)	6588(2)	20(1)
C(18)	8833(2)	2055(4)	7198(2)	22(1)
C(10)	5583(2)	-3281(4)	1948(2)	22(1)

Table 3. Bond lengths [A] and angles [deg] for 14.

S(1)-C(18)	1.725(2)
S(1)-C(15)	1.734(2)
O(1)-C(2)	1.340(2)
O(1)-C(1)	1.445(2)
O(2)-C(2)	1.210(3)
C(1)-H(1A)	0.9600
C(1)-H(1B)	0.9600
C(1)-H(1C)	0.9600
C(2)-C(3)	1.493(3)
C(3)-C(4)	1.369(3)
C(3)-C(16)	1.425(3)
C(4)-C(5)	1.413(3)
C(4)-H(4)	0.9300
C(5)-C(14)	1.415(3)
C(5)-C(6)	1.449(3)

C(6)-C(7)	1.411(3)
C(6)-C(11)	1.423(3)
C(7)-C(8)	1.374(3)
C(7)-H(7)	0.9300
C(8)-C(9)	1.402(3)
C(8)-H(8)	0.9300
C(9)-C(10)	1.371(3)
C(9)-H(9)	0.9300
C(11)-C(10)	1.414(3)
C(11)-C(12)	1.431(3)
C(12)-C(13)	1.343(3)
C(12)-H(12)	0.9300
C(13)-C(14)	1.427(3)
C(13)-H(13)	0.9300
C(14)-C(15)	1.417(3)
C(15)-C(16)	1.403(3)
C(16)-C(17)	1.437(3)
C(17)-C(18)	1.349(3)

C(17)-H(17)	0.9300
C(18)-H(18)	0.9300
C(10)-H(10)	0.9300
C(18)-S(1)-C(15)	91.06(10)
C(2)-O(1)-C(1)	115.48(17)
O(1)-C(1)-H(1A)	109.5
O(1)-C(1)-H(1B)	109.5
H(1A)-C(1)-H(1B)	109.5
O(1)-C(1)-H(1C)	109.5
H(1A)-C(1)-H(1C)	109.5
H(1B)-C(1)-H(1C)	109.5
O(2)-C(2)-O(1)	123.2(2)
O(2)-C(2)-C(3)	125.15(19)
O(1)-C(2)-C(3)	111.62(17)
C(4)-C(3)-C(16)	119.52(19)
C(4)-C(3)-C(2)	119.87(18)
C(16)-C(3)-C(2)	120.57(18)
C(3)-C(4)-C(5)	123.12(19)

C(3)-C(4)-H(4)	118.4
C(5)-C(4)-H(4)	118.4
C(4)-C(5)-C(14)	118.76(19)
C(4)-C(5)-C(6)	122.36(18)
C(14)-C(5)-C(6)	118.76(19)
C(7)-C(6)-C(11)	117.86(19)
C(7)-C(6)-C(5)	122.78(19)
C(11)-C(6)-C(5)	119.34(19)
C(8)-C(7)-C(6)	121.3(2)
C(8)-C(7)-H(7)	119.4
C(6)-C(7)-H(7)	119.4
C(7)-C(8)-C(9)	120.6(2)
C(7)-C(8)-H(8)	119.7
C(9)-C(8)-H(8)	119.7
C(10)-C(9)-C(8)	119.9(2)
C(10)-C(9)-H(9)	120.0
C(8)-C(9)-H(9)	120.0

C(10)-C(11)-C(6)	119.75(19)
C(10)-C(11)-C(12)	120.99(19)
C(6)-C(11)-C(12)	119.26(19)
C(13)-C(12)-C(11)	121.3(2)
C(13)-C(12)-H(12)	119.4
C(11)-C(12)-H(12)	119.4
C(12)-C(13)-C(14)	121.3(2)
C(12)-C(13)-H(13)	119.4
C(14)-C(13)-H(13)	119.4
C(5)-C(14)-C(15)	117.66(19)
C(5)-C(14)-C(13)	120.01(19)
C(15)-C(14)-C(13)	122.31(19)
C(16)-C(15)-C(14)	123.24(19)
C(16)-C(15)-S(1)	111.64(16)
C(14)-C(15)-S(1)	125.07(16)
C(15)-C(16)-C(3)	117.68(19)
C(15)-C(16)-C(17)	111.13(18)
C(3)-C(16)-C(17)	131.2(2)

C(18)-C(17)-C(16)	112.9(2)
C(18)-C(17)-H(17)	123.6
C(16)-C(17)-H(17)	123.6
C(17)-C(18)-S(1)	113.27(17)
C(17)-C(18)-H(18)	123.4
S(1)-C(18)-H(18)	123.4
C(9)-C(10)-C(11)	120.6(2)
C(9)-C(10)-H(10)	119.7
C(11)-C(10)-H(10)	119.7

Symmetry transformations used to generate equivalent atoms:

Table 4. Anisotropic displacement parameters (A^2 x 10^3) for 14.

The anisotropic displacement factor exponent takes the form:

-2 pi^2 [h^2 a*^2 U11 + ... + 2 h k a* b* U12]

	U11	U22	U33	U23	U13	U12
S(1)	26(1)	22(1)	17(1)	5(1)	12(1)	5(1)
O(1)	20(1)	16(1)	16(1)	0(1)	7(1)	-3(1)
O(2)	23(1)	25(1)	17(1)	-3(1)	6(1)	-5(1)
C(1)	20(1)	16(1)	25(1)	1(1)	11(1)	-3(1)

C(2)	15(1)	15(1)	17(1)	-1(1)	8(1)	4(1)
C(3)	13(1)	16(1)	16(1)	1(1)	7(1)	4(1)
C(4)	16(1)	15(1)	14(1)	2(1)	8(1)	4(1)
C(5)	12(1)	15(1)	17(1)	1(1)	7(1)	4(1)
C(6)	12(1)	15(1)	20(1)	-2(1)	9(1)	2(1)
C(7)	15(1)	17(1)	19(1)	-2(1)	8(1)	-1(1)
C(8)	19(1)	25(1)	19(1)	-2(1)	9(1)	1(1)
C(9)	19(1)	24(1)	23(1)	-9(1)	9(1)	-2(1)
C(11)	12(1)	16(1)	23(1)	-1(1)	8(1)	2(1)
C(12)	20(1)	14(1)	31(1)	1(1)	17(1)	0(1)
C(13)	22(1)	18(1)	25(1)	5(1)	16(1)	3(1)
C(14)	16(1)	16(1)	19(1)	1(1)	11(1)	4(1)
C(15)	18(1)	18(1)	16(1)	2(1)	10(1)	5(1)
C(16)	15(1)	16(1)	16(1)	-1(1)	7(1)	4(1)
C(17)	18(1)	25(1)	16(1)	-3(1)	7(1)	2(1)
C(18)	21(1)	27(1)	15(1)	1(1)	8(1)	6(1)
C(10)	17(1)	18(1)	31(1)	-6(1)	12(1)	-3(1)

19: Table 1. Crystal data and structure refinement for 19.

Identification code	compound_19
Empirical formula	C64 H54 O8 S4
Formula weight	1079.31
Temperature	120(2) K
Wavelength	0.71073 A
Crystal system, space group	Triclinic, P-1
Unit cell dimensions	a = 11.146(4) A alpha = 83.625(18) deg.
	b = 13.739(5) A beta = 76.563(17) deg.
	c = 17.971(6) A gamma = 87.14(2) deg.
Volume	2659.3(16) A^3
Z, Calculated density	2, 1.348 Mg/m^3
Absorption coefficient	0.237 mm^-1
F(000)	1132
Crystal size	0.11 x 0.10 x 0.07 mm
Theta range for data collection	1.80 to 25.60 deg.
Limiting indices	-12<=h<=13, -16<=k<=15, -21<=l<=21
Reflections collected / unique	27569 / 9042 [R(int) = 0.1054]
Completeness to theta = 25.00	94.0 %
Absorption correction	Semi-empirical from equivalents
Max. and min. transmission	0.9836 and 0.9743
Refinement method	Full-matrix least-squares on F^2
Data / restraints / parameters	9042 / 30 / 688
Goodness-of-fit on F^2	1.045
Final R indices [I>2sigma(I)]	R1 = 0.1081, wR2 = 0.2698
R indices (all data)	R1 = 0.2447, wR2 = 0.3730
Largest diff. peak and hole	0.825 and -0.741 e.A^-3

23: Table 1. Crystal data and structure refinement for 23.

Identification code	compound_23
Empirical formula	C14 H10 O4 S2
Formula weight	306.34
Temperature	100(2) K

Wavelength	0.71073 A
Crystal system, space group	Orthorhombic, Pca2(1)
Unit cell dimensions	a = 17.3421(10) A alpha = 90 deg.
	b = 7.5256(4) A beta = 90 deg.
	c = 19.9689(11) A gamma = 90 deg.
Volume	2606.1(2) A^3
Z, Calculated density	8, 1.562 Mg/m^3
Absorption coefficient	0.418 mm^-1
F(000)	1264
Crystal size	0.26 x 0.08 x 0.02 mm
Theta range for data collection	2.35 to 29.14 deg.
Limiting indices	-23<=h<=23, -10<=k<=9, -27<=l<=27
Reflections collected / unique	51728 / 6936 [R(int) = 0.0659]
Completeness to theta = 29.14	99.7 %
Absorption correction	Semi-empirical from equivalents
Max. and min. transmission	0.9917 and 0.8991
Refinement method	Full-matrix least-squares on F^2
Data / restraints / parameters	6936 / 1 / 366
Goodness-of-fit on F^2	1.059
Final R indices [I>2sigma(I)]	R1 = 0.0458, wR2 = 0.1135
R indices (all data)	R1 = 0.0594, wR2 = 0.1237
Absolute structure parameter	0.44(7)
Largest diff. peak and hole	0.572 and -0.542 e.A^-3

3.9. References

[1] R. Scholl, C. Seer, and R. Weitzenböck; *Berichte der deutschen chemischen Gesellschaft*, vol. 43, no. 2, pp. 2202–2209, Apr. 1910.

[2] R. Scholl and C. Seer, *Justus Liebig's Annalen der Chemie*, vol. 394, no. 2, pp. 111–177, 1912.

[3] M. Müller, C. Kübel, and K. Müllen, *Chem. Eur. J.*, vol. 4, no. 11, pp. 2099–2109, 1998.

[4] A. C. Grimsdale and K. Müllen, *Angewandte Chemie International Edition*, vol. 44, no. 35, pp. 5592–5629, Sep. 2005.

[5] B. T. King, J. Kroulík, C. R. Robertson, P. Rempala, C. L. Hilton, J. D. Korinek, and L. M. Gortari, *The Journal of Organic Chemistry*, vol. 72, no. 7, pp. 2279–2288, Mar. 2007.

[6] L. Zhai, R. Shukla, S. H. Wadumethrige, and R. Rathore, *The Journal of Organic Chemistry*, vol. 75, no. 14, pp. 4748–4760, Jul. 2010.

[7] E. Clar and M. Zander, *Journal of the Chemical Society (Resumed)*, p. 4616, 1957.

[8] *Clar, E. Polycyclic Hydrocarbons; Academic Press: New York, 1964; Vol. I/II. .*

[9] H. Langhals and S. Kirner, *Eur. J. Org. Chem.*, vol. 2000, no. 2, pp. 365–380, 2000.

[10] S. Alibert-Fouet, I. Seguy, J.-F. Bobo, P. Destruel, and H. Bock, *Chemistry - A European Journal*, vol. 13, no. 6, pp. 1746–1753, Feb. 2007.

[11] T. S. Navale, K. Thakur, and R. Rathore; *Organic Letters*, vol. 13, no. 7, pp. 1634–1637, Apr. 2011.

[12] Mallory, F. B.; Mallory, C. W. Org. React, 3.0, 1, 1984.

[13] W. H. Perkin, *Journal of the Chemical Society*, vol. 21, p. 181, 1868.

[14] W. H. Perkin, *Journal of the Chemical Society*, vol. 32, p. 660, 1877.

[15] Rosen, T.; Comp. Org. Syn., 2, 395-408, 1991.

[16] T. Hassheider, S. A. Benning, H.-S. Kitzerow, M.-F. Achard, and H. Bock, *Angewandte Chemie International Edition*, vol. 40, no. 11, pp. 2060–2063, 2001.

[17] H. Bock, A. Babeau, I. Seguy, P. Jolinat, and P. Destruel, *ChemPhysChem*, vol. 3, no. 6, pp. 532–535, 2002.

[18] S. Saïdi-Besbes, É. Grelet, and H. Bock, *Angewandte Chemie International Edition*, vol. 45, no. 11, pp. 1783–1786, Mar. 2006.

[19] H. Bock, M. Rajaoarivelo, S. Clavaguera, and É. Grelet, *European Journal of Organic Chemistry*, vol. 2006, no. 13, pp. 2889–2893, Jul. 2006.

[20] J. Kelber, M.-F. Achard, B. Garreau-de Bonneval, and H. Bock, *Chemistry - A European Journal*, vol. 17, no. 29, pp. 8145–8155, Jul. 2011.

[21] J. Kelber, H. Bock, O. Thiebaut, E. Grelet, and H. Langhals, *European Journal of Organic Chemistry*, vol. 2011, no. 4, pp. 707–712, Feb. 2011.

[22] J. Kelber, M.-F. Achard, F. Duroal, H. Bock, Angew. Chem. Int. ed., in press.

[23] K. Wang, M. Lü, A. Yu, X. Zhu, and Q. Wang, *The Journal of Organic Chemistry*, vol. 74, no. 2, pp. 935–938, Jan. 2009.

[24] M. Wu, L. Li, B. Su, Z. Liu, and Q. Wang, *Organic & Biomolecular Chemistry*, vol. 9, no. 1, p. 141, 2011.

[25] A. J. Liepa and R. E. Summons, *Journal of the Chemical Society, Chemical Communications*, no. 22, p. 826, 1977.

[26] R. E. Buckles and J. A. Cooper, *The Journal of Organic Chemistry*, vol. 30, no. 5, pp. 1588–1592, May 1965.

[27] E. Lee-Ruff, H. Kruk, and M. Katz, *The Journal of Organic Chemistry*, vol. 49, no. 3, pp. 553–555, Feb. 1984.

[28] F. H. Herbstein and G. M. J. Schmidt, *Journal of the Chemical Society (Resumed)*, p. 3302, 1954.

[29] M. Pomerantz, Y. Cheng, R. K. Kasim, and R. L. Elsenbaumer, *Journal of Materials Chemistry*, vol. 9, no. 9, pp. 2155–2163, 1999.

[30] G. Koshkakaryan, D. Cao, L. M. Klivansky, S. J. Teat, J. L. Tran, and Y. Liu, *Organic Letters*, vol. 12, no. 7, pp. 1528–1531, Apr. 2010.

[31] C. F. Koelsch and S. Wawzonek, *The Journal of Organic Chemistry*, vol. 6, no. 5, pp. 684–689, Sep. 1941.

[32] E. K. Fields, S. J. Behrend, S. Meyerson, M. L. Winzenburg, B. R. Ortega, and H. K. Hall, *The Journal of Organic Chemistry*, vol. 55, no. 17, pp. 5165–5170, Aug. 1990.

[33] S. Amin, S. S. Hecht, E. LaVoie and D. Hoffmann, *J. Med. Chem.*, vol. 22, pp. 1336-, 1979.

Chapter 4

Aromatic laths by palladium-catalysed dehydrodebrominations of Perkin condensation products

The synthesis of lath-shaped polycyclic arene-polycarboxylic esters and imides of discrete length by Perkin coupling of dibromoarylene-diacetic acids and arylene-dicarboxaldehydes or arylene-diglyoxylic acids followed by ring closure with palladium acetate is examined. A modular approach to graphene nanoribbons with tunable electronic properties is elaborated based on Perkin condensations of 2,5-dibromophenylene-1,4-diacetic acid and pyrenylene-1,8-diglyoxylic acid and their monoprotected derivatives followed by in-situ imidifications.

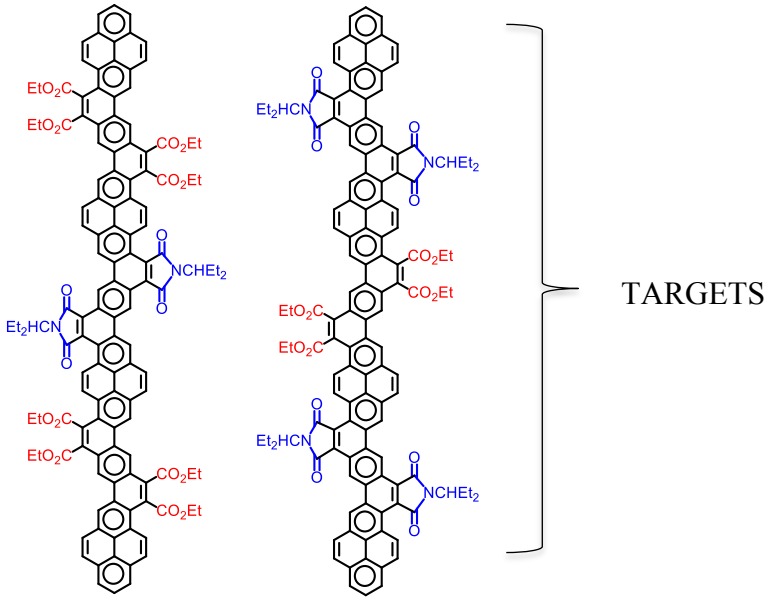

4.1. The build-up of aromatic rings by palladium catalysed dehydrodebrominations and their combination with Perkin reactions

The elimination of HBr to cyclise Perkin products bearing bromo substituents suitably placed in ortho to the ethylene bridge has been achieved in some cases in molten potassium hydroxide at elevated temperatures (200 to 300°C), but the cases reported are limited to Perkin products obtained from 1-bromonaphthyl-2-acetic acid or 1-bromonaphthaldehyde, where the bromine is in the activated position of the naphthalene nucleus. The violent reaction conditions lead in some cases to

rearrangements of the carbon skeleton and thus to a mixture of isomeric products, and the yields seem to be poorly reproducible because the poor solubility of 2,3-diarylacrylic acids in molten KOH necessitates vigourous trituration, whilst reaction times are to be kept short (5min to 1h) to avoid extensive decomposition.[1, 2, 3]

When we tried to cyclise the Perkin products **4** and **5**, obtained from 2-bromophenylacetic acid **1** and either 1-naphthaldehyde **2** or 1,5-diformylbenzene **3** in molten KOH, to obtain, after subsequent esterification, the butyl esters **6** and **7** of chrysene-6-carboxylic acid and fulminene-8,16-dicarboxylic acid, we obtained the two esters in overall yields of only 22% and 14%, respectively.

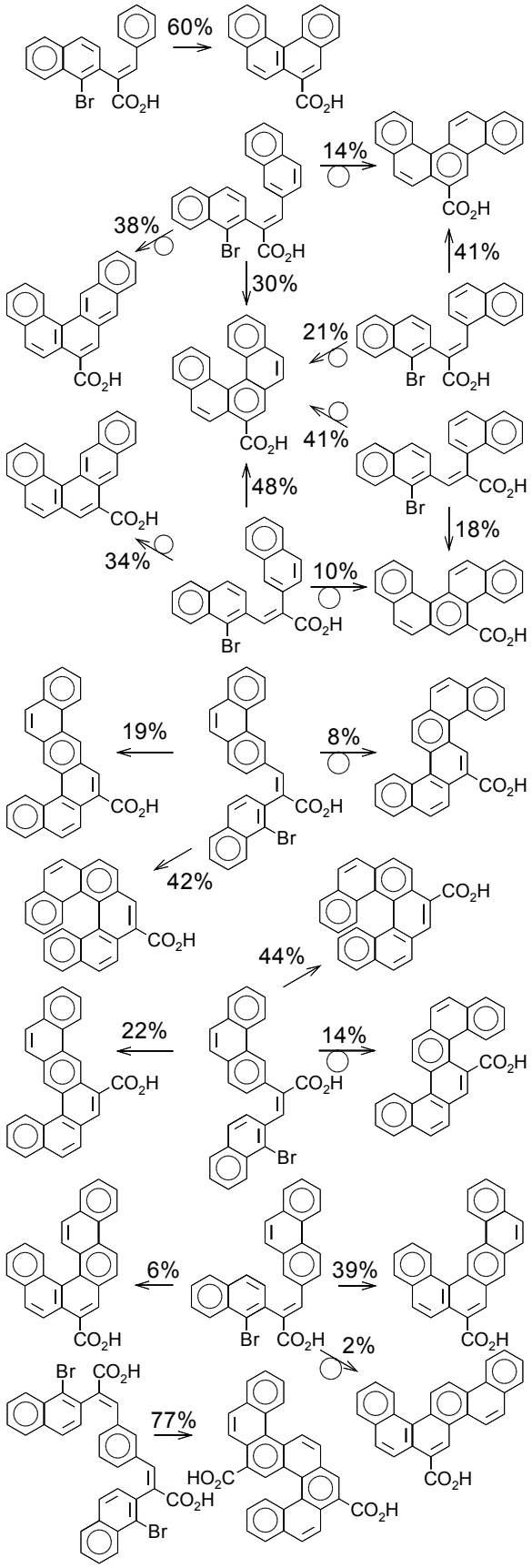

Fig. 1 Reported cyclisations of 3(or 2)-(1-bromonaphth-2-yl)-2(or 3)-aryl-acrylic acids in molten KOH. Reactions involving rearrangements of the carbon skeleton are marked by looped arrows. [1, 2, 3]

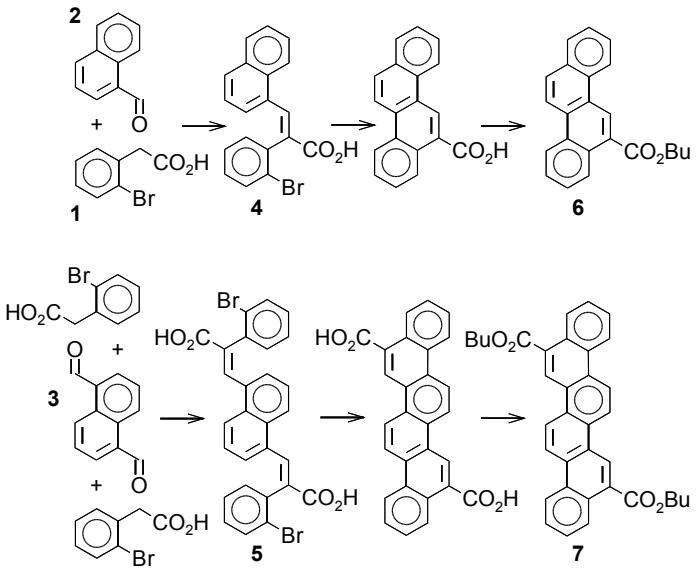

Fig. 2 Syntheses of chrysene and fulminene esters in low yield from 2-bromophenylacetic acid, *via* cyclisation in molten KOH.

Very recently, the ring closure under loss of HBr of 3-(2-bromophenyl)-2-phenyl-acrylic acid esters to phenanthrene-9-carboxylates has been reported to proceed efficiently in DMF or dimethylacetamide (DMAc) at 110 to 130°C in the presence of excess potassium carbonate and catalytic amounts of palladium diacetate.[4]

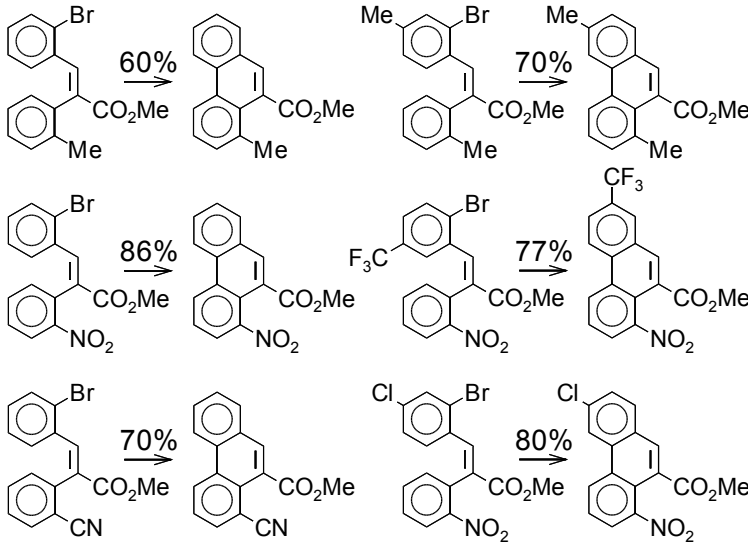

Fig. 3 Reported syntheses of substituted phenanthrenecarboxylates by $Pd(OAc)_2$-catalysed ring closures of bromostilbenecarboxylates.[4]

Even though the authors did not prepare their precursor stilbene-carboxylates by Perkin condensations but by Heck couplings of aryldiazonium salts with 2-(2-phenyl)-acrylates, the Perkin reaction followed by esterification seems to be the easiest approach to appropriately brominated cylisation substrates, as long as the necessary ortho-brominated arylacetic acids and reactive arylcarbonyl compounds are easily accessible.

The ability of palladium acetate to cyclise appropriately brominated precursors under sterical hindrance is illustrated by the reported formation of dimethoxy-helicenes from bis((bromoaryl)vinyl)veratroles: The [5]helicene forms in 75% yield, the [6]helicene in 30% yield, the [7]helicene could not be obtained (reaction conditions: 10mol% $Pd(OAc)_2$, 20mol% P(cyclohexyl)$_3$-HBF_4, 14h in DMAc at 130°C).[5]

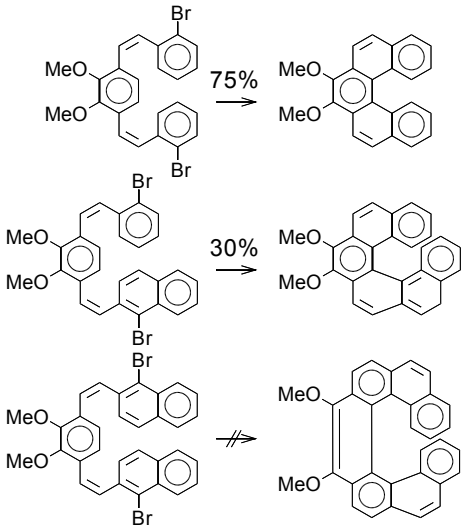

Fig. 4 Reported double cyclisations of dibrominated substrates with $Pd(OAc)_2$ to helicenes.[5]

To avoid more than one possible isomeric cyclisation product, the nonbrominated Perkin precursor should have only one aromatic ortho-hydrogen available next to the Perkin-reactive carbonyl, so eg. 1-naphthaldehyde **2** and 1,5-diformylnaphthalene **3** are preferable precursors compared to 2-naphthaldehyde or 2,6-diformylnaphthalene. We thus coupled 2-bromophenylacetic acid **1** with the two aldehydes **2** and **3** using our previously established mild procedure (3h reflux in THF in the presence of Et_3N and Ac_2O), esterified the resulting Perkin products **4** and **5** to obtain the butyl ester **4a** and the dibutyl ester **5a** (*c.*50% yield over 2 steps in both cases, i.e. no decrease in isolated yield between single and double Perkin reaction) and then treated these with $Pd(OAc)_2$ (5 mol%) and K_2CO_3 in DMF at 110°C for 16h to obtain butyl chrysene-6-carboxyate **6** and dibutyl fulminene-8,16-dicarboxylate **7** in 85% and 30% yield, respectively. The latter yield is not optimal, but considering that we made no attempt to optimise it by changing the solvent (DMAc is reported to give better yields

than DMF[4]) or adding ligands such as tricyclohexylphosphine,[4] these results illustrate that the palladium coupling approach to carboxy-substituted elongated polycyclic arenes is clearly superior to coupling in molten KOH.

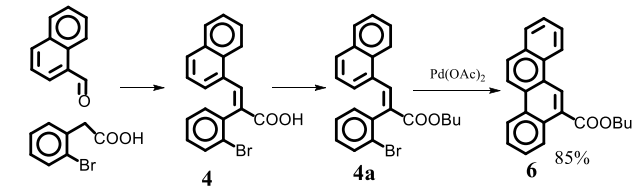

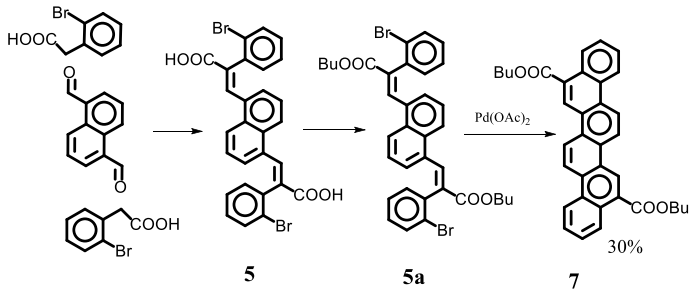

4.2. Perkin reactions of arylglyoxylic acids with arylacetic acids

The above results show that the Perkin condensation – palladium dehydrodebromination sequence offers a straightforward access from bromoarylacetic acids and formylarenes to elongated alkoxycarbonyl-substituted laths with one ester substituent per condensation site. To exploit this approach for the development of laths with a greater variety of electronic properties, it would be beneficial to replace the formylarene substrate by an arylglyoxylic acid. This should yield two vicinal carboxy substituents on the double bond created by the Perkin reaction, which could, depending on the post-Perkin treatment, either give two ester substituents with only a weak electron-withdrawing effect on the arene π system, or give one imide substituent with a pronounced depleting effect on the π system.

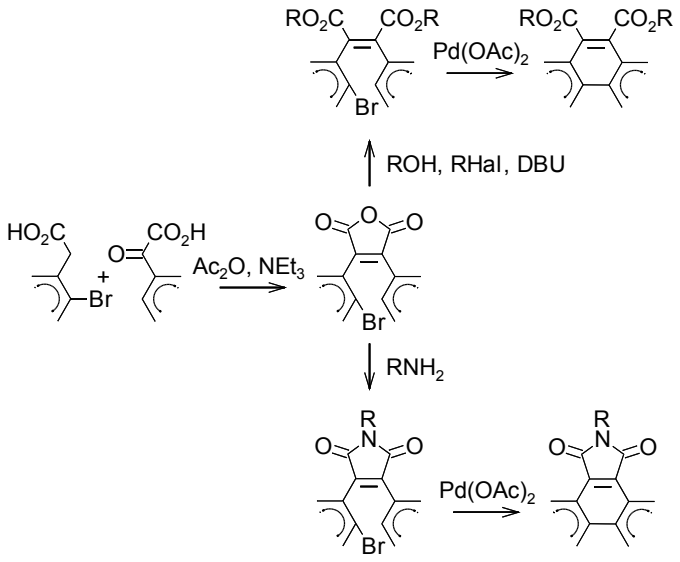

Fig. 5 Envisaged access to either *vic*-diester or imide functionalised arenes via Perkin reactions with arylglyoxylic acids

Whilst acetylarenes are not known to give the Perkin reaction, the successful formation of diphenylmaleic anhydride by condensation of potassium phenylglyoxylate with phenylacetic acid in acetic anhydride was first reported by Koelsch and Wawzonek in 1941,[6] and the analogous formation of substituted diphenylmaleic anhydrides from various para-substituted phenylacetic acids has been reported with 72 to 89% yield,[7] including the double Perkin reaction of p-phenylenediacetic acid with two equivalents of phenylglyoxylic acid **8** in 87% yield.

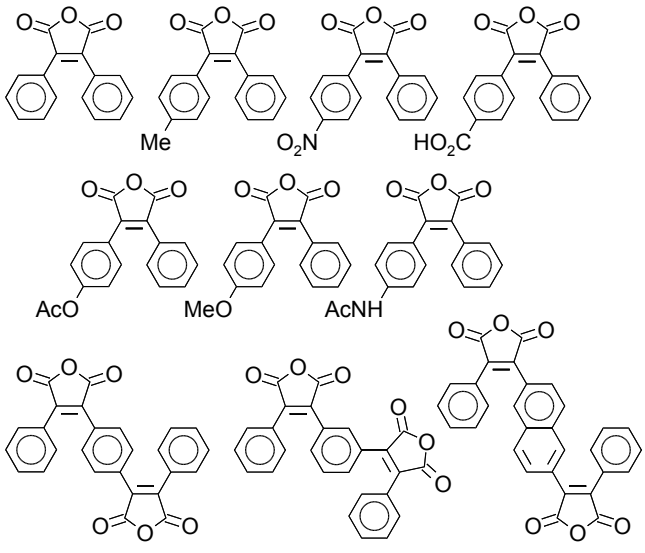

Fig. 6 Products of reported Perkin condensations of substituted phenylacetic acids with phenylglyoxylic acid (all yields >50%).[6, 7]

4.3. Bifunctional reagents for glyoxylic Perkin reactions followed by cyclising dehydrodebrominations

For the eventual elaboration of elongated condensed arenes by multiple Perkin reactions followed by cyclising dehydrobrominations, readily accessible bifunctional substrates are necessary.

As bifunctional homologue of 2-bromophenylacetic acid **1**, the evident target substrate is 2,5-dibromophenylene-1,4-diacetic acid **9**. The bromination of 4-cyanophenylacetic acid with one equivalent NBS in 50% aqueous sulphuric acid at room temperature has been reported to give 2-bromo-4-cyanophenylacetic acid in 70% yield.[8] Given that the deactivating effect of a first bromo substituent should be weaker than the one of a cyano substituent and that the deactivating effect of a second carboxymethyl should be negligible, we assumed that the entry of two bromine atoms into 1,4-phenylenediacetic acid should be feasible with two equivalents of NBS under similar reaction conditions. Indeed, we found that the 2,5-dibromophenylene-1,4-diacetic acid **9** is obtained as major product, accompanied by 2,3-dibromophenylene-1,4-diacetic acid and smaller amounts of monobromo- and tribromo-phenylene-1,4-diacetic acid. The desired unpolar 2,5-isomer **9** could be separated from the polar 2,3-isomer by profiting from its lower solubility in the quite polar solvents THF and acetone and its higher solubility in the less polar solvent ethyl acetate, allowing its isolation on a 100g scale in yields of 40 to 50%.

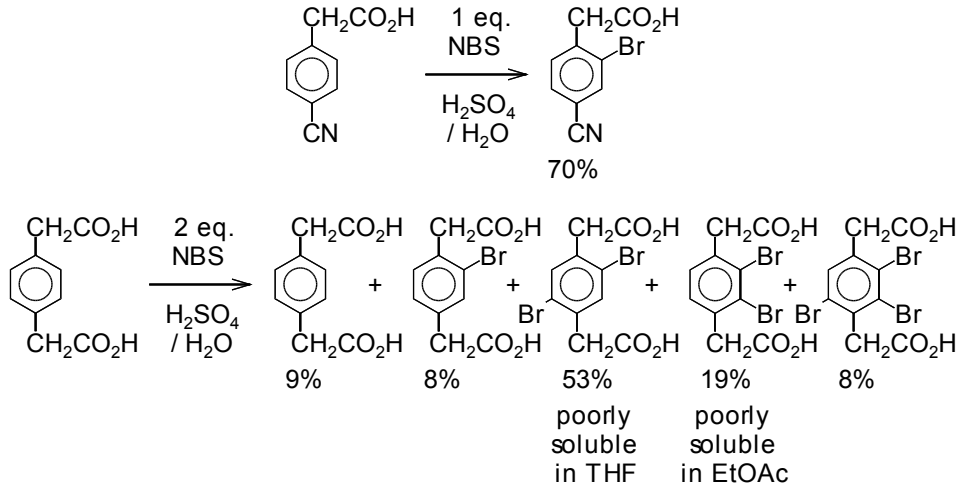

Fig. 7 Reported bromination of 4-cyanophenylacetic acid,[8] and analogous bromination of phenylene-1,4-diacetic acid, with yields (by ^{1}H-NMR of crude product mixture).

To obtain a arylenediglyoxylic acid as complementary Perkin substrate, an apparently very direct approach would be the double Friedel-Crafts acylation of pyrene with ethyl chloroglyoxylate (EtO_2CCOCl). Pyrene is highly reactive in its four equivalent positions 1, 3, 6 and 8, and is known to undergo double acylations with acyl chlorides in the presence of aluminium trichloride at room temperature very easily and selectively to yield mixtures of 1,6- and 1,8-diacylpyrenes. Only acetyl chloride, the smallest stable acyl chloride, is known to give also the 1,3-diacylpyrene besides the 1,6 and 1,8 isomers (the latter being the major product),[9] whereas e.g. chloroacetyl chloride and benzoyl chloride give exclusively the latter two.[10] We thus supposed that the acylation of pyrene with excess ethyl chloroglyoxylate[11, 12, 13, 14] should lead to pyrenylene-1,6- and -1,8-diglyoxylic acid ethyl esters directly and exclusively. The same approach with naphthalene should be less viable because its double Friedel-Crafts acylation requires harsh conditions[15, 16] and its monoacylation with one equivalent of ethyl chloroglyoxylate is known to give a mixture of naphthyl-1- and 2-glyoxylic acids.[11] Diacylation of naphthalene with this sterically demanding acyl chloride should thus, if feasible, give a hard-to-separate mixture of many isomers (1,4/1,5/1,3/1,6/1,7/2,6/2,7 if we consider vicinal disubstitution in 1,2/2,3/1,8 improbable).

To our surprise, we found that in contrast to its reaction with acetyl, chloroacetyl or benzoyl chloride, pyrene undergoes mostly monoacylation with excess ethyl chloroglyoxylate and $AlCl_3$ in DCM at room temperature over night, with only traces of diacylation products. A longer reaction time of 5d led to substantial ester hydrolysis (in spite of the anhydrous reaction conditions; one may assume that the HCl formed during acylation splits the ester $ArCOCO_2Et$ into acid chloride and alcohol), but only moderately improved the extent of diacylation. The deactivating effect of a $–COCO_2R$ substituent is apparently significantly stronger than the one of a $-CO_2R$ substituent. After reesterification of hydrolysed products, we were nevertheless able to isolate a mixture of diesters in about 15% yield, surprisingly containing more 1,3- than 1,6-isomer, and we could isolate the major 1,8-isomer by column chromatography in 8% yield.

We then considered acylation with EtO_2CCOCl of 1-acetylpyrene. The latter is smoothly obtained in large quantities and high yields if the acetylation of pyrene is conducted with acetic anhydride in the presence of zinc dichloride, both less reactive than acetyl chloride and aluminium trichloride, respectively.[10] We were delighted to not only find that the reaction of 1-acetylpyrene with EtO_2CCOCl and $AlCl_3$ in DCM at room temperature smoothly gives the expected mixture of three diacylpyrenes, but also that the major isomer, ethyl 1-acetylpyrenyl-8-glyoxylate, is conveniently separable from the minor 1,6- and 1,3-isomers by crystallisation from ethyl acetate.

Oxidation of the acetyl group with selenium dioxide[17, 18] yields pyrenylene-1,8-diglyoxylic acid monoethyl ester **10** in 71% yield.

Hydrolysis of the diester or of the ester-acid **9** gives pyrenylene-1,8-diglyoxylic acid **11** as bifunctional Perkin reagent.

4.4. Elongated polycyclic aromatic di- and tetraesters

Having thus in hand bifunctional Perkin substrates of two types – a dibromo-arylene-diacetic acid (**9**) and an arylene-diglyoxylic acid (**11**), we tested their efficiency in combination with commercial or easily accessible monofunctional counterparts: phenylglyoxylic acid **8** and 1-pyrenylglyoxylic acid **13** on the one hand, and 2-bromophenylacetic acid **1** on the other, and 1-naphthylglyoxylic acid **12** with 2,5-Dibromophenylene-1,4-diacetic acid **9**. We also reacted 2-bromophenylacetic acid **1** with **11** and 2,5-Dibromophenylene-1,4-diacetic acid **9** with **13** to compare the double Perkin condensation – double dehydrodebromination sequences with single Perkin – single cyclisation sequences.

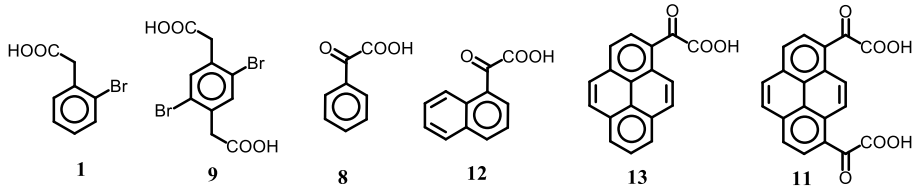

1 **9** **8** **12** **13** **11**

Isolated yields of the Perkin condensations plus subsequent esterifications were again on average as good with double as with single condensations, and slightly better with glyoxylic acids (around 60%, see fig. 8) than with aldehydes (*c.*50%, *see above*) under essentially identical reaction conditions. The palladium coupling reactions of the so obtained vicinal diethyl esters **14**-**19**, carried out as before, gave excellent yields – 92% and 90% for single cyclisations, and 89%, 66%, 79% and 91% for double cyclisations (**20**-**25**, see fig. 8). The yield of **14** increased from 80% to 92% when increasing the quantity of Pd(II)acetate used from 2.5 to 5 mol%. We thereupon stuck to the use of 5 mol% of $Pd(OAc)_2$ per cyclisation site in all cyclisation reactions.

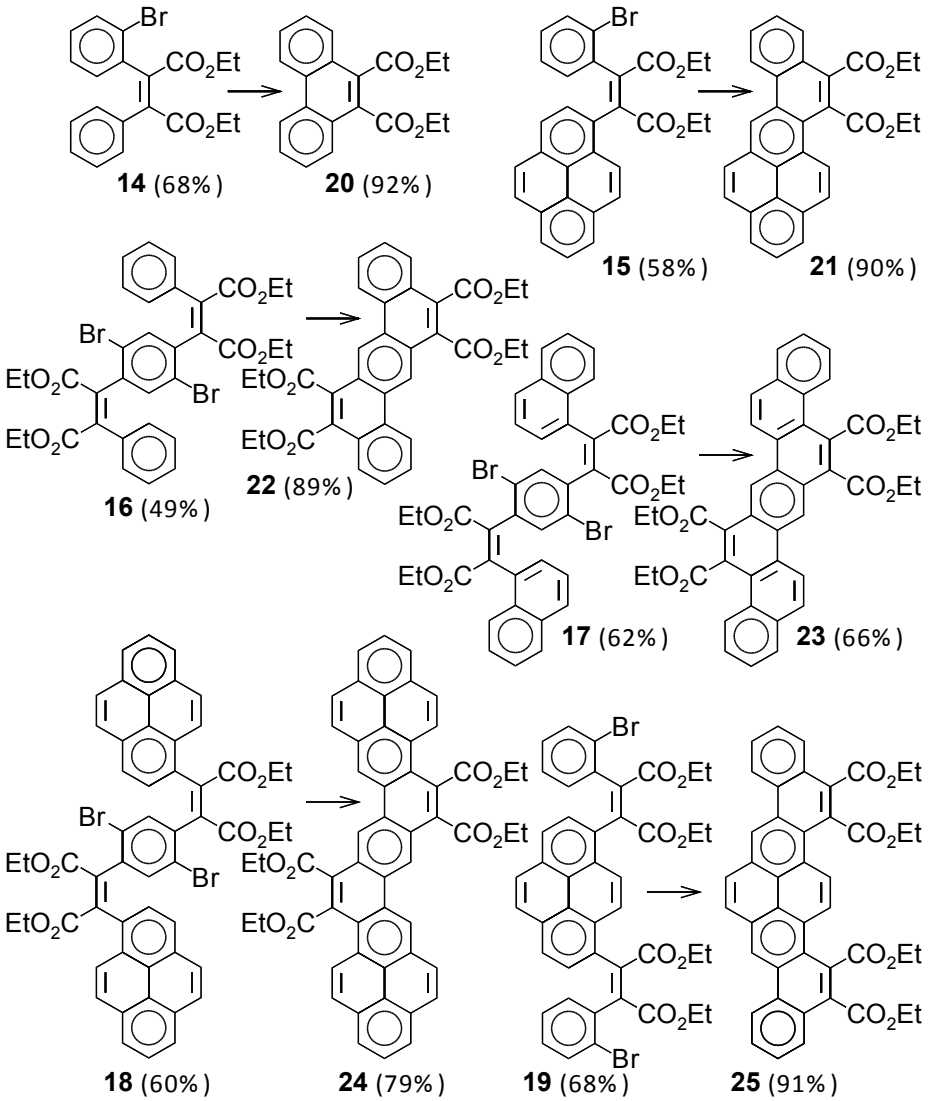

Fig. 8 Products of single and double glyoxylic Perkin condensations (bromoarylacetic acid, arylglyoxylic acid, Et_3N, Ac_2O, THF, reflux, 3h, then EtOH, EtI, DBU, reflux, 4h) and dehydrodebrominations (5 mol% $Pd(OAc)_2$, K_2CO_3, DMF, 110°C, 16h). Yields are given in parentheses.

4.5. Towards more extended carboxy-substituted lath-shaped arenes with the help of monoprotected bifunctional bricks and one-pot Perkin reaction – imidification sequences

Having established that the two complementary bifunctional Perkin substrates 2,5-dibromophenylene-1,4-diacetic acid **9** and pyrenylene-1,8-diglyoxylic acid **11** are accessible with limited effort in

multigram quantities and are smoothly condensed with monofunctional counterparts via the three-step condensation – esterification – cyclisation sequence to elongated polycyclic aromatic tetraesters, we considered the controlled build-up of longer ribbon-type homologues. A monoester of either of the diacids **9** and **11** would allow the double condensation with half an equivalent of the other diacid **11** or **9**. Thereafter the anhydride moieties of the dianhydride-diester obtained by this double condensation should be transformed into solubilising substituents that are inert during the hydrolysis of the terminal ester groups prior to a second iteration of the Perkin condensation – functional group modification sequence. If no such solubilising groups are introduced, failure of later Perkin condensations due to insufficient solubility is to be expected. Esterification of the anhydride groups seems inappropriate because these ester groups would a priori not be more stable than the terminal ester groups that are to be hydrolysed. Cyclic alkylimide moieties on the other hand are much more stable towards hydrolysis than alkyl esters, and our group recently showed that perylene-tetracarboxylic monoimide-diesters could be hydrolysed conveniently to the imide-anhydride without affecting the alkylimide group.[19] Besides the prospect of more variable electronic properties of the final ribbons, the possibility to introduce hydrolysis-resistant solubilising alkylimide groups is another feature that makes the glyoxylic approach more attractive than the use of aldehydes as Perkin substrates.

Cyclic *n*-alkylimide substituents are less efficient solubilising moieties than *vic*-di-*n*-alkylester groups, but the use of α-branched alkyl groups dramatically increases the solubilising effect of the alkylimide substituent if both alkyl branches are longer than methyl.[20] The only appropriate non-terminal aminoalkane that is commercially cheaply available is 3-aminopentane (*c.*0.15€/mmol). 4-aminoheptane is available at higher price (*c.*0.9€/mmol), and longer swallow-tail alkylamines can be obtained efficiently from the commercially available ketones in two steps via the oximes.[20, 21]

To obtain a monoprotected derivative of 2,5-dibromophenylene-1,4-diacetic acid **9**, we considered that the statistically controlled saponification of its dialkylester with one equivalent of KOH should lead to 50% yield of the monoester, besides 25% of unchanged diester and 25% of diacid, which both can be recycled. To obtain the necessary homogeneous reaction conditions, we found that a mixture of THF and methanol is appropriate to dissolve both the dimethylester (insoluble in methanol) and KOH. Thus we indeed obtained the monomethylester **26** in 50% yield, plus 44% recuperated diester and diacid **9**, and the separation of these three products proved to be easy by chromatography in chloroform on silica.

As concerns a monoprotected derivative of pyrenylene-1,8-diglyoxylic acid **11**, the synthesis from ethyl 1-acetylpyrenyl-8-glyoxylate by oxidation with SeO_2 yields not only the monoethylester-monoacid **10**, but offers also an alternative monoprotection in the form of an oxidisable acetyl group if instead of oxidation, saponification is chosen to yield 1-acetylpyrenyl-8-glyoxylic acid **27**. **27** could

e.g. be used in a Perkin reaction with **9**, followed, after transformation of the anhydride moieties, by oxidation of both terminal acetyl groups with selenium dioxide.

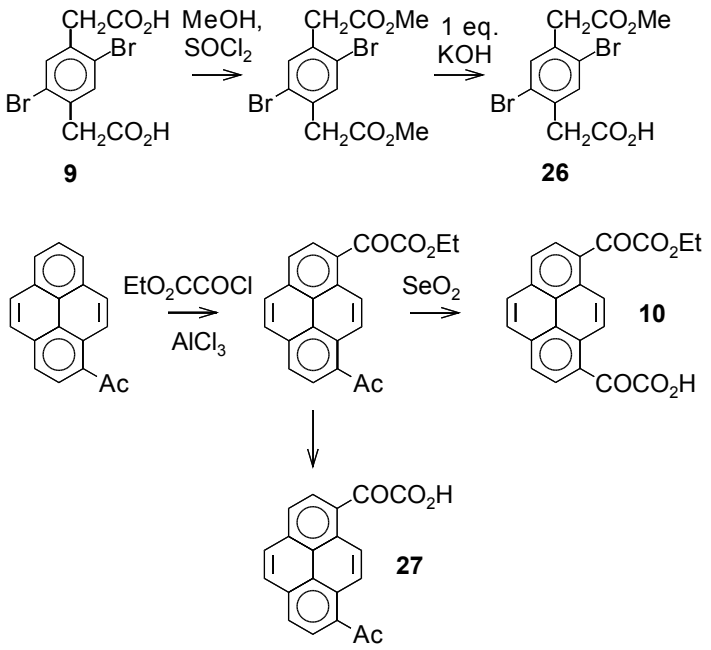

Fig. 9 Syntheses of monoprotected bifunctional Perkin substrates.

To elaborate an efficient approach to imidified Perkin products, we tried to combine the condensation and imidification steps in a one-pot procedure. After 2h at reflux in dioxane (bp. 101°C), instead of working up the Perkin reaction, we added excess 3-aminopentane and continued reflux for 16h. We chose boiling dioxane as solvent because we feared that refluxing THF (66°C) was not hot enough to ensure ring closure of the initially formed amide-acid to the imide – conventional imidifications are often carried out at even higher temperatures, *e.g.* in refluxing DMF.[22] When applied to pyrenyl-1-glyoxylic acid **13** and 2-bromophenylacetic acid **1**, this procedure led directly to the expected imide **28** in excellent yield (82%), whilst the yield of diimides **29** and **30** from the double condensations **13**+**9**+**13** and **1**+**11**+**1** were similar (>50%) to the two-step procedure used to obtain the corresponding tetraesters.

The Pd(II) catalysed cyclisation of **28** gave the expected naphthopyrenylene-dicarboxylic (3-pentyl)imide **31** near-quantitatively (93% yield).

We then checked whether the monoester-monoacids **26** and **10** would give the expected imides when reacted with their monofunctional counterparts **13** and **1**. Whilst **26** condensed with **13** to give the imido-arylacetic ester **32** in 50% yield, we could not isolate the expected imido-arylglyoxylic ester from the reaction of **10** with **1** due to apparent decomposition to unidentified polar substances. When we then replaced **10** by 1-acetylpyrenyl-8-glyoxylic acid **27**, the expected acetyl-imide **33** was

obtained in low yield (22%). Both glyoxylic ester substituents and acyl groups seem thus to be too fragile to survive either the Perkin condensation or the imidification step when carried out in refluxing dioxane, but the successful isolation of **33** indicates that slight modifications should lead to more satisfying yields when using one or the other of these protected substituents.

It is noteworthy that the orthobrominated diarylmaleic esters and imides **14**-**19**, **28**-**30**, **32** & **33** show strongly broadened ^{1}H-NMR spectra due to hindered aryl rotation between conformational energy minima, whereas the signals of their cyclised derivatives **20**-**25** & **31** are sharp in the absence of conformational multiplicity (see fig.11).

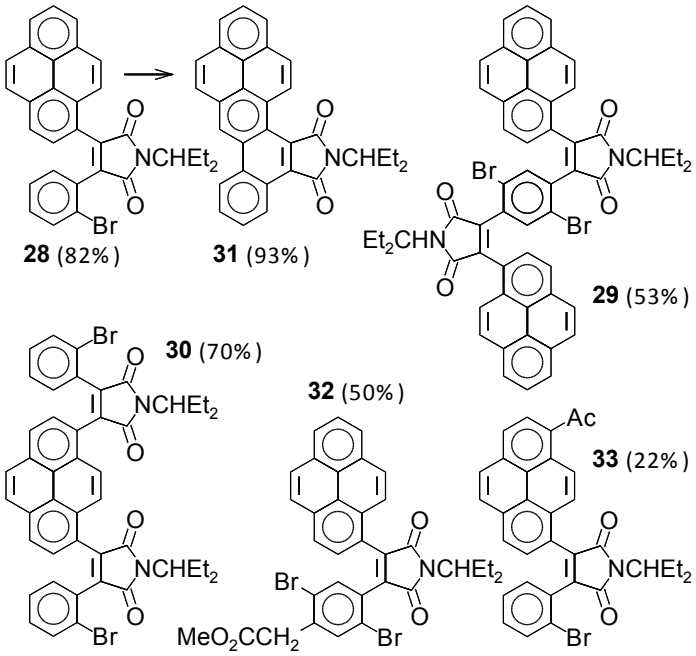

Fig. 10 Imides obtained by one-pot Perkin condensation – imidification sequences in refluxing dioxane, with yields.

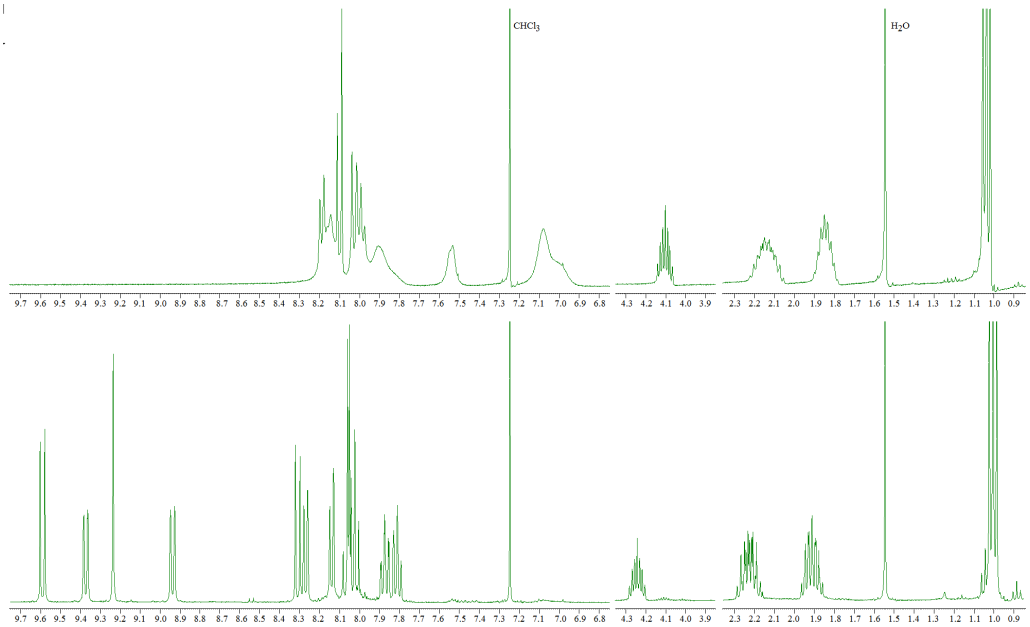

Fig. 11 characteristically broadened ^{1}H-NMR spectrum of brominated imide **28** (top) and sharp spectrum of the cyclised imide **31** (bottom).

To check whether milder reaction conditions were feasible, we returned to boiling THF as solvent and to the simplest possible test reaction, the reaction of phenylacetic acid with phenylglyoxylic acid. To our satisfaction, we could isolate diphenylmaleic acid butylimide **34** in excellent yield (91%, we used 1-aminobutane here instead of 3-aminopentane to ensure good recrystallisability in such a small molecule). Apparently, the dehydrating ring closure of maleic acid-amides to maleimides is efficient already in refluxing THF. It is thus not far-fetched to believe that acetyl-imides such as **33** or even imido-arylglyoxylic esters **32** can be obtained in satisfactory yield as well.

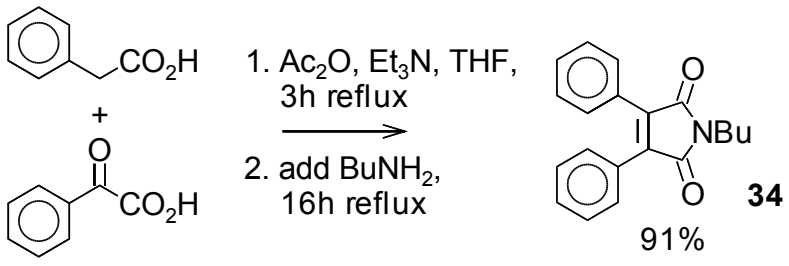

Fig. 12 High-yield synthesis of diphenylmaleic butylimide.

4.6. Conclusion and outlook

We found that the palladium diacetate catalysed cyclo-dehydrodebromination of orthobrominated Perkin condensation products is of satisfactory efficiency both on diarylacrylate and diarylmaleate substrates, without need of sophisticated or expensive ligands. The yields of Perkin condensations as well as Pd(II) catalysed cyclisations does not markedly decrease when passing from single to double condensations and cyclisations. Compared to the initially pursued approach based on the condensation of orthobromoarylacetic acids with aromatic aldehydes followed by esterification and cyclisation, the use of arylglyoxylic acids instead of aldehydes, followed by same-pot imidification and subsequent cyclisation, appears superior. This is due to the greater variability of the electronic properties of the final lath- or ribbon-shaped products, and to the possibility to maintain the solubilising alkylimide substituents during the saponification of protective ester groups prior to a second iteration of Perkin condensations. In order to pursue this approach, we not only elaborated the large-scale synthesis of two complementary bifunctional Perkin substrates, 2,5-dibromophenylene-1,4-diacetic acid **9** and pyrenylene-1,8-diglyoxylic acid **11**, but also of their monoprotected ester-acid variants **26** and **10** as well of the acetyl-acid **27** as alternative to **10**, and partially proved the viability of **26** and **27** in one-pot condensation-imidification sequences. Further optimisation is necessary to obtain satisfactory yields with the monoprotected diglyoxylic bricks **27** and **10**, but the successful obtention of diarylmaleimide **32** in high yield under milder reaction conditions indicates that we are not far from obtaining high yields with **27** or **10**. Second-iteration laths such as depicted in Fig. 12 thus appear to be feasible targets, and true GNR polymers as well as fully condensed macrocycles (nanobelts) become envisageable.

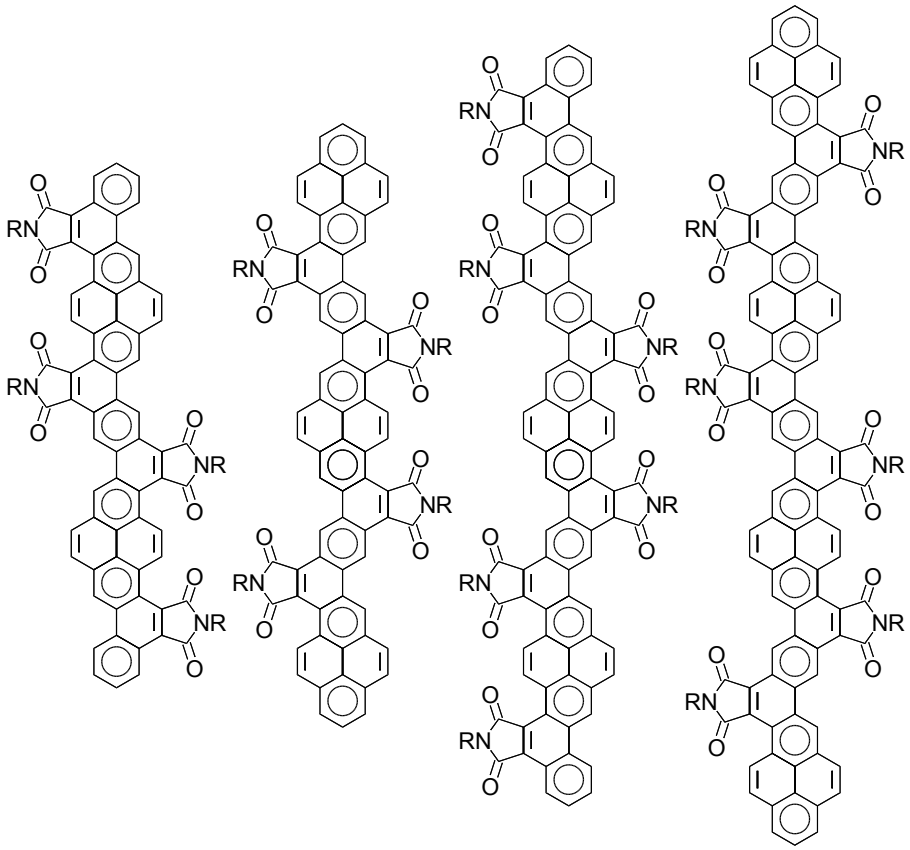

Fig. 13 Hypothetical tetra- and hexaimides based on **26** and **10** or **27**, plus **1** or **13** as end bricks, by two iterations of the condensation/imidification – cyclisation sequence.

4.7. Experimental

Substrates for Perkin condensations:

2,5-Dibromophenylene-1,4-diacetic acid (9)

With ice bath cooling, conc. sulfuric acid (800 g) is cautiously added to water (400 g) in a 2 L flask. Once the mixture has cooled back down to approximately room temperature, phenylene-1,4-diacetic acid (126.2 g, 650 mmol) is added with vigorous stirring, followed by N-bromo-succinimide (131.4 g, 1.30 mol), and the resulting suspension is stirred at room temperature for 16 h. The suspension is added with stirring to an ice/water mixture (2 L), the raw product is filtered off with a large glass filter, washed on the filter with water, oven-dried ands recrystallised twice from THF to yield 66.1 g of product. The majority of the also formed 2,3-dibromophenylene-1,4-diacetic acid (poorly soluble in boiling ethyl acetate, not isolated pure) is eliminated from the evaporation residue of the THF mother liquors by crystallisation from ethyl acetate. A further crop of 43.7 g of the major 2,5-dibromo isomer (poorly soluble in acetone) is then obtained from the evaporation residue of the ethyl acetate mother liquors by boiling in acetone followed by hot filtration. Combined yield: 99.8 g (284 mmol, 44%).
^{1}H-NMR (d_6-DMSO, 400MHz): δ = 12.55 (broad s, 2H), 7.68 (s, 2H), 3.72 (s, 4H) ppm. ^{13}C-NMR (d_6-DMSO, 100MHz): δ = 171.1, 135.9, 135.2, 123.4, 40.3 ppm.

2,5-Dibromophenylene-1,4-diacetic acid dimethyl ester

2,5-Dibromophenylene-1,4-diacetic acid (42.2 g, 60 mmol) is dissolved in refluxing methanol (1 L). Thionyl chloride (100 g) is cautiously added through the reflux condenser and reflux is continued for 16 h under exclusion of humidity. The product crystallises upon cooling, and is filtered off on a glass filter, washed with methanol and dried under vacuum. Yield: 42.6 g (112 mmol, 93%).
^{1}H-NMR ($CDCl_3$, 400MHz): δ = 7.50 (s, 2H), 3.74 (s, 4H), 3.72 (s, 6H) ppm.

2,5-Dibromophenylene-1,4-diacetic acid monomethyl ester (26)

The dimethyl ester (36.0 g, 95 mmol) is dissolved in THF (100 mL). At reflux and with stirring, methanol (200 mL) is added slowly through the reflux condenser, upon which the diester may repricipitate temporarily. Reflux is continued until full dissolution, whereupon a solution of an equimolar amount of potassium hydroxide (5.3 g, 95 mmol) in methanol (25 mL) is added and stirring at reflux is continued for 2 h. The solvent is evaporated, 5% aqueous hydrochloric acid (600 mL) and ethyl acetate (600 mL) are added, the mixture is thoroughly shaken until full dissolution, the phases are separated, the organic phase is dried with sodium sulphate and the ethyl acetate is evaporated. The residue is boiled in chloroform, the part insoluble in hot chloroform is filtered off (5.2 g, mainly

diacid, c.15 mmol), and the chloroform-soluble part is chromatographed on silica. Chloroform elutes unreacted diester (10.2 g, 27 mmol), followed by ethyl acetate to elute the ester-acid. Yield: 17.2 g (47 mmol, 50%). Yield of recuperated recyclable side products (diester and diacid): c.44% (c.42 mmol).

^{1}H-NMR ($CDCl_3$, 400MHz): δ = 7.51 (s, 2H), 3.78 (s, 2H), 3.74 (s, 2H), 3.72 (s, 3H) ppm (acid proton not detected).

1,5-Bis(bromomethyl)naphthalene[23]

1,5-Dimethylnaphthalene (15 g, 96 mmol) and azobisisobutyronitrile (0.4 g, 2 mmol) are dissolved in tetrachloromethane (100 mL). At reflux, a solution of bromine (10 mL, 31 g, 194 mmol) in tetrachloromethane (30 mL) is added dropwise, and reflux is continued for 16 h. The product crystallises during the reaction. After cooling to room temperature, the precipitate is filtered off, washed with pentane and recrystallised from chloroform. Yield: 16.7g (53mmol, 55%).

^{1}H-NMR ($CDCl_3$, 400MHz): δ = 8.18 (d, 8Hz, 2H), 7.59 (d, 8Hz, 2H), 7.54 (t, 8Hz, 2H), 4.95 (s, 4H) ppm.

1,5-Diformylnaphthalene (3)[23]

1,5-Bis(bromomethyl)naphthalene (16.7 g, 53 mmol), N-methyl-morpholine-N-oxide (28 g, 239 mmol) and powdered 4Å molecular sieves (100 g) are refluxed for 16 h under exclusion of moisture. The solids are filtered off hot and boiled out with chloroform twice, the solvents of combined filtrate and extracts are evaporated and the residue is purified by chromatography on silica in chloroform. Yield: 5.0 g (27 mmol, 51%).

^{1}H-NMR ($CDCl_3$, 400MHz): δ = 10.39 (s, 2H), 9.61 (d, 8.5Hz, 2H), 8.09 (d, 7Hz, 2H), 7.86 (dd, 7Hz & 8.5Hz, 2H) ppm.

Naphthyl-1-glyoxylic acid (12)[11]

Naphthyl-1-acetic acid methyl ester (8.0 g, 40 mmol, 7 mL) and selenium dioxide (7.9 g, 71 mmol) are refluxed in dry diglyme under argon and exclusion of moisture for 5 h. DCM (300 mL) is added, the solids (mainly metallic selenium) are filtered off, the solvents are mostly evaporated (100° C, 20 mbar) and the residue purified by chromatography on silica in dichloromethane. The crude naphthyl-1-glyoxylic methyl ester (6.8 g) is saponified by refluxing with ethanol (10 mL) and 10% aquesous sodium carbonate (40 mL) for 5 h. Water and DCM are added, the phases are separated, the organic phase is washed with 5% aqueous hydrochloric acid and dried with sodium sulfate, and the solvent is evaporated. The product is recrystallised from toluene. Yield: 5.8 g (29 mmol, 72%).

^{1}H-NMR ($CDCl_3$, 400MHz): δ = 8.91 (d, 8Hz, 1H), 8.90 (broad s, 1H), 8.37 (d, 8Hz, 1H), 8.14 (d, 8Hz, 1H), 7.92 (d, 8Hz, 1H), 7.69 (t, 8Hz, 1H), 7.60 (t, 8Hz, 1H), 7.57 (t, 8Hz, 1H) ppm. ^{13}C-NMR

($CDCl_3$, 100MHz): δ = 187.0, 164.3, 136.7, 135.1, 134.1, 131.3, 129.7, 129.2, 127.6, 127.3, 125.6, 124.6 ppm.

Pyrenyl-1-glyoxylic acid ethyl ester

A solution of pyrene (20.2 g, 100 mmol) and ethyl chloroglyoxylate (EtO_2CCOCl, 30 g, 220 mmol) in DCM (150 mL) is added dropwise to an ice-cooled stirred suspension of aluminium trichloride (40 g, 300 mmol) in DCM (200 mL). Stirring is continued at room temperature under exclusion of humidity for 16 h. The mixture is poured into ice/water, acidified with aqueous hydrochloric acid and extracted with chloroform. The chloroform solution is dried with sodium sulfate and concentrated. Column chromatograpy on silica in chloroform separates the product from traces of diethyl pyrenylene-diglyoxylates The product is further purified by recrystallisation from butanol. Yield: 19.5 g (65 mmol, 65%).

^{1}H-NMR ($CDCl_3$, 400MHz): δ = 9.33 (d, 9Hz, 1H), 8.33 (d, 8Hz, 1H), 8.30 (d, 9Hz, 1H), 8.30 (d, 8Hz, 1H), 8.28 (d, 8Hz, 1H), 8.21 (d, 9Hz, 1H), 8.16 (d, 8Hz, 1H), 8.08 (t, 8Hz, 1H), 8.06 (d, 9Hz, 1H), 4.54 (q, 7.5Hz, 2H), 1.48 (t, 7.5Hz, 3H) ppm. ^{13}C-NMR ($CDCl_3$, 100MHz): δ = 189.3, 165.2, 135.9, 131.8, 131.24, 131.18, 130.9, 130.5, 130.4, 127.4, 127.2, 127.1, 126.8, 125.0, 124.5, 124.4, 124.0, 123.9, 62.5, 14.3 ppm.

Pyrenyl-1-glyoxylic acid ethyl ester and **pyrenylene-1,8-diglyoxylic acid diethyl ester**

A solution of pyrene (20.2 g, 100 mmol) and ethyl chloroglyoxylate (30 g, 220 mmol) in DCM (150 mL) is added dropwise to an ice-cooled stirred suspension of aluminium trichloride (40 g, 300 mmol) in DCM (200 mL). Stirring is continued at room temperature under exclusion of humidity for 5 days. The mixture is poured into ice/water and acidified with aqueous hydrochloric acid. The insoluble precipitate (a mixture of pyrenyl-glyoxylic and pyrenylene-diglyoxylic acids) is filtered off and dissolved in THF. The solution is dried with sodium sulfate and the solvent is evaporated. The residue is dissolved in anhydrous ethanol (500 mL), thionyl chloride (50 g) is added and the solution is stirred under reflux for 16 h. The solvent is evaporated and the product mixture is chromatographied on silica in DCM. Pyrenyl-1-glyoxylic acid ethyl ester elutes first (8.5 g, 28 mmol, 28%), followed by the three pyrenylene-diglyoxylic acid diethyl esters, of which the 1,6-isomer is formed only in traces and elutes before the 1,8-isomer (3.2 g, 8 mmol, 8%) and, as last, the 1,3-isomer (*c.*3 g, 7 mmol, 7%). The unwanted 1,6- and 1,3-isomers were not isolated in pure form.

Pyrenylene-1,8-diglyoxylic acid diethyl ester: ^{1}H-NMR ($CDCl_3$, 400MHz): δ = 9.37 (s, 2H), 8.42 (d, 9Hz, 2H), 8.29 (d, 9Hz, 2H), 8.21 (s, 2H), 4.55 (q, 7.5Hz, 4H), 1.49 (t, 7.5Hz, 6H) ppm. ^{13}C-NMR (CD_2Cl_2, 100MHz): δ = 189.3, 165.0, 135.5, 131.2, 130.7, 130.4, 127.7, 126.51, 126.46, 124.3, 63.2, 14.5 ppm.

Pyrenyl-1-glyoxylic acid (13)[24, 25]

Pyrenyl-1-glyoxylic acid ethyl ester (9 g, 30 mmol) is dissolved in refluxing absolute ethanol (90 mL). A 10 % aqueous sodium bicarbonate solution is added with stirring, whereupon a fine precipitate forms. The mixture is stirred at reflux for 16 h (complete dissolution occurs within the first hour). The solution is poured onto 1 % aqueous hydrochloric acid (1 L) to form a yellow precipitate, which is filtered off on a glass filter, washed with water on the filter and dried under vacuum. Yield: 8.2 g (30 mmol, 100 %).

^{1}H-NMR (d_6-DMSO, 400MHz): δ = 9.22 (d, 9Hz, 1H), 8.47-8.38 (m, 6H), 8.25 (d, 9Hz, 1H), 8.18 (t, 8Hz, 1H) ppm (acid proton not detected). ^{13}C-NMR (d_6-DMSO, 100MHz): δ = 191.4, 166.9, 135.2, 131.2, 131.1, 130.54, 130.49, 130.45, 129.7, 127.6, 127.1 (×3), 124.5, 124.0, 123.8, 123.5, 123.0 ppm.

Pyrenylene-1,8-diglyoxylic acid (11)

Pyrenylene-1,8-diglyoxylic acid diethyl ester (1.7 g, 4.3 mmol) is refluxed in 10% aqueous Na_2CO_3 solution (200 mL) and methanol (20 mL) for 3 h. The clear solution was acidified with concentrated hydrochloric acid to obtain a yellow precipitate that is filtered off via a glass frit, washed with water on the frit and dried in vaccum. Yield: 1.5 g (100 %). ^{1}H-NMR (d_6-DMSO, 400MHz): δ = 9.18 (s, 1H), 8.46 (m, 2H), 8.35 (s, 1H) ppm (acid proton not detected). ^{13}C-NMR (d_6-DMSO, 100MHz): δ = 191.6, 166.7, 135.2, 131.4, 131.0, 129.6, 127.3 (x2), 126.3, 123.9 ppm.

1-Acetylpyrene[10]

Pyrene (80.8 g, 400 mmol) is dissolved at 120 °C in acetic anhydride (300 mL). This solution is allowed to cool to 90 °C and added to a hot (90 °C) solution of zinc dichloride (100 g) in acetic acid (300 mL). After stirring for 1h at 90 °C, during which time a yellow precipitate forms, the mixture is allowed to cool to room temperature, and the precipitate is filtered off on a large glass filter and washed with acetic acid. The precipitate is dissolved with vigorous stirring in a biphasic mixture of water (800 mL) and chloroform (800 mL), the phases are separated and the chloroform phase is dried with sodium sulfate. The chloroform is evaporated and the product is purified by chromatography in DCM on silica. Yield: 74.5 g (300 mmol, 75 %).

^{1}H-NMR ($CDCl_3$, 400MHz): δ = 9.05 (d, 9Hz, 1H), 8.38 (d, 8Hz, 1H), 8.25 (d, 8Hz, 1H), 8.24 (d, 8Hz, 1H), 8.22 (d, 9Hz, 1H), 8.16 (d, 9Hz, 1H), 8.16 (d, 8Hz, 1H), 8.06 (d, 9Hz, 1H), 8.05 (t, 8Hz, 1H), 2.90 (s, 3H) ppm.

1-Acetylpyrenyl-8-glyoxylic acid ethyl ester and **1-Acetylpyrenyl-8-glyoxylic acid (27)**

A solution of 1-acetylpyrene (74.5 g, 300 mmol) and ethyl chloroglyoxylate (59 g, 242 mmol) in DCM (200 mL) is added dropwise with ice bath cooling to a stirred suspension of aluminium

trichloride (120 g, 900 mmol) in DCM (500 mL). After stirring under exclusion of humidity for 16 h at room temperature, the mixture is poured into ice/water (1 L). Hot (c. 50 °C) chloroform (2 L) and acetone (1 L) are added and the mixture is stirred until complete dissolution. The organic phase is separated and dried with sodium sulfate, and the solvent is evaporated. The residue is boiled out with chloroform (500 mL) and filtered hot, to remove insoluble 8-acetylpyrenyl-1-glyoxylic acid (10.9 g, 34 mmol, 11 %). The chloroform is evaporated and the residue is purified by chromatography in chloroform on silica and recrystallisation from ethyl acetate to yield 1-acetylpyrenyl-8-glyoxylic acid ethyl ester (27.6 g, 80 mmol, 27 %).

1-Acetylpyrenyl-8-glyoxylic acid ethyl ester: ^{1}H-NMR ($CDCl_3$, 400MHz): δ = 9.32 (d, 10Hz, 1H), 9.12 (d, 10Hz, 1H), 8.41 (d, 8Hz, 1H), 8.37 (d, 8Hz, 1H), 8.26 (d, 8Hz, 1H), 8.22 (d, 8Hz, 1H), 8.18 (d, 9Hz, 1H), 8.12 (d, 9Hz, 1H), 4.54 (q, 7Hz, 2H), 2.91 (s, 3H), 1.48 (t, 7Hz, 3H) ppm.

1-Acetylpyrenyl-8-glyoxylic acid **27**: ^{1}H-NMR (d_6-DMSO, 400MHz): δ = 9.23 (d, 10Hz, 1H), 9.04 (d, 10Hz, 1H), 8.68 (d, 8Hz, 1H), 8.54 (d, 8Hz, 1H), 8.52 (d, 8Hz, 1H), 8.49 (d, 8Hz, 1H), 8.45 (d, 9Hz, 1H), 8.38 (d, 9Hz, 1H), 2.91 (s, 3H) ppm (acid proton not detected).

Pyrenylene-1,8-diglyoxylic acid monoethyl ester (10)

1-Acetylpyrenyl-8-glyoxylic acid ethyl ester (5 g, 14.5 mmol) and SeO_2 (2.6 g, 23.4 mmol, 1.6 eq.) are stirred in anhydrous pyridine (20 mL) at reflux (c. 115 °C) under argon and under exclusion of moisture and oxygen for 2 h. The dark precipitate is filtered off and washed with hot THF, and the solution is concentrated. The residue is chromatographed through silica with THF as eluent. Yield: 4.3 g (79 %) of yellow solid. ^{1}H-NMR (d_6-DMSO, 400MHz): δ = 9.12 (d, 10Hz, 1H), 8.57 (d, 5.5Hz, 1H), 8.39 (m, 4H), 8.23 (s, 2H), 4.50 (m, 2H), 1.37 (t, 7Hz, 3H) ppm

Perkin condensations between bromoarylacetic acids and formylnaphthalenes in THF, followed by esterification:

General procedure

2-Bromophenylacetic acid **1** (2.16 g, 10 mmol) is dissolved in triethylamine (5.05 g, 50 mmol) and acetic anhydride (10.2 g, 100 mmol). A solution of naphthalene-1-carbaldehyde (1.56 g, 10 mmol) or 1,5-diformylnaphthalene **3** (0.92 g, 5 mmol in THF (50 mL) is added. The reaction mixture is refluxed for 16 h, quenched by adding 50 ml of water into it and refluxing again for 1h, and then concentrated at reduced pressure. The residue is dissolved in aqueous KOH (15 g in 300 mL) and the crude Perkin product is precipitated by adding concentrated hydrochloric acid. The precipitate is filtered off by a glass frit, washed with water on the frit and dried on the air.

This crude condensation product is stirred with DBU (4.55 g, 30 mmol) and 1-bromobutane (6.9 g, 50 mmol) in butanol (150 mL) at 60 °C for 4h under exclusion of moisture, then concentrated at reduced pressure and chromatographed in chloroform through silica. The product ester is recrystallised from butanol.

Butyl 2-(2-bromophenyl)-3-(1-napthyl)-acrylate (4a)

Yield from **1** and naphthalene-1-carbaldehyde: 2.0 g (50 %) of white powder. ^{1}H NMR (400 MHz, $CDCl_3$): ∂ =8.55 (s, 1H), 8.11 (d, 8Hz, 1H), 7.81 (d, 8Hz, 1H), 7.70 (d, 8Hz, 1H), 7.57 (d, 9Hz, 1H), 7.52 (m, 1H), 7.16 (t, 8Hz, 1H), 7.07 (m, 2H), 6.99 (d, 7Hz, 1H), 6.92 (d, 7Hz, 1H), 4.26 (broad s, 2H), 1.65 (m, 2H), 1,35 (m, 2H), 0.90 (t, 7Hz, 3H) ppm. ^{13}C NMR (100MHz, $CDCl_3$) : ∂ = 166.8, 139.3, 137.5, 135.1, 133.4, 132.4, 132.0, 131.8, 131.6, 129.2 (X 2), 128.7, 127.5, 127.4, 126.7, 126.2, 125.2, 125.0, 124.2, 65.4, 30.7, 19.3, 13.8 ppm. HRMS (m/z (%)): calcd. For $C_{23}H_{21}BrO_2$ [M] 428.0725; found 408.0711.

Bis-1,6-(2-butoxycarbonyl-2-(2-bromophenyl)-vinyl)-naphthalene (5a)

Yield from **1** and **3**: 1.7g (49%) of white powder. ^{1}H NMR (400 MHz, $CDCl_3$): ∂ = 8.47 (s, 1H), 7.98 (d, 8Hz, 1H), 7.57 (d, 8Hz, 1H), 7.24 (pseudo t, 7Hz & 9Hz, 1H), 7.06 (m, 3H), 6.90 (d, 7Hz, 1H), 4.24 (broad s, 2H), 1.63 (m, 2H), 1.32 (m, 2H), 0.88 (t, 7Hz, 3H) ppm. ^{13}C NMR (100MHz, $CDCl_3$) : ∂ = 166.7, 139.2, 137.2, 132.5, 132.4, 131.8, 131.5, 129.3, 127.6, 127.4, 125.8, 125.3 (X 2), 124.9, 65.4, 30.6, 19.2, 13.8 ppm. HRMS (m/z (%)): calcd. For $C_{36}H_{34}Br_2O_4$ [M] 688.0824; found 688.0818.

Perkin condensations between bromoarylacetic acids and arylglyoxylic acids in THF, followed by esterification:

General procedure

2-Bromophenylacetic acid **1** (2.16 g, 10 mmol) or 2,5-dibromophenylene-1,4-diacetic acid **9** (1.76 g, 5 mmol) is dissolved in triethylamine (5.05 g, 50 mmol) and acetic anhydride (10.2 g, 100 mmol). A solution of phenylglyoxylic acid **8** (1.5 g, 10 mmol) or naphthyl-1-glyoxylic acid **12** (2.00 g, 10 mmol) or pyrenyl-1-glyoxylic acid **13** (2.74 g, 10 mmol) or pyrenylene-1,8-diglyoxylic acid **11** (1.73 g, 5 mmol) in THF (50 mL) is added. The reaction mixture is refluxed for 3 h, quenched by adding 50 ml of water into it and refluxing again for 1h, and then concentrated at reduced pressure. The residue is dissolved in aqueous KOH (10 g in 200 mL) and the crude Perkin product is precipitated by adding concentrated hydrochloric acid. The precipitate is filtered off by a glass frit, washed with water on the frit and dried on the air.

This crude condensation product is stirred with DBU (4.55 g, 30 mmol) and iodoethane (7.8 g, 50 mmol) in ethanol (150 mL) at 60 °C for 4 h under exclusion of moisture, then concentrated at reduced pressure and chromatographed in chloroform through silica. The product ester is recrystallised from ethanol.

Diethyl 2-(2-bromophenyl)-1-phenyl-maleate (14)

Yield from **1** and **8**: 2.74 g (68 %). ^{1}H NMR (400 MHz, $CDCl_3$): ∂ = 7.52 (m, 1H), 7.15 (m, 3H), 7.09 (m, 4H), 6.94 (m, 1H), 4.34 (m, 2H), 4.22 (broad s, 1H), 1.33 (t, 7Hz, 3H), 1.22 (t, 7Hz, 3H) ppm. HRMS (m/z (%)): calcd. For $C_{20}H_{19}BrO_4$ [M] 402.0467; found 402.0471.

Diethyl 2-(2-bromophenyl)-1-pyrenyl-maleate (15)

Yield from **1** and **13**: 3.06 g (49 %). ^{1}H NMR (400 MHz, $CDCl_3$): ∂ = 8.39 (s, 1H), 8.16 (s, 3H), 8.00 (m, 3H), 7.26 (broad s, 1H), 6.90 (s, 1H), 6.80 (broad s, 1H), 6.68 (s, 1H), 4.35 (s, 2H), 4.29 (broad s, 2H), 1.34 (t, 7Hz, 3H), 1.24 (t, 7Hz, 3H) ppm.

16

Yield from **9** and **8**: 1.78 g (49 %) ^{1}H NMR (400 MHz, $CDCl_3$): ∂ = 7.25 (s, 1H), 7.17 (t, 7Hz, 2H), 7.10 (s, 1H), 7.06 (broad s, 2H), 4.33 (m, 2H), 4.18 (broad s, 2H), 1.31 (t, 7Hz, 3H), 1.15 (broad s, 3H) ppm. HRMS (m/z (%)): calcd. For $C_{34}H_{32}Br_2O_8$ [M] 726.0464; found 726.0490.

17

Yield from **9** and **12**: 2.57 g (62 %). ^{1}H NMR (400 MHz, $CDCl_3$): ∂ = 7.98 (broad s, 2H), 7.70 (broad s, 2H), 7.43 (broad s, 2H), 7.14 (broad s, 1H), 6.83 (broad s, 1H), 4.20 (broad s, 4H), 1.19 (t, 7Hz, 3H), 1.02 (broad s, 3H) ppm. HRMS (m/z (%)): calcd. For $C_{42}H_{36}Br_2O_8$ [M] 826.0777; found 826.0814

18

Yield from **9** and **13**: 2.93 g (60 %) of yellow solid. ^{1}H NMR (400 MHz, $CDCl_3$): ∂ = 8.4 – 7.5 (broad s, 9H), 6.75 (broad s, 1H), 4.3 – 3.4 (broad s, 4H), 1.15 – -0.3 (broad s, 6H). ^{13}C NMR (100MHz, $CDCl_3$) : ∂ =. HRMS (m/z (%)): calcd. For $C_{54}H_{40}Br_2O_8$ [M] 974.1089; found 974.1084.

19

Yield from **1** and **11**: 2.90 g (68 %) of yellow solid. ^{1}H NMR (400 MHz, $CDCl_3$): ∂ = 8.43 (broad s, 1H), 7.89 (broad s, 3H), 7.37 (broad s, 1H), 6.83 (broad s, 2H), 6.67 (broad s, 1H), 4.32 (broad s, 4H), 1.30 (m, 6H).

Perkin condensations between bromoarylacetic acids and arylglyoxylic acids in dioxane, followed by same-pot esterification:

General procedure

The bromoarylacetic acid [2-bromophenylacetic acid **1** (2.15 g, 10 mmol) or 2,5-dibromophenylene-1,4-diacetic acid **9** (1.76 g, 5 mmol) or 2,5-dibromophenylene-1,4-diacetic acid monomethylester **26** (3.66 g, 10 mmol)] and the arylglyoxylic acid [pyrenyl-1-glyoxylic acid **13** (2.74 g, 10 mmol) or pyrenylene-1,8-diglyoxylic acid **11** (1.73 g, 5 mmol) or 1-acetylpyrenyl-10glyoxylic acid **27** (3.16 g, 10 mmol)] are dissolved in a solution of triethylamine (2.02 g, 20 mmol) and acetic anhydride (3.06 g, 30 mmol) in dioxane (50 mL) and refluxed for 2 h under exclusion of moisture. Then a solution of 3-aminopentane (4.5 g, 50 mmol) in dioxane (20 mL) is added and reflux is continued for 16 h. The solution is poured into water (400 mL), the formed precipitate is filtered off on a glass frit, washed with water on the frit, dried in vacuum and purified by chromatography in chloroform on silica followed by recrystallisation from ethanol (**28**) or butanol (**29**, **30**, **33**) or methanol (**32**).

28

Yield from **1** and **13**: 4.31 g (82 %) of orange powder. ^{1}H NMR (400 MHz, $CDCl_3$): ∂ = 8.20 – 8.09 (m, 5H), 8.01 (m, 3H), 7.90 (broad s, 2H), 7.54 (broad s, 1H), 7.08 (broad s, 3H), 4.10 (m, 1H), 2.13 (m, 2H), 1.85 (m, 2H), 1.03 (t, 7Hz, 6H) ppm.

29

Yield from **9** and **13**: 2.56 g (53 %) of orange powder. ^{1}H NMR (400 MHz, $CDCl_3$): ∂ = 8.30 – 7.70 (broad s, 9H), 7.30 (broad s, 1H), 4.04 (broad s, 1H), 2.07 (broad s, 2H), 1.80 (broad s, 2H), 0.97 (m, 6H) ppm.

30

Yield from **1** and **11**: 2.95 g (70 %) of orange powder. ^{1}H NMR (400 MHz, $CDCl_3$): ∂ = 8.20-8.07 (broad, 2H), 8.05 (s, 2H), 7.99-7.68 (broad, 4H), 7.58-7.49 (broad, 2H), 7.16-6.89 (broad, 6H), 4.09 (sept, 7.5Hz, 2H), 2.15 (broad, 4H), 1.85 (broad, 4H), 1.03 (t, 7.5Hz, 6H) ppm.

32

Yield from **26** and **13**: 3.38 g (50 %) of orange powder. ^{1}H NMR (400 MHz, $CDCl_3$): ∂ = 8.20 (d, 8Hz, 1H), 8.15 (d, 5.5 Hz, 1H), 8.12 (d, 3Hz, 1H), 8.10 (s, 1H), 8.01 (m, 3H), 7.85 (dd, 1Hz & 14 Hz,

2H), 7.44 (broad s, 1H), 7.35 (broad s, 1H), 4.10 (m, 1H), 3.61 (s, 3H), 3.46 (s, 2H), 2.12 (broad s, 2H), 1.84 (m, 2H), 1.03 (t, 7Hz, 6H) ppm.

33

Yield from **1** and **27**: 1.27 g (22 %) of orange powder. ^{1}H NMR (400 MHz, $CDCl_3$): ∂ = 8.95 (broad s, 1H), 8.36 (d, 8Hz, 1H), 8.17 (d, 8Hz, 2H), 8.10 (m, 3H), 7.90 (broad s, 1H), 7.53 (broad s, 1H), 7.09 (broad s, 3H), 4.10 (m, 1H), 2.86 (s, 3H), 2.13 (m, 2H), 1.84 (m, 2H), 1.04 (t, 7Hz, 6H) ppm.

Perkin condensation between a bromoarylacetic acid and an arylglyoxylic acid in THF, followed by same-pot esterification:

Butyl diphenylmaleimide (34)

Phenylacetic acid (2.72 g, 20 mmol) and phenylglyoxylic acid (3.00 g, 20 mmol) are dissolved in a solution of triethylamine (4.04 g, 40 mmol) and acetic anhydride (6.12 g, 60 mmol) in THF (40 mL) and refluxed for 3 h under exclusion of moisture. Then 1-aminobutane (7.3 g, 100 mmol) is added and reflux is continued for 16 h. The solution is poured into water (400 mL), the formed precipitate is filtered off on a glass frit, washed with water on the frit, dried in vacuum and purified by chromatography in DCM : pentane 1 : 1 on silica followed by recrystallisation from methanol. Yield: 5.53 g (91 %) of pale yellow strongly fluorescent powder.

^{1}H NMR (400 MHz, $CDCl_3$): ∂ = 7.46 (d, 8Hz, 2H), 7.39-7.31 (m, 3H), 3.65 (d, 7.5Hz, 2H), 1.66 (quint, 7.5Hz, 2H), 1.38 (sext, 7.5Hz, 2H), 0.95 (t, 7.5Hz, 3H) ppm.

Cyclisations by $Pd(OAc)_2$-catalysed dehydrodebromination:

General procedure

The esterified Perkin condensation product (2.5 mmol) is stirred with $Pd(OAc)_2$ (5 mol% per cyclisation site) and K_2CO_3 (5mmol per cyclisation site) in anhydrous DMF (30mL) at 110 °C under argon and with exclusion of moisture and oxygen for 16 h. The mixture is allowed to cool to room temperature, diluted with DCM (100 mL) and filtered through silica to separate the palladium black formed. The solvent is evaporated under reduced pressure and the product is purified by chromatography in DCM on silica and recrystallisation from ethanol (ethyl esters) or butanol (butyl esters).

Butyl chrysene-6-carboxylate (6)

Yield from **4a**: 700 mg (85 %) of white powder. ^{1}H NMR (400 MHz, $CDCl_3$): ∂ = 9.41 (s, 1H), 9.0 (d, 6hz, 1H), 8.80 (m, 2H), 8.69 (d, 9Hz, 1H), 8.08 (d, 9Hz, 1H), 8.00 (d, 8Hz, 1H), 7.75 (m, 3H), 7.66 (t, 7Hz, 1H), 4.52 (t, 7Hz, 2H), 1.91 (m, 2H), 1.61 (m, 2H), 1.05 (t, 7Hz, 3H) ppm. ^{13}C NMR (100MHz,

$CDCl_3$) : ∂ = 168.2, 132.2, 131.1, 130.9, 130.8, 129.8, 129.5, 128.8, 127.5, 127.4, 127.0, 126.9, 126.7, 126.6, 126.5, 126.1, 123.4, 123.1, 121.0, 65.4, 31.0, 19.6, 13.0 ppm. HRMS (m/z (%)): calcd. For $C_{23}H_{20}O_2$ [M] 328.1463; found 328.1455.

Dibutyl fulminene-8,16-dicarboxylate (7)

Yield from **5a**: 400 mg (30 %) of white powder. ^{1}H NMR (400 MHz, $CDCl_3$): ∂ = 9.32 (s, 1H), 8.88 (d, 9Hz, 1H), 8.81 (m, 2H), 8.71 (d, 9Hz, 1H), 7.59 (2t, 2H), 4.38 (t, 7Hz, 2H), 1.77 (m, 2H), 1.44 (m, 2H), 0.91 (t, 7Hz, 3H) ppm. ^{13}C NMR (100MHz, $CDCl_3$) : ∂ = 168.0, 130.8, 130.7, 129.3, 129.2, 127.6, 127.2, 127.1, 126.6, 126.5, 126.1, 124.0, 123,3, 122.1, 65.3, 30.9, 19.4, 13.8 ppm. HRMS (m/z (%)): calcd. For $C_{36}H_{32}O_4$ [M] 528.2301; found 528.2318.

Diethyl phenanthrene-9,10-dicarboxylate (20)

Yield from **14**: 740 mg (92 %) of white needles. ^{1}H NMR (400 MHz, $CDCl_3$): ∂ = 8.68 (d, 8Hz, 1H), 8.16 (d, 8H, 1H), 7.71 (t, 8Hz, 1H), 7.65 (t, 8Hz, 1H), 4.52 (q, 7Hz, 2H), 1.45 (t, 7Hz, 3H). ^{13}C NMR (100MHz, $CDCl_3$): ∂ = 168.0, 131.1, 130.0, 128.4, 127.7, 127.2, 126.8, 122.9, 62.0, 14.3 ppm. HRMS (m/z (%)): calcd. For $C_{20}H_{18}O_4$ [M] 322.1205; found 322.1204.

Diethyl naphthopyrene-dicarboxylate 21

Yield from **15**: 1.0 g (90 %) of yellow powder. ^{1}H NMR (400 MHz, $CDCl_3$): ∂ = 9.32 (s, 1H), 9.00 (d, 9Hz, 1H), 8.56 (d, 9Hz, 1H), 8.24 (d, 8Hz, 1H), 8.20 (d, 7Hz, 1H), 8.15 (m, 3H), 8.04 (m, 2H), 7.83 (pseudo t, 8Hz & 7Hz, 1H), 7.72 (pseudo t, 7Hz & 8Hz, 1H), 4.60 (m, 2H), 4.51 (m, 2H), 1.50 (t, 7Hz, 3H), 1.31 (t, 7Hz, 3H) ppm. ^{13}C NMR (100MHz, $CDCl_3$): ∂ = 170.8, 168.7, 131.4, 131.3, 131.1, 130.8, 129.2, 129.0, 128.7, 128.1, 128.0 (x2), 127.9, 127.8, 127.1 (x2), 126.9, 126.6, 126.4, 125.9, 125.8, 125.3, 124.5, 123.7, 121.7, 119.2, 62.4, 62.3, 14.3, 14.0 ppm.

Tetraethyl dibenzanthracene-tetracarboxylate 22

Yield from **16**: 1.24 g (89 %) of white powder. ^{1}H NMR (400 MHz, $CDCl_3$): ∂ = 9.62 (s, 1H), 8.82 (d, 8Hz, 1H), 8.13 (d, 8Hz, 1H), 7.81 (t, 7Hz, 1H), 7.70 (t, 7Hz, 1H), 4.62 (m, 2H), 4.56 (m, 2H), 1.56 (t, 7Hz, 3H), 1.50 (t, 7H, 3H) ppm. ^{13}C NMR (100MHz, $CDCl_3$) : ∂ = 168.0, 167.7, 132.4, 131.1, 129.6, 129.2, 129.1, 128.3, 127.2 (x 2), 126.7, 123.4, 121.4, 62.3, 62.2, 14.4, 14.3 ppm. HRMS (m/z (%)): calcd. For $C_{34}H_{30}O_8$ [M] 566.1941; found 566.1951.

Tetraethyl dinaphthanthracene-tetracarboxylate 23

Yield from **17**: 1.1 g (66 %) of yelow powder ^{1}H NMR (400 MHz, $CDCl_3$): ∂ = 9.62 (s, 1H), 8.82 (d, 9Hz, 1H), 8.32 (d, 8Hz, 1H), 8.18 (d, 9Hz, 1H), 8.03 (d, 8Hz, 1H), 7.62 (m, 2H), 4.70 (m, 2H), 4.49

(m, 2H), 1.56 (t, 7Hz, 3H), 1.34 (t, 7Hz, 3H) ppm. ^{13}C NMR (100MHz, $CDCl_3$) : ∂ = 170.5, 168.3, 133.3, 131.3, 130.4 (x 2), 130.0, 129.7, 129.5, 128.8, 127.0, 126.7, 126.5, 126.3, 124.3, 121.4, 120.8, 62.6, 62.5, 14.4, 13.9 ppm. HRMS (m/z (%)): calcd. For $C_{42}H_{34}O_8$ [M] 666.2254; found 666.2272.

Tetraethyl dipyrenoanthracene-tetracarboxylate 24

Yield from **18**: 1.6 g (79 %) of orange powder. ^{1}H NMR (400 MHz, $CDCl_3$): ∂ = 9.89 (s, 1H), 9.53 (s, 1H), 8.63 (d, 9Hz, 1H), 8.30 (m, 4H), 8.21 (d, 9Hz, 1H), 8.07 (t, 7hz, 1H), 4.81 (m, 2H), 4.57 (m, 2H), 1.66 (t, 7Hz, 3H), 1.35 (t, 7Hz, 3H) ppm. HRMS (m/z (%)): calcd. For $C_{54}H_{38}O_8$ [M] 814.2567; found 814.2599.

Tetraethyl dinaphthopyrene-tetracarboxylate 25

Yield from **19**: 1.6 g (91 %) of orange powder. ^{1}H NMR (400 MHz, $CDCl_3$): ∂ = 8.80 (s, 1H), 8.65 (d, 8Hz, 1H), 8.56 (s, 1H), 8.05 (d, 8Hz, 1H) 7.75 (s, 1H), 7.65 (t, 7Hz, 1H), 7.56 (t, 7Hz, 1H), 4.62 (m, 2H), 1.55 (t, 7Hz, 3H), 1.34 (t, 7Hz, 3H). ^{13}C NMR (100MHz, $CDCl_3$) : ∂ = 170.6, 168.7, 131.4, 131.1 (x 2), 130.7, 129.4, 129.0, 128.6, 128.0, 127.9, 127.3, 127.0, 126.2 (x 2), 124.6, 123.6, 119.8, 62.5, 62.4, 14.4, 14.1 ppm.

Naphthoperylene-dicarboxylic (3-pentyl)imide 31

Yield from **28**: 1.1 g (93 %) of orange powder. ^{1}H NMR (400 MHz, $CDCl_3$): ∂ = 9.59 (d, 9Hz, 1H), 9.38 (d, 8Hz, 1H), 9.24 (s, 1H), 8.94 (d, 8Hz, 1H), 8.31 (d, 9Hz, 1H), 8.27 (d, 7Hz, 1H), 8.14 (d, 7Hz, 1H), 8.04 (m, 3H), 7.88 (t, 7Hz, 1H), 7.81 (t, 7Hz, 1H), 4.24 (m, 1H), 2.22 (m, 2H), 1.91 (m, 2H), 1.00 (t, 7Hz, 6H) ppm. ^{13}C NMR (100MHz, $CDCl_3$): ∂ = 170.4, 170.3, 133.7, 132.03, 131.99, 131.36, 131.32, 129.8, 129.6, 128.7 (× 2), 128.5, 128.0, 127.72, 127.66, 126.8, 126.7, 126.5, 126.1, 125.8, 125.5, 124.6, 124.0, 123.8, 121.1, 119.5, 56.0, 25.6, 11.5 ppm.

4.8. Notes and references

[1] C. L. Hewett, *Journal of the Chemical Society (Resumed)*, p. 1286, 1938.
[2] D. Bogaert-Verhogen and R. H. Martin *Tetrahedron Letters*, vol. 8, no. 32, pp. 3045–3048, Jan. 1967.
[3] J. Brison and R. H. Martin, *Bull. Soc. Chim. Belges*, vol. 92, no. 10, pp. 893–899, 1983.
[4] L. Nassar-Hardy, C. Deraedt, E. Fouquet, and F.-X. Felpin; *Eur. J. Org. Chem.*, vol. 2011, no. 24, pp. 4616–4622, 2011.
[5] K. Kamikawa, I. Takemoto, S. Takemoto, and H. Matsuzaka; *J. Org. Chem.*, vol. 72, no. 19, pp. 7406–7408, 2007.
[6] C. F. Koelsch and S. Wawzonek, *J. Org. Chem.*, vol. 06, no. 5, pp. 684–689, 1941.
[7] E. K. Fields, S. J. Behrend, S. Meyerson, M. L. Winzenburg, B. R. Ortega, and H. K. Hall; *J. Org. Chem.*, vol. 55, no. 17, pp. 5165–5170, 1990.
[8] Patent, 2009, WO2009037294.
[9] R. G. Harvey, J. Pataki, and H. Lee, *Organic Preparations and Procedures International*, vol. 16, no. 2, pp. 144–148, Apr. 1984.

[10] H. Vollmann, H. Becker, M. Corell, and H. Streeck; *Justus Liebigs Ann. Chem.*, vol. 531, no. 1, pp. 1–159, 1937.

[11] F. F. Blicke and R. F. Feldkamp, *J. Am. Chem. Soc.*, vol. 66, no. 7, pp. 1087–1091, 1944.

[12] G. Lock, *Monatshefte für Chemie*, vol. 86, no. 3, pp. 511–516, 1955.

[13] G. Lock and R. Schneider, *Chem. Ber.*, vol. 88, no. 4, pp. 564–565, 1955.

[14] R. G. Micetich, *Organic Preparations and Procedures*, vol. 2, no. 4, pp. 249–252, Nov. 1970.

[15] R. Stephan, *Chem. Ber.*, vol. 90, no. 2, pp. 296–298, 1957.

[16] German Patent 576253 (1933, R. Sedlmayr & W. Eckert / IG Farben AG).

[17] X. Beebe, A. M. Nilius, P. J. Merta, N. B. Soni, M. H. Bui, R. Wagner, and B. A. Beutel, *Bioorganic & Medicinal Chemistry Letters*, vol. 13, no. 19, pp. 3133–3136, Oct. 2003.

[18] J. Zhuang, C. Wang, F. Xie, and W. Zhang, *Tetrahedron*, vol. 65, no. 47, pp. 9797–9800, Nov. 2009.

[19] J. Kelber, H. Bock, O. Thiebaut, E. Grelet, and H. Langhals, *Eur. J. Org. Chem.*, vol. 2011, no. 4, pp. 707–712, 2011.

[20] S. Demmig and H. Langhals, *Chem. Ber.*, vol. 121, no. 2, pp. 225–230, 1988.

[21] L. D. Wescott and D. L. Mattern, *J. Org. Chem.*, vol. 68, no. 26, pp. 10058–10066, 2003.

[22] S. Alibert-Fouet, I. Seguy, J.-F. Bobo, P. Destruel, and H. Bock, *Chem. Eur. J.*, vol. 13, no. 6, pp. 1746–1753, 2007.

[23] G. Koshkakaryan, D. Cao, L. M. Klivansky, S. J. Teat, J. L. Tran, and Y. Liu, *Org. Lett.*, vol. 12, no. 7, pp. 1528–1531, 2010.

[24] Cymerman-Craig, J.; Loder, J. W.; Moore, B. Australian Journal of Chemistry (1956), 9, 222-7.

[25] N. Watanabe, M. Hamano, S. Todaka, T. Asaeda, H. K. Ijuin, and M. Matsumoto, *J. Org. Chem.*, vol. 77, no. 1, pp. 632–639, 2011.

Chapter 5

Conclusion and outlook on a new approach to functionalised polycyclic aromatic ribbons

This work aimed at elaborating new synthetic approaches to two types of target ribbons: heteronanoribbons with specific electronic properties, and carboxysubstituted nanoribbons where the easily modifiable substituents allow 1. tuning of solubility and processability, 2. tuning of electronic properties, and 3. access to the parent unsubstituted ribbons.

5.1. The ceramidonine approach

To obtain coordinating heteronanoribbons, we considered as most promising an approach based on the coupling of bifunctional anthraquinones and azaarylenediamines followed by cyclisations in strong acid, in analogy to the formation of ceramidonine from 1-phenylamino-anthraquinone. This approach has proven unworkable as we were unable to develop bifunctional substrates with sufficiently stable solubilising substituents. Besides this, the yields of the final cyclisations proved to be only moderate and very dependent on the reaction conditions. Consequently, only short tetraazaarene units with terminal solubilising substituents could be synthesised. Such species may be of interest for organic optoelectronics as electron deficient (acceptor-type) materials with better light absorption than fullerene derivatives, and as doubly chelating bridging ligands in bimetallic complexes. For the latter use, our synthesis of tetraaza-dinaphthoperylenes might be modified appropriately by using 8-nitro- instead of 5-nitro-3-bromoquinoline, *ie*. the minor isomer obtained upon nitration of 3-bromoquinoline.[1] This would bring the quinolinic nitrogens into appropriate positions for chelation in the final product.

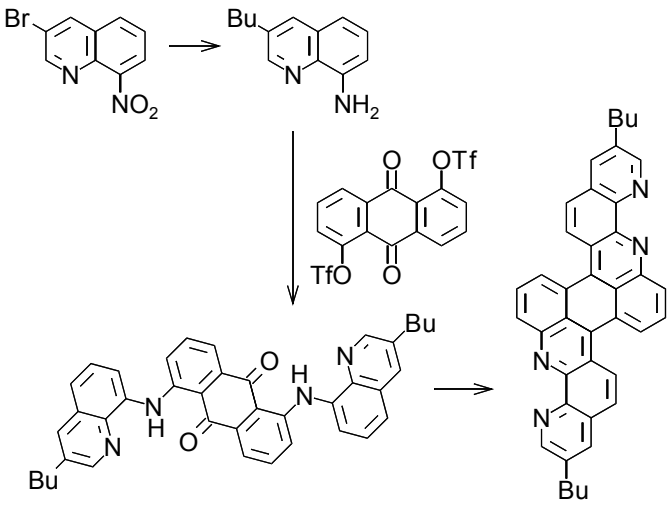

Fig. 1 Hypothetical synthesis, from 3-bromo-8-nitro-quinoline, of a dibutyl-tetraaza-dinaphthoperylene with the nitrogen atoms in appropriate positions for chelation.

5.2. The cyclodehydrogenation variant of the Perkin approach

To obtain carboxysubstituted nanoribbons, two strategies were followed. The first relied on Scholl-type cyclisations of diarylacrylate moieties with a quinone oxidant in strong acid, in analogy to recent work with hydrocarbon substrates by R. Rathore and co-workers. The second was based on the combination of Perkin condensations of bromoarylacetic acids with aromatic aldehydes or arylglyoxylic acids followed by Pd(II)-catalysed cyclisations.

In a systematic study, the quinone approach proved to be limited to substrates with relatively activated aryl moieties such as naphthyl or, especially, thienyl. Albeit a quite exotic outcome including the formation of a seven-membered carbocycle was observed when we tried to obtain a chrysenodithiophene from 1,5-diformylnaphthalene and 3-thienylacetic acid, the expected product could be obtained at higher dilution. As neighbouring thienylene units in polythiophenes are known to be transoid and coplanar[2] if no sterically hindering substituents vicinal to the thiophene-thiophene single bond are present, polymerisation of our chrysenodithiophene (*eg*. by methods established for the coupling of thiophene-3-carboxylic esters[2, 3]) may lead to highly conjugated, partially condensed "quasi-ribbons".

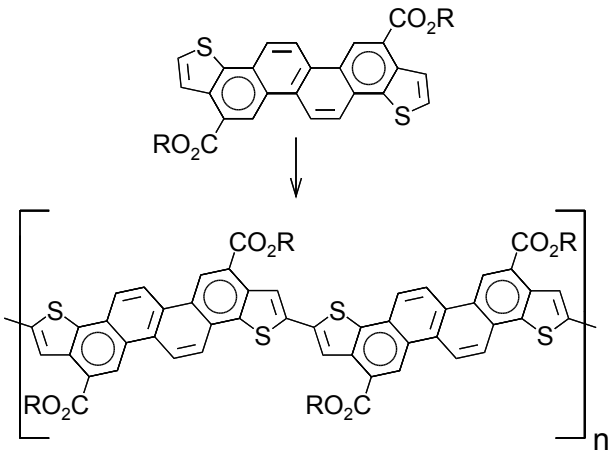

Fig. 2 Hypothetical "quasi-ribbon" polymer based on the chrysenodithiophene obtained from 3-thienylacetic acid and 1,5-diformylnaphthalene.

We also obtained benzodithiophenes that may be used similarly. Our benzodithiophene based on 3-thienylacetic acid and 2-thienylglyoxylic acid may lead, due to the preferred transoid orientation of neighbouring thiophene units, to cyclic hexamers and to helical polymers with potentially good intramolecular π-π stacking between adjacent helix loops, if controlled head-to-tail polymerisation can be achieved.

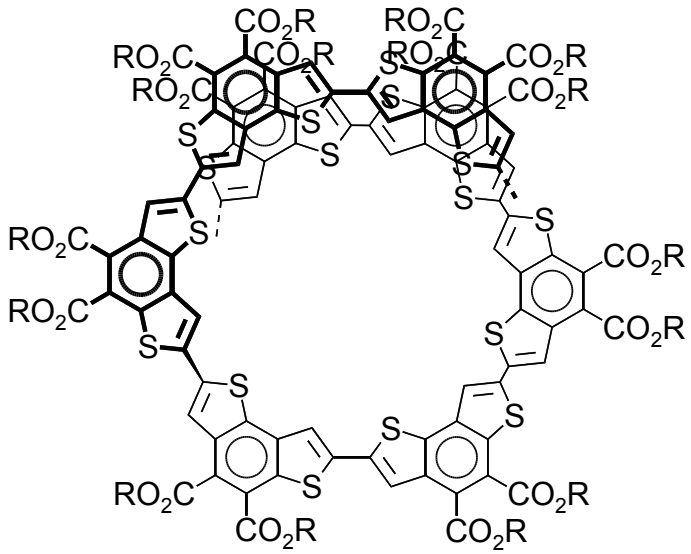

Fig. 3 Hypothetical helical polymer based on head-to-tail polymerisation of the unsymmetrical benzodithiophene obtained from 3-thienylacetic acid and 2-thienylglyoxylic acid.

5.3. The cyclodehydrodebromination variant of the Perkin approach

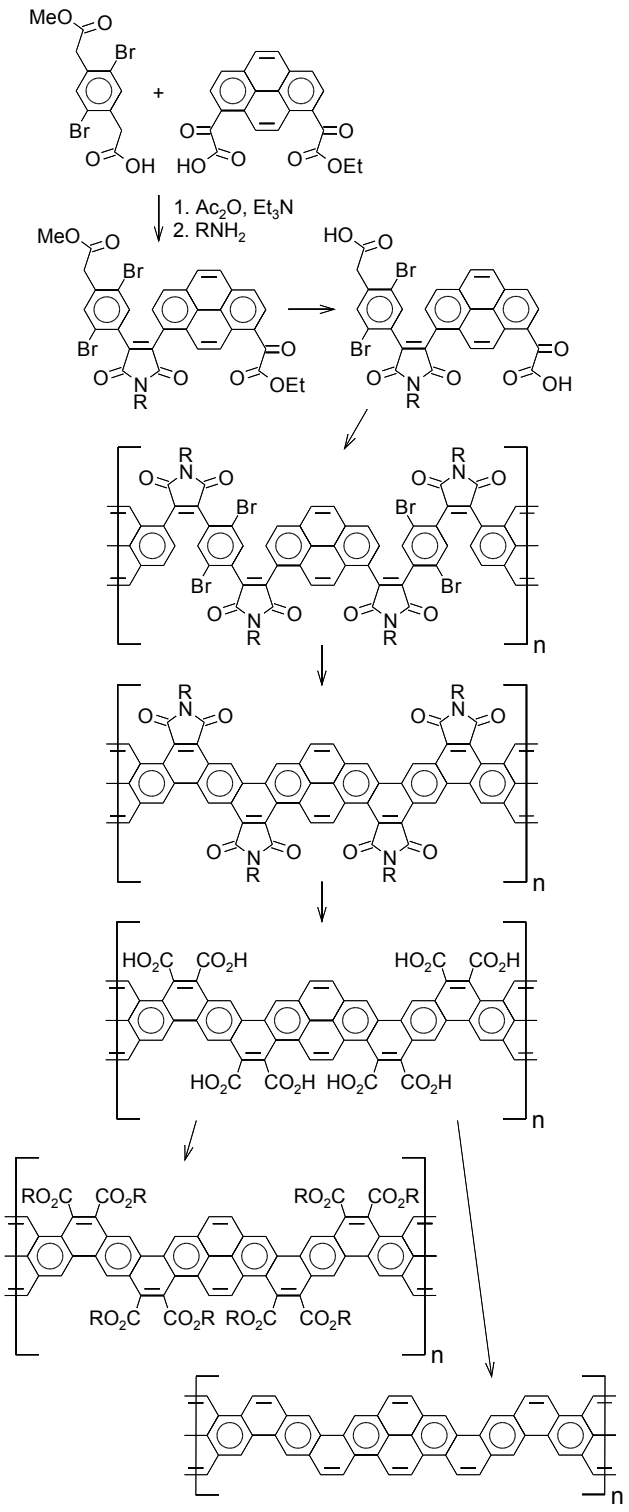

Fig. 4 Hypothetical polymers based on 2,5-dibromophenylene-1,4-diacetic acid and pyrenylene-1,8-diglyoxylic acid.

The second of the two strategies towards carboxy-ribbons proved to be more generalisable than the first. The glyoxylic Perkin condensation followed by diesterification or same-pot imidification and $Pd(OAc)_2$-catalysed dehydrodebromination proved to be an efficient and robust means to obtain fully condensed elongated arenes. Especially the elaboration of 2,5-dibromophenylene-1,4-diacetic acid and pyrenylene-1,8-diglyoxylic acid as a regiospecific bricks allowed the obtention of lath-shaped tetraesters as proof-of-principle. Monoprotected derivatives of both bricks were elaborated in view of the synthesis of longer oligomers and truly polymeric ribbons. An imidified Perkin condensation product of these two monoprotected bifunctional bricks could serve as key monomer, already bearing a solubilising substituent, for the synthesis of a variety of differently functionalised polymeric ribbons.

This strategy may also offer access, under high dilution conditions, to cyclic oligomers that may be dehydrodebrominated to functionalised carbon nanobelts, *ie*. extremely short carbon nanotubes. Such belts might serve, after decarboxylation, as seeds for the controlled growth of carbon nanotubes of homogeneous chirality and diameter.[4, 5, 6]

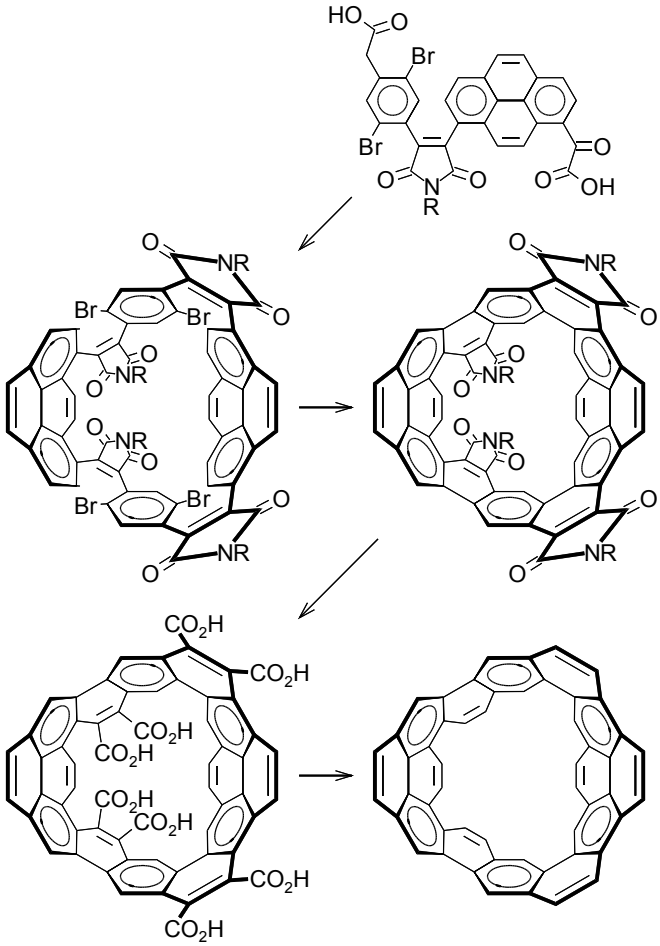

Fig. 5 Hypothetical nanobelts based on 2,5-dibromophenylene-1,4-diacetic acid and pyrenylene-1,8-diglyoxylic acid.

5.4. References

[1] J. D. Crowley, I. M. Steele, B. Bosnich, *Chem. Eur. J.* **12**, 8935, 2006.

[2] M. Pomerantz, A. S. Amarasekara, H. V. R. Dias, *J. Org. Chem.*, **67**, 6931, 2002.

[3] M. Pomerantz, Y. Cheng, R. K. Kasim, R. L. Elsenbaumer, *J. Mater. Chem.*, **9**, 2155, 1999.

[4] M. Iyoda, J. Yamakawa, M. J. Rahman, *Angew. Chem. Int. Ed.*, **50**, 10522, 2011.

[5] D. Eisenberg, R. Shenhar, M. Rabinovitz, *Chem. Soc. Rev.*, **39**, 2879, 2010.

[6] M. A. Petrukhina, L. T. Scott (eds.), *Fragments of Fullerenes and Carbon Nanotubes: Designed Synthesis, Unusual Reactions, and Coordination Chemistry*, John Wiley & Sons, 2011.